

LYAPUNOV-BASED NONLINEAR ESTIMATION METHODS WITH APPLICATIONS
TO MACHINE VISION

By
ASHWIN P. DANI

A DISSERTATION PRESENTED TO THE GRADUATE SCHOOL
OF THE UNIVERSITY OF FLORIDA IN PARTIAL FULFILLMENT
OF THE REQUIREMENTS FOR THE DEGREE OF
DOCTOR OF PHILOSOPHY

UNIVERSITY OF FLORIDA

2011

© 2011 Ashwin P. Dani

To my parents, Chhaya and Kishor, wife, Uttara, and brother, Ketan for their unwavering support

ACKNOWLEDGMENTS

I would like to express sincere gratitude to my advisor, Warren E. Dixon, whose experience and motivation were instrumental for this dissertation. As an advisor, he provided guidance in my research, and encouragement in developing my own ideas. The dynamic and free work culture he has developed in the NCR lab has encouraged and facilitated my learning. As a mentor, he helped me understand the intricacies of working in a professional environment by exposing me to various professional activities such as journal/conference reviews, grant proposal writing, teaching classroom lectures, conducting robot camps as a part of societal outreach activity, etc. I feel fortunate to have had the opportunity to work with him and would like to thank him for all the technical as well as non-technical knowledge he has given me.

I would like to thank Prabir Barooah for his suggestions and technical discussions during various occasions over my graduate school career. During his class and other discussions, I not only received a training about technical matter but also received a training on questioning each and every step. I am slowly assimilating this habit and this has played a crucial role for the technical development in this dissertation.

I would also like to express my thankfulness to Carl D. Crane III for time and the help he provided me during the classroom meetings, various project discussion meetings, and oral qualifiers. I would like to thank him for the support and encouragement he provided me during our visit to Air Force base in Virginia, for a project demonstration.

I would like to extend my gratitude to Pramod Khargonekar for his technical suggestions, during oral qualifiers and during one-on-one meetings, to improve the quality of the dissertation. During his ‘Advanced Topics in Systems and Controls’ class I have learnt many different aspects of systems and controls which I was totally ignorant of. His encouraging and philosophical lectures in the classroom changed my perspective for the systems and controls field and for doing research in general.

I would also like to thank my coworkers, and friends for their support and encouragement. Various technical discussions with my coworkers from the NCR lab have helped me learn and understand the subject in detail. Also, I appreciate all the help they provided me for conducting various experiments.

Last but not the least, I would like to thank my parents for their love and support, my wife, for all the support and encouragement she provided, my brother for his constant support to my higher education.

TABLE OF CONTENTS

	<u>page</u>
ACKNOWLEDGMENTS	4
LIST OF TABLES	9
LIST OF FIGURES	10
ABSTRACT	12
CHAPTER	
1 INTRODUCTION	16
1.1 Motivation	16
1.2 Problem Statement and Overview	16
1.3 Literature Review	17
1.4 Contributions	25
1.5 Dissertation Outline	29
2 CAMERA MOTION MODEL	31
2.1 Euclidean and Image Space Relationships	31
2.2 Camera-Object Relative Motion Model	34
2.3 Assumptions	35
3 GLOBALLY EXPONENTIALLY STABLE OBSERVER FOR VISION-BASED RANGE ESTIMATION	37
3.1 Vision-based Range Estimation	38
3.1.1 Range Observer	38
3.1.2 Stability Analysis	40
3.2 Stability Analysis in the Presence of Disturbances	44
3.3 Discussion	46
3.4 Simulations and Experiments	48
3.5 Summary	58
4 STRUCTURE AND MOTION USING A SINGLE KNOWN CAMERA LINEAR VELOCITY	59
4.1 Structure and Motion Estimation	60
4.1.1 Estimation with a Known Linear Velocity	60
4.1.1.1 Step I: Angular velocity estimation	62
4.1.1.2 Step II: Structure estimation	63
4.1.2 Stability Analysis	64
4.2 Simulation	67
4.3 Summary	70

5	A LYAPUNOV-BASED OBSERVER FOR A CLASS OF NONLINEAR SYSTEMS WITH APPLICATION TO IMAGE-BASED STRUCTURE AND MOTION ESTIMATION	71
5.1	Nonlinear Observer	71
5.1.1	System Dynamics	71
5.1.2	State Estimator	72
5.1.3	Stability Analysis	74
5.2	Application to Structure and Motion Problem	80
5.2.1	Structure and Motion from Motion (SaMfM) Objective	80
5.2.2	State Dynamics Formulation	81
5.2.3	Structure and Motion Observer	83
5.2.4	Conditions on the Moving Object Trajectory	84
5.3	Simulation	86
5.4	Summary	91
6	LYAPUNOV-BASED UNKNOWN INPUT OBSERVER FOR A CLASS OF NONLINEAR SYSTEMS	92
6.1	Nonlinear Unknown Input Observer	92
6.1.1	Nonlinear Dynamics	92
6.1.2	UIO Design	93
6.1.3	Necessary and Sufficient Condition	95
6.1.4	Conditions for Choosing Matrix A	100
6.1.5	LMI Formulation	103
6.2	Summary	104
7	APPLICATION OF THE UNKNOWN INPUT OBSERVER TO THE STRUCTURE ESTIMATION	105
7.1	Structure and Motion Estimation	105
7.1.1	Structure and Motion from Motion (SaMfM) Objective	105
7.1.2	Nonlinear Unknown Input Observer	106
7.1.3	Stability Analysis	108
7.1.4	Conditions for Stability	109
7.1.5	Conditions on Object Trajectories	109
7.2	Simulation	110
7.3	Summary	112
8	CONCLUSION AND FUTURE WORK	114
8.1	Conclusion	114
8.2	Future Work	116
APPENDIX		
A	PROOF OF POSITIVENESS OF P	118

B	OBSERVABILITY CONDITIONS	120
B.1	Observability Condition in Chapter 4	120
B.2	Observability Condition in Chapter 5	120
	REFERENCES	122
	BIOGRAPHICAL SKETCH	131

LIST OF TABLES

<u>Table</u>		<u>page</u>
3-1	Comparison of the presented observer with observers in [1] and [2].	47
3-2	Comparison of the RMS depth estimation errors.	49

LIST OF FIGURES

<u>Figure</u>	<u>page</u>
2-1 Coordinate frame relationships of a moving camera and an object.	31
2-2 Moving camera looking at the static scene.	33
3-1 Comparison between the true and estimated depth in the presence of measurement noise A) top subplot shows the estimated depth using the proposed observer. B) middle subplot shows the estimated depth using the observer in [1]. C) bottom subplot shows the estimated depth using the observer in [2].	49
3-2 Comparison of the depth estimation using the proposed observer and the observer in [2] when camera motion does not satisfy Assumption 3.1.	50
3-3 Evolution of the signal $h_1^2(t) + h_2^2(t)$ against time.	50
3-4 Depth estimation using the observer in [1].	51
3-5 Estimation of $\hat{y}_3(t)$ starting from large initial condition $\alpha(t_0) = 300$ using the proposed observer.	51
3-6 Depth estimation with large initial condition $\alpha(t_0) = 300$ using the proposed observer.	52
3-7 State estimation using the observer in [2] for large initial conditions. Since the state estimate is very large, simulation fails to integrate at $t = 0.03$	52
3-8 AUV experimental setup.	53
3-9 An image frame displaying the tracked buoy target by the AUV.	54
3-10 Comparison of the estimated and ground truth range of the buoy with respect to the underwater vehicle.	55
3-11 States $y_1(t)$ and $y_2(t)$ computed using image pixels.	56
4-1 State $[y_3 \ u_1 \ u_2]^T$	68
4-2 State $[y_3 \ u_1 \ u_2]^T$	69
4-3 State $[y_3 \ u_1 \ u_2]^T$	69
5-1 The velocity of the moving object measured in the inertial reference frame.	88
5-2 State estimation errors using the proposed observer.	88
5-3 State estimation errors using the observer in [3].	89

5-4	Comparison of the actual and estimated 3D relative position of the object and the camera.	89
5-5	The velocity of the moving object measured in the inertial reference frame. . . .	90
5-6	State estimation errors for time varying velocity, $v_p(t)$, using the proposed observer.	90
5-7	Comparison of the actual and estimated 3D relative position of the object and the camera for time-varying object velocity $v_p(t)$	91
7-1	Comparison of the actual and estimated X,Y and Z positions of a moving object with respect to a moving camera.	111
7-2	Error in the range estimation of the moving object.	111

Abstract of Dissertation Presented to the Graduate School
of the University of Florida in Partial Fulfillment of the
Requirements for the Degree of Doctor of Philosophy

LYAPUNOV-BASED NONLINEAR ESTIMATION METHODS WITH APPLICATIONS
TO MACHINE VISION

By

Ashwin P. Dani

August 2011

Chair: Warren E. Dixon

Major: Mechanical and Aerospace Engineering

Recent advances in image-based information estimation has enabled the use of vision sensor in many robotics and surveillance applications. The work in this dissertation, is focused on developing online techniques for image-based structure and motion (SaM) estimation. Since traditional batch methods are not useful for the online vision-based control tasks, observer-based approaches to the problem have been developed. Starting from the Kalman-filter for SaM problem by L. Matthies in 1990, many contributions to the observer approach for the SaM problem exist in literature. Various models are introduced in literature for SaM estimation but two models are prevalent, viz; a kinematic relative motion affine model with implicit outputs and a transformed nonlinear state model with the linear output equation. The existing SaM observers are designed for the case of a stationary object, requires full camera velocity information and cannot be used for certain camera motions. In this dissertation, new solutions to the SaM are presented using the transformed nonlinear state model which can be used for larger set of camera motions, does not require full camera velocity information, and are reduced-order. Solutions for the stationary as well as moving objects viewed by a moving camera are presented.

Chapter 2 introduces a camera projection model and a camera-object relative motion model. The model is generic and can be used to describe relative motion of a moving camera looking at a moving object or a stationary object. Chapters 3 and 4 develops

solution to structure estimation of a stationary object while Chapters 5, 6, and 7 extend the solutions to the structure estimation of a moving object.

In Chapter 3, a reduced order nonlinear observer is developed to estimate the distance from a moving camera to a feature point on a static object (i.e., structure estimation or range identification), where full velocity and linear acceleration feedback of the calibrated camera is provided. The contribution of this work is to develop a global exponential range observer which can be used for a larger set of camera motions than existing observers. The observer is shown to be robust against external disturbances in the sense that the observer is $\mathcal{L}_p \forall p \in [1, \infty]$ stable even if the target object is moving or the camera motion is perturbed. The proposed observer estimates the structure provided an observability condition commonly used in literature is satisfied and is shown to be exponentially stable even if camera motion satisfies a less restrictive observability condition. A sufficient condition on the observer gain is derived to prove stability using a Lyapunov-based analysis. Experimental results are provided to show robust performance of the observer using an autonomous underwater vehicle (AUV).

A natural question arises, is the structure estimation feasible when all six camera velocities are not known? Motivated by this question, Chapter 4 focuses on the development of a reduced order nonlinear observer for the “structure and motion (SaM)” estimation of a stationary object observed by a moving calibrated camera. In comparison to existing work which requires some knowledge of the Euclidean geometry of an observed object or full knowledge of the camera motion, the developed reduced order observer only requires one camera linear velocity and corresponding acceleration to asymptotically identify the Euclidean coordinates of the feature points attached to an object (with proper scale reconstruction) and the remaining camera velocities. The unknown linear velocities are assumed to be generated using a model with unknown parameters. The unknown angular

velocities are estimated using a robust estimator and a standard Homography decomposition algorithm. A Lyapunov analysis is provided to prove that the observer asymptotically estimates the unknown states under a persistency of excitation (PE) condition.

The results in Chapter 3 and 4 assume that the object is stationary. If the object is moving, the system dynamics presents a new challenge for the observer design because of the presence of unmeasurable signals. To solve this challenge, in Chapter 5 an observer design is presented for a specific class of nonlinear systems where the output dynamics is affine in the unmeasurable state and the dynamics of the unmeasurable state are nonlinear. The observer design is based on a strategy of identifying the unmeasurable part of the state from the output dynamics and using the identifier to stabilize the corresponding error dynamics. The estimation error asymptotically converges to zero in the presence of $\mathcal{L}_2[0, \infty)$ disturbances. To illustrate the implications of such an observer, the method is applied to simultaneously estimate the structure (i.e., the range of an object with respect to a camera) and motion (i.e., velocities of an object) of a moving object seen by a moving camera.

Another strategy to the observer design in the presence of an unmeasurable disturbance is an unknown input observer (UIO) design. Chapter 6 provides a solution to an UIO design for a general class of nonlinear systems. Stability and convergence of the estimation error is proven using a Lyapunov-based stability analysis. Necessary and sufficient conditions for the observer error convergence are provided. Similarities to the existence conditions of UIO theory for linear systems and the existence conditions of an observer for Lipschitz nonlinear systems with a known input are established.

In Chapter 7, the UIO developed in Chapter 6 is applied to the structure estimation of an object moving with time-varying velocities viewed by a moving camera. The object's velocity is considered as an unknown input to the perspective dynamical system introduced in Chapter 2. A few scenarios are discussed where the moving object velocity and the camera velocity satisfy the assumptions required for the feasibility of the UIO

developed in Chapter 6. The developed method provides the first causal, observer-based structure estimation algorithm for a moving camera viewing a moving object with unknown time-varying object velocities.

Chapter 1 INTRODUCTION

1.1 Motivation

Camera images provide a dense data set in an encrypted form. Estimation of the data encoded in the images is a pervasive problem across multiple disciplines. From the large amount of information encoded in the images, structure and motion (SaM) of the objects in the scene is of particular interest. SaM estimation is important for robotic applications such as vision-based urban navigation of an autonomous agent, manipulation of unknown and moving targets, or human-machine interaction applications. For military applications such as, automated missile navigation, guidance, and control, GPS-denied autonomous flight, autonomous visual surveillance and video-based geo-location; for medical robotics applications, image-based estimation of SaM is critical. Given the crosscutting need for SaM estimation, this dissertation is motivated by the following questions.

1. How can the structure of stationary objects be accurately estimated in real-time for a static scene given all the camera motion information?
2. How can the structure of a stationary object be estimated given minimal information about the camera motion?
3. How can the structure and motion in dynamic scenes be estimated when the objects are moving with unknown motion?

1.2 Problem Statement and Overview

Observers for SaM estimation of a target object in the field-of-view of a moving camera are developed. For the general SaM problem, the camera and the target are allowed to move freely. The objective of the classic “structure from motion (SfM)” problem is to estimate the Euclidean coordinates of feature points attached to an object (i.e., 3D structure) provided the relative motion between the camera and the object is known. The converse of the SfM problem is the “motion from structure (MfS)” problem where the relative motion between the camera and the object is estimated based on known

geometry of the feature points attached to an object. An extended problem is “structure and motion (SaM)” where the objective is to estimate the Euclidean geometry of the feature points as well as the relative motion between the camera and feature points. The SaM problem is fundamental and some examples indicate that SaM estimation is only possible up to a scale when a pinhole camera model is used [4]. The work presented in this dissertation examines a moving camera capturing images of either a static or moving object. For these scenarios, a reduced order observer is developed using a specific state-space model to estimate structure of a stationary object either given all the camera velocities (see Chapter 3) or given partial knowledge of the camera motion (see Chapter 4). Nonlinear observer is developed in Chapter 5 for a general class of systems, and this observer is applied to estimate the structure and motion of a moving object given all camera velocities. An unknown input observer for a general class of systems is developed in Chapter 6 and its application to the structure estimation of a moving object given all camera velocities is presented in Chapter 7. The observer designs in Chapters 5 and 6 are based on a nonlinear model of the moving object and moving camera relative motion. A pinhole camera projection model is assumed and the measurement of feature points in each camera frame can be obtained using existing feature point identification, and tracking algorithms (see [5–7]).

1.3 Literature Review

This section provides a review of relevant related literature for each chapter.

Chapter 3: Structure estimation of a stationary object given all six camera velocities.

Solutions to the SfM problem can be broadly classified as offline methods (batch methods) and online methods (iterative methods). References and critiques of batch methods can be found in [8–13] and the references therein. Online methods typically formulate the SfM problem as a continuous differential equation, where the image dynamics are derived from a continuous image sequence (see [3, 14–23] and the references therein). Online methods often rely on the use of an Extended Kalman filter (EKF) [14, 24–26]. Kalman

filter based approaches also lack a convergence guarantee and could diverge in practical scenarios. Also, *a priori* knowledge about the noise is required for such solutions. In comparison to Kalman filter-based approaches, some researchers have developed nonlinear observers for SfM with analytical proofs of stability. For example, a high-gain observer called the identifier-based observer (IBO) is presented for range estimation in [23] under the assumption of known camera motion. In [3], a discontinuous sliding-mode observer is developed which guarantees exponential convergence of the states to an arbitrarily small neighborhood, i.e., uniformly ultimately bounded (UUB) result. A continuous observer which guarantees asymptotic range estimation is presented in [19] under the assumption of known camera motion. A semi-globally asymptotically stable reduced-order observer is presented in [27] to estimate the range, given known camera motion. In [21], an asymptotically converging nonlinear observer is developed based on Lyapunov’s indirect method. An application of IBO is presented in [28] to estimate the range of features in the static scene.

The dynamics of the unknown state are nonlinear and the unknown state appears linearly in the dynamics of the known states. In the previous work, the nonlinearities are dominated using sliding mode techniques as shown in [3, 19] which achieves UUB or asymptotic stability. Recently, in [2] a nonlinear observer is developed and using converse Lyapunov theorem exponential convergence of the estimation error is shown, but the result is local in nature, meaning the initial condition has to be within some bound of the ‘true’ depth. The nonlinearities are treated as a perturbation and Lyapunov-based stability analysis is presented to show the local stability of the error system. It is pointed out in [2] that the observer is guaranteed to converge with initial conditions in an arbitrarily large compact set if the linear velocity in Z-direction, and angular velocities in X and Y directions are small. The authors in [2] propose that these velocities can be scaled down suitably in a visual servoing controller scheme. Thus, the observer can be initialized within an arbitrarily large compact set only when the camera velocities

are small, which restricts the domain of applications of this observer. In another recent work [1], an immersion and invariance (I&I) based observer is designed which computes the output injection functions by solving a partial differential equation and achieves global exponential stability. The observer requires camera acceleration measurements along with camera velocity and image feature measurements. In [1], the authors state that the observer has to satisfy the Extended Output Jacobian (EOJ) observability rank condition, which is stricter than the persistency of excitation condition. Thus, the observer in [1] cannot address all the camera motions, which can be addressed by the observer in [2]. The gain condition of the observer in [1] is a function of image features, camera velocities and camera acceleration. Motivated by the desire to achieve globally exponentially convergence observer for the range estimation with less stringent observability conditions a new nonlinear observer is developed in Chapter 3.

Chapter 4: Structure estimation of a stationary object with one known camera linear velocity.

Various batch and iterative methods have been developed to solve the SaM problem up to a scale, such as [11, 29]. However, in comparison to SfM and MfS results, sparse literature is available where the SaM problem is formulated in terms of continuous image dynamics with associated analytical stability analysis. In [30], an algorithm is presented to estimate the structure and motion parameters up to a scaling factor. In [31], a perspective realization theory for the estimation of the shape and motion of a moving planar object observed using a static camera up to a scale is discussed. Recently, a nonlinear observer is developed in [21] to asymptotically identify the structure given the camera motion (i.e., the SfM problem) or to asymptotically identify the structure and the unknown time-varying angular velocities given all three linear velocities. In [14, 32] structure and linear velocities are estimated given partial structure information such as length between two points on an object, which may be difficult in practice for random objects. In another recent result in [28], the IBO approach in [23] is used to estimate the structure and

the constant angular velocity of the camera given all three linear velocities, which may not be possible in practical scenarios such as a camera attached to a unmanned vehicle where side-slip velocities may not be available. The problem of estimating structure, time varying angular velocities, and time varying linear velocities of the camera without knowledge of partial structure information remains an unsolved problem.

The technical challenge presented by the SaM problem is that the image dynamics are scaled by an unknown factor, and the unknown structure is multiplied by unknown motion parameters. The challenge is to estimate a state in the open loop dynamics that appears nonlinearly inside a matrix that is multiplied by a vector of unknown linear and angular velocity terms (see (2–12)). By assuming that the velocities are known, or some model knowledge exists, previous online efforts have been able to avoid the problem of separately estimating multiplicative uncertainties. The contribution of this work is a strategy to segregate the multiplicative uncertainties, and then to develop a reduced order nonlinear observer to address the SaM problem where the structure (i.e., the properly scaled relative Euclidean coordinates of feature points), the time-varying angular velocities, and two unknown time-varying linear velocities are estimated (i.e., one relative linear velocity is assumed to be known along with a corresponding acceleration).

Chapter 5: Structure and motion estimation of a moving object using a moving camera.

Solutions to the SfM problem when the object is stationary, can be used for self-localization and map building of an environment using a moving camera. Since the object is stationary, a moving camera can capture snapshots of the object from two different locations and triangulation can be used to estimate the structure. If object is moving SfM techniques cannot be used to recover the structure. In this dissertation, the structure and motion estimation of a moving object using a moving camera is referred to as SaMfM.

The pioneering work in [33] provides a solution to the SaMfM problem where at least five views are required if the motion of the object is constrained to a straight line and at

least nine views are required if the object is moving with conic trajectories. In [34], the structure and motion of the objects moving with linear or conic trajectories are recovered from tangent projections, provided at least nine views are available. In [35], an object is assumed to be moving with constant velocities while being observed by an approximate orthographic projection camera model. In [36], a stereo camera is used to provide a solution to the SaMfM with at least four views. In [37], a batch algorithm is presented for object motions represented by more general curves. In [38], a factorization-based batch algorithm is proposed where objects are assumed to be moving with constant speed in a straight line, observed by a weak perspective camera. An algebraic geometry approach is presented in [39] to estimate the motion of objects up to a scale given a minimum number of point correspondences. In [40], authors propose a batch algorithm to estimate the structure and motion of objects moving on a ground plane observed by a moving airborne camera. The method relies on a static scene for estimating the projective depth, approximated by the depth of feature points on a static background assuming that one of the feature points of the moving object lies on the static background. In [41], a batch algorithm is developed by approximating the trajectories of a moving object using a linear combination of discrete cosine transform (DCT) basis vectors.

Traditionally, SaMfM problem is tackled using batch algorithms which uses algebraic relationships between 3D coordinates of points in the camera coordinate frame and corresponding 2D projections on the image frame collected over n images to estimate the structure. Batch algorithms are not useful in real-time control algorithms (such as formation control of unmanned ground vehicles, autonomous missile guidance, navigation, and control) where state estimation is required at every camera image capture. Instead of algebraic relationships and geometric constraints used by batch algorithms, a rigid body kinematic motion model can be used to design nonlinear observers/estimators using the data from images up to the current time step. Nonlinear observer algorithm generate

the estimates at every time instant and hence can be implemented online along with the control algorithm.

In [42], an H_∞ approach to the SaMfM problem is presented where the moving object velocities are considered as external disturbances, and only the structure estimation problem is solved. The estimator in [42] converges to a ball around the origin (i.e., an UUB result). In this dissertation, two approaches to the problem of structure and motion estimation for a moving object are presented. In the first approach, an extended state space is created by combining the moving object velocity with the unknown state. The extended state space dynamics are expressed as a nonlinear system where output (measurable state) dynamics is affine in the unmeasurable state and the dynamics of the unmeasurable state is nonlinear. A nonlinear observer is designed for this class of nonlinear systems. In the second approach, the linear velocity of the moving object is viewed as an unknown exogenous input and an unknown input observer approach is developed. In the following, various observer design techniques for nonlinear systems present in literature are discussed and the proposed approach is contrasted against the existing literature.

One of the earliest observer design techniques for nonlinear systems is based on a strategy of linearizing a plant up to a nonlinear function of outputs by a change of coordinates. The method requires the output equation to be linear in the state. A Luenberger observer can be developed for the transformed system, but the conditions for simultaneous transformation of the state dynamics and output equation are very stringent and are based on a solution to a partial differential equation (PDE) [43, 44]. In [45], a method to approximately solve a state transformation PDE is developed. The observer design in [45] does not require the output equation to be linear in the state, hence, it imposes less stringent conditions on system transformation. The results in [45] are extended in [46] by increasing the domain of feasible coordinate transformations. Extension of the result in [45] can also be found in [47]. Another approach to nonlinear

observer design utilizes a strategy where gains are selected large enough to dominate the unmeasurable state dependent nonlinearity [48–50].

Lyapunov-based observer design solutions for Lipschitz nonlinear systems can be found in [51–54]. In [52], a necessary and sufficient observer existence condition is developed for Lipschitz nonlinear systems. In [53], the conditions in [52] are related to a H_∞ problem which satisfy all the regularity assumptions. However, for the design methods in [52] and [53] the Lipschitz constant of the non-linearity has to be small. This limitation is overcome in [54] by developing a robust observer based on the loop-transfer recovery (LTR) observer design technique [55]. All of these observer designs require the system dynamics to contain a linear time-invariant term, i.e., Ax along with a nonlinear term.

In [3, 23, 27], observers for a class of nonlinear systems are developed, where the dynamics of the measurable part of the state is affine in the unmeasurable part of the state, and the dynamics of the unmeasurable part of the state is nonlinear. Systems of this class do not contain a linear time-invariant part in the system dynamics. In [23], the observer design is based on the use of high gain and parameter identification theory from [56]. However, the observer in [23] can only be designed for systems where the dimension of the unmeasurable part of the state is less than the measurable part of the state. An observer is developed in [3] which is not restricted by the dimensions of the measurable and the unmeasurable parts of the state. The design in [3] is based on a sliding mode strategy and yields a state estimation which is uniformly ultimately bounded (UUB) around the origin of the system. Recently, a reduced-order observer design for a general class of nonlinear systems (where the dynamics of measurable part of the state is not required to be affine in the unmeasurable part) is presented in [57]. The observer in [57] can also be used to design an observer for the class of systems in [3, 23, 27] but the observer design relies on finding an appropriate invariant manifold which can be rendered attractive. Finding such invariant manifold involves solving a PDE which may be a tedious task. Motivated by the desire to design an asymptotically converging observer for

the class of nonlinear systems presented in [3] and overcome the limitations in [3, 23, 27], a new observer is presented in Chapter 5.

Chapter 6: Unknown input observer and its application to structure and motion estimation of a moving object

In the relative rigid body motion dynamics for structure and motion estimation, the moving object's linear velocity can be viewed as an exogenous time-varying disturbance. An unknown input observer (UIO) approach is used to estimate the state of the dynamical system where the moving object's velocity is considered as an unknown input. This approach does not require creating an extended state space as required by the observer design approach in the Chapter 5. To motivate the UIO design in this dissertation, the existing UIO design approaches are discussed in the following section.

One of the earliest UIO results introduced the concept of system observability with respect to unknown inputs [58]. Presently, several UIO algorithms exist in literature for estimating the state when a time-varying disturbance, considered as an exogenous input, is present in the system (cf., [59–71]). UIO solutions for linear time-invariant (LTI) systems are broadly studied (cf., [59–68, 72–75]).

Linear UIO algorithms are extended to nonlinear systems in [69–71, 76–81]. In [69], an UIO is designed for SISO nonlinear systems. In [70], a nonlinear UIO is presented based on H_∞ optimization. The observer is called a dynamic UIO which provides an extra degree of design freedom but increases the order of the system. In [78], a nonlinear UIO is presented for a class of nonlinear systems based on an LMI approach but no necessary and sufficient observer existence conditions are developed. In [79], a high gain observer for a class of nonlinear systems is presented for state and unknown input estimation but is achieved only up to a small bound which can be reduced by increasing the observer gains, (i.e., an uniformly ultimately bounded (UUB) result). A higher order sliding mode UIO is presented for nonlinear systems in [80] which requires the original nonlinear system to satisfy geometric conditions for transforming the system into the Brunovsky canonical

form. Based on a detectability notion, a sufficient condition for the existence of an UIO is derived in [81] for state-affine systems up to an output injection. Based on the geometric approach of [59], necessary and sufficient conditions are derived in [71] for the existence of an UIO for state affine systems up to a nonlinear unknown input dynamics; hence, the UIO can be used for a larger class of unknown inputs. UIOs are used extensively in fault detection and isolation for various classes of systems such as linear systems [82], control affine systems [83], bilinear systems [84], and nonlinear systems [76, 85]. In [76], an unknown input observer for a class of nonlinear systems is presented for fault diagnosis. The observer design relies on a coordinate transformation which decouples the nonlinear system into a system independent of unknown inputs and a system with the states that can be expressed as linear combinations of the outputs and the states of the first subsystem. The observer gain is obtained by solving a parametric Lyapunov equation which can be challenging to compute [78]. To overcome the limitations of the current UIO designs, a solution for a general class of nonlinear systems is desired and is presented in Chapter 6.

1.4 Contributions

This dissertation focuses on developing nonlinear observers for vision-based range and motion estimation. The observers are developed to overcome the technical challenges such as global estimation in the presence of locally Lipschitz nonlinearity and nonlinear multiplicative uncertainty. The contributions of the proposed results are as follows.

1. Chapter 3, *Globally Exponentially Convergent Observer for Vision-based Range Estimation*: This chapter presents a new reduced order observer for vision based range estimation. The main contributions of the observer are summarized as follows.
 - (a) Global exponential convergence is achieved under a gain conditions and the observability condition required by the range observers present in the literature.

- (b) The observer is proven to be exponentially convergent even under a relaxed observability condition which allows camera motion to be zero along all three direction for sufficiently small duration of time.
- (c) The observer is shown to be finite gain \mathcal{L}_p stable with respect to an exogenous disturbance input. Thus, the observer errors remain bounded even if the stationary object assumption is violated where the object motion is considered as an exogenous input.

In comparison with the observer in [1], the gain condition in this chapter is only a function of upper bounds on camera velocities and image size.

2. Chapter 4, *Structure and Motion with a Single Known Linear Velocity*: In this chapter an observer for range (structure) and motion estimation is presented. The technical challenge presented by the SaM problem is that the image dynamics are scaled by an unknown scale factor, and the unknown structure is multiplied by unknown motion parameters. As described in Chapter 4, the challenge is to estimate a state in the open loop dynamics that appears nonlinearly inside a matrix that is multiplied by a vector of unknown linear and angular velocity terms (see Eq. 2–12). By assuming that the velocities are known, or some model knowledge exists, previous online efforts have been able to avoid the problem of separately estimating multiplicative uncertainties. The contribution of this work is a strategy to segregate the multiplicative uncertainties, and then to develop a reduced order nonlinear observer to address the SaM problem where the structure (i.e., the properly scaled relative Euclidean coordinates of feature points), the time-varying angular velocities, and two unknown time-varying linear velocities are estimated (i.e., one relative linear velocity is assumed to be known along with a corresponding acceleration). The result exploits an uncertain locally Lipschitz model of the unknown linear velocities of the camera. The strategic use of a standard homography decomposition is used to estimate the angular velocities, provided the intrinsic camera calibration parameters

are known and feature points can be between images. A persistency of excitation (PE) condition is formulated, which provides an observability condition that can be physically interpreted as the known camera linear velocity should not be zero over any small interval of time, and the camera should not be moving along the projected ray of a point being during any small interval of time. A Lyapunov-based analysis is provided that indicates the SaM observer errors are asymptotically regulated provided the PE condition is satisfied. By developing a reduced order observer to segregate and estimate the multiplicative uncertainties, new applications can be addressed including: range and velocity estimation using a camera fixed to a moving vehicle where only the forward velocity/acceleration of the vehicle is known, range and velocity estimation using an unmanned air vehicle (UAV) using only a forward velocity/acceleration sensors, etc.

3. Chapter 5, *Observer Design for a Class of Nonlinear Systems with an Application to Structure and Motion*: In this chapter, the problem of structure and motion estimation of a moving object is cast into a specific class of nonlinear systems and an observer design is presented. For the systems of this class, output dynamics (measurable part of the state) is affine in the unmeasurable part of the state, and dynamics of the unmeasurable part of the state is nonlinear. There is no restriction on the dimensions of the measurable part and the unmeasurable part of the state. The observer design does not require the transformation of the plant dynamics into the observer canonical form or solving a PDE, hence, assumption of uniform observability of the system dynamics is not required. Additionally, the system dynamics does not require a linear time invariant term. The state estimation error asymptotically converges to zero in the presence of $\mathcal{L}_2[0, \infty)$ time-varying disturbances. The design is based on identifying the linear unmeasurable part of the state from the dynamics of the measurable part of the state using a robust identifier called the robust integral of the signum of the error (RISE) [86, 87]. The identifier is

then used to stabilize the estimation error dynamics of the unmeasurable state. The proposed observer provides a real-time solution to structure and motion and extends the existing results to objects moving independently with unknown time-varying velocity converging to a constant. The proposed method has no requirements of the minimum number of point correspondences or the minimum number of views.

4. Chapter 6, *Lyapunov-based Unknown Input Observer Design for a Class of Nonlinear Systems*: In this chapter, a nonlinear UIO is developed for a general class of multi-input multi-output (MIMO) nonlinear systems. Based on the existence of a solution to the Riccati equation, necessary and sufficient existence conditions are derived. The conditions provide guidelines for choosing the observer gain matrix based on the Lipschitz constant of the nonlinearity present in the dynamics. An algorithm for choosing the gain matrix based on the Eigenvalue placement is suggested in [52]. The gain matrix is obtained by solving an LMI feasibility problem. Contributions of Chapter 6 include the design of an UIO for a general class of nonlinear systems and an extension of the observer existence conditions derived in [52] for systems with known inputs to a general class of nonlinear systems with unknown inputs.
5. Chapter 7, *Application of the Unknown Input Observer for the Structure and Motion*: The contribution of this work is to provide a causal algorithm for estimating the structure of a moving object using a moving camera with relaxed assumptions on the object's motion. The object is assumed to be moving on a ground plane with arbitrary velocities observed by a downward looking camera with arbitrary linear motion in 3D space. No assumptions are made on the minimum number of points or minimum number of views required to estimate the structure. Feature point data and camera velocity data from each image frame is required. Estimating the structure of a moving object is re-cast into an unknown input observer design problem.

1.5 Dissertation Outline

Chapter 1 serves as an introduction. The motivation, problem statement and the contributions of the dissertation are discussed in this chapter. Chapter 2 describes the relative motion model of a camera-object system and states the common assumptions of the model used in rest of the chapters. Chapter 3 illustrates a nonlinear observer for range estimation when all six camera velocities are known. The observer presented in this chapter achieves global exponential convergence result for a nonlinear system with a locally Lipschitz nonlinearity. Simulation results compare the performance of the observer with the recently published observers for the range estimation problem. The observer performance is validated using experiments conducted on autonomous underwater vehicle (AUV). Chapter 4 provides a solution to an extended structure and motion problem where out of the six camera velocities (three angular and three linear) only one of the linear velocities is known. A reduced order observer is developed which asymptotically estimates the unknown depth and two unknown linear camera velocities given a persistency of excitation (PE) condition is satisfied. Angular velocities are estimated using homography matrix decomposition between consecutive camera frames. Simulation results are provided to illustrate the performance of the observer. Chapter 5 develops a new observer for a class of nonlinear systems which can be used to solve the structure and motion estimation problem when an object is moving. Physical constraints on the object's motion are discussed. Performance of the observer is illustrated via comparison with the existing observers in simulation. Chapter 6 provides a new solution to a general class of unknown input observers (UIO). Necessary and sufficient existence conditions are developed for the observer. A linear matrix inequality (LMI) is developed to compute the observer gain matrix. Chapter 7 presents an application of the UIO to the SaMfM problem. Specific scenarios are discussed when the SaMfM state dynamics can be transformed into the structure of UIO developed in Chapter 6. Chapter 8 concludes the dissertation

by summarizing the work in this dissertation and giving directions to a few future open problems in the observer design and structure and motion estimation.

Chapter 2
CAMERA MOTION MODEL

The purpose of this chapter is to provide background information pertaining to coordinate frames attached to the camera and object, their relationship, geometric projections of the object on a camera image and camera-object relative motion model.

2.1 Euclidean and Image Space Relationships

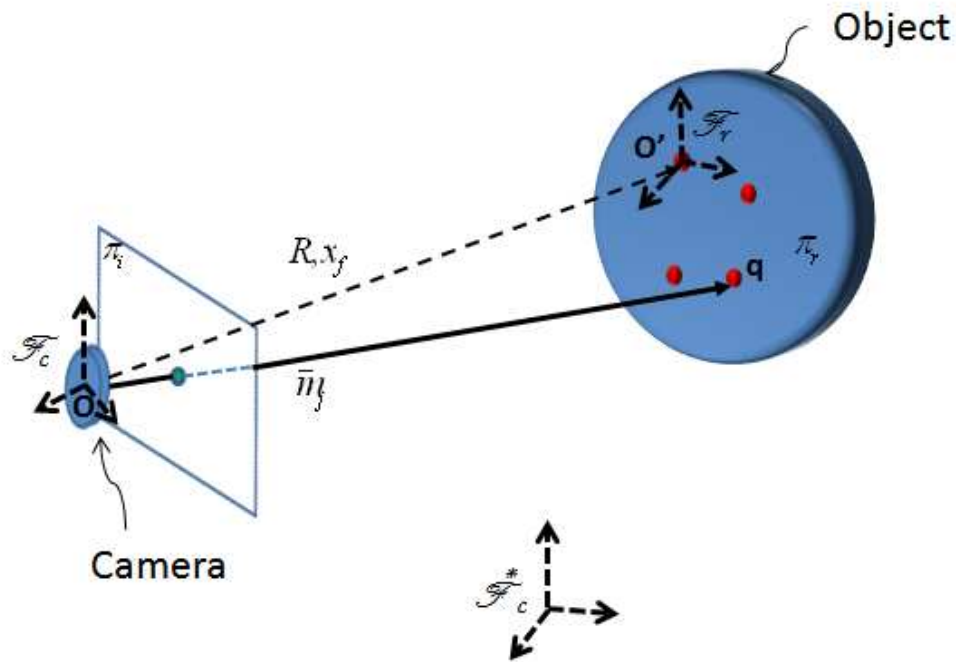


Figure 2-1. Coordinate frame relationships of a moving camera and an object.

A moving camera observing a scene induces a motion in the image plane. Point correspondences in successive image to image can be computed using existing feature tracking techniques [5–7]. Consider a moving camera that views four or more planar¹ and non-collinear feature points (denoted by $j = \{1, 2, \dots, n\} \forall n \geq 4$) lying fixed in a visible plane π_r , attached to an object in front of the camera as shown in Fig. 2-1. Let \mathcal{F}_r be a

¹ Four planar points are needed to compute the homography. The homography can also be computed with 8 non-coplanar and non-collinear feature points using the “virtual parallax” algorithm [88].

static coordinate frame attached to the object. A static reference orthogonal coordinate frame \mathcal{F}_c^* is attached to the camera at the location corresponding to an initial point in time t_0 where the object is in the camera field of view (FOV). After the initial time, an orthogonal coordinate frame \mathcal{F}_c attached to the camera undergoes some rotation $\bar{R}(t) \in SO(3)$ and translation $\bar{x}_f(t) \in \mathbb{R}^3$ away from \mathcal{F}_c^* .

The Euclidean coordinates $\bar{m}(t) \in \mathbb{R}^3$ of a point² observed by a camera expressed in the camera frame \mathcal{F}_c and the respective normalized Euclidean coordinates $m(t) \in \mathbb{R}^3$ are defined as

$$\bar{m}(t) = \begin{bmatrix} x_1(t), & x_2(t), & x_3(t) \end{bmatrix}^T, \quad (2-1)$$

$$m(t) = \begin{bmatrix} \frac{x_1(t)}{x_3(t)}, & \frac{x_2(t)}{x_3(t)}, & 1 \end{bmatrix}^T. \quad (2-2)$$

The constant Euclidean coordinates and the normalized coordinates of the feature points expressed in the camera frame \mathcal{F}_c^* are denoted by $\bar{m}^* \in \mathbb{R}^3$, and $m^* \in \mathbb{R}^3$ respectively and are given by Eq. 2-2 super-scripted by a ‘*’. To facilitate the subsequent development, the state vector $y(t) = [y_1(t), y_2(t), y_3(t)]^T \in \mathcal{Y} \subset \mathbb{R}^3$ is constructed from Eq. 2-2 as

$$y = \begin{bmatrix} \frac{x_1}{x_3}, & \frac{x_2}{x_3}, & \frac{1}{x_3} \end{bmatrix}^T. \quad (2-3)$$

The corresponding feature points m^* and $m(t)$ viewed by the camera from two different locations (and two different instances in time) are related by a depth ratio $\alpha(t) \triangleq \frac{x_3^*}{x_3(t)} \in \mathbb{R}$ and a homography matrix $H(t) \in \mathbb{R}^{3 \times 3}$ as

$$m = Hm^* \quad (2-4)$$

where $H \triangleq \frac{x_3^*}{x_3} \left(\bar{R} + \frac{\bar{x}_f}{d^*} n^{*T} \right)$. The homography matrix can be estimated using four coplanar points or eight non-coplanar points. The homography matrix $H(t)$ can be

² Subsequent technical development is shown for a single point. In practice, results can be extended to multiple points in a similar manner.

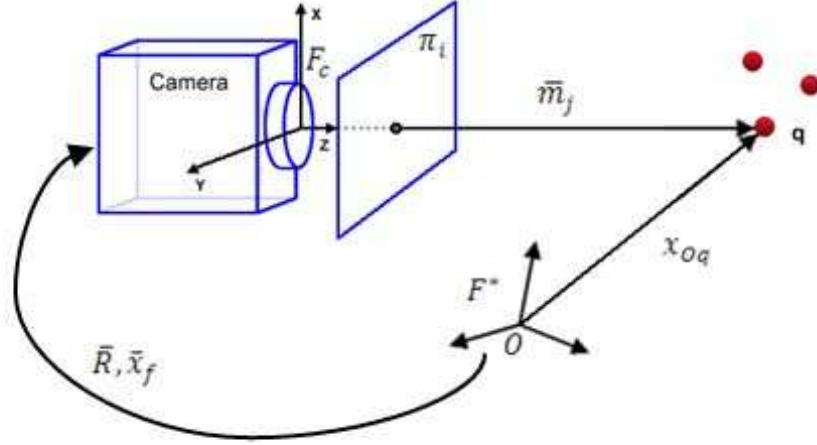


Figure 2-2. Moving camera looking at the static scene.

decomposed using various methods (see e.g., [89, 90]) to obtain the rotation $\bar{R}(t)$, depth ratio $\alpha(t)$, the scaled translation $\frac{\bar{x}_f(t)}{d^*}$ where $\bar{x}_f(t)$ is the absolute translation between \mathcal{F}_c^* and \mathcal{F}_c , d^* and n^* represents the perpendicular distance and normal vector between \mathcal{F}_c^* and the object plane. The decomposition of the homography leads to two solutions, one of which is physically relevant. An in-depth discussion about the homography estimation and decomposition and how to obtain the physically relevant solution can be found in [4, 89]. Using projective geometry, the normalized Euclidean coordinates m^* and $m(t)$ can be related to the pixel coordinates in the image space as

$$p = A_c m, \quad p^* = A_c m^* \quad (2-5)$$

where $p(t) = [u, v, 1]^T$ is a vector of the image-space feature point coordinates $u(t)$, $v(t) \in \mathbb{R}$ defined on the closed and bounded set $\mathcal{I} \subset \mathbb{R}^3$, and $A_c \in \mathbb{R}^{3 \times 3}$ is a constant,

known, invertible intrinsic camera calibration matrix [4] given by

$$A_c = \begin{bmatrix} \lambda_m & -\lambda_m \cot \phi & u_0 \\ 0 & \frac{\lambda_m}{\sin \phi} & v_0 \\ 0 & 0 & 1 \end{bmatrix}. \quad (2-6)$$

In Eq. 2-6 $u_0, v_0 \in \mathbb{R}$ denote the pixel coordinates of the principal point, $\lambda_m \in \mathbb{R}$ represents the focal length in pixels and $\phi \in \mathbb{R}$ is the skew angle between the camera axes. Since A_c is known, Eq. 2-5 can be used to recover $m(t)$, which can be used to partially reconstruct the state $y(t)$.

2.2 Camera-Object Relative Motion Model

As seen from Fig. 2-2, the static scene point q can be expressed in the coordinate system \mathcal{F}_c as

$$\bar{m} = \bar{x}_f + \bar{R}x_{oq} \quad (2-7)$$

where x_{oq} is a vector from the origin of coordinate system \mathcal{F}_c^* to the point q expressed in the coordinate system \mathcal{F}_c . Differentiating Eq. 2-7, the relative motion of q as observed in the camera coordinate system can be expressed by the following kinematics [4, 91]

$$\dot{\bar{m}} = [\omega]_{\times} \bar{m} + v_r \quad (2-8)$$

where $\bar{m}(t)$ is defined in Eq. 2-1, $[\omega]_{\times} \in \mathbb{R}^{3 \times 3}$ denotes a skew symmetric matrix formed from the angular velocity vector of the camera $\omega(t) = \begin{bmatrix} \omega_1 & \omega_2 & \omega_3 \end{bmatrix}^T \in \mathcal{W} \subset \mathbb{R}^3$, and $v_r(t)$ represents the relative velocity of the camera with respect to the moving point, defined as

$$v_r = v_c - \bar{R}\bar{v}_p. \quad (2-9)$$

In Eq. 2-9, $v_c(t) = \begin{bmatrix} v_{cx} & v_{cy} & v_{cz} \end{bmatrix}^T \in \mathcal{V}_c \subset \mathbb{R}^3$ denotes the camera velocity in the inertial reference frame, $\bar{R}\bar{v}_p(t) \triangleq v_p(t) = \begin{bmatrix} v_{px} & v_{py} & v_{pz} \end{bmatrix}^T \in \mathcal{V}_p \subset \mathbb{R}^3$ denotes the velocity of the moving point q expressed in camera reference frame \mathcal{F}_c , and $\bar{v}_p(t) =$

$\begin{bmatrix} \bar{v}_{px} & \bar{v}_{py} & \bar{v}_{pz} \end{bmatrix}^T \in \bar{\mathcal{V}}_p \subset \mathbb{R}^3$ denotes the velocity of the moving point in the inertial reference frame \mathcal{F}^* . Subsequent development in Chapters 3 and 4 is based on the fact that, for stationary object, $\bar{v}_p(t) = 0$, hence, $v_r(t) = v_c(t)$.

Using Eqs. 2-3 and 2-8, the dynamics of the partially measurable state $y(t)$ can be expressed as

$$\dot{y}_1 = (v_{cx} - y_1 v_{cz})y_3 - y_1 y_2 \omega_1 + (1 + y_1^2)\omega_2 - y_2 \omega_3 - (v_{px} - y_1 v_{pz})y_3 \quad (2-10)$$

$$\dot{y}_2 = (v_{cy} - y_2 v_{cz})y_3 - (1 + y_2^2)\omega_1 + y_1 y_2 \omega_2 + y_1 \omega_3 - (v_{py} - y_2 v_{pz})y_3 \quad (2-11)$$

$$\dot{y}_3 = -y_3^2 v_{cz} - y_2 y_3 \omega_1 + y_1 y_3 \omega_2 + y_3^2 v_{pz} \quad (2-12)$$

where the states $y_1(t)$ and $y_2(t)$ can be measured as the output of the system through the invertible transformation given by Eq. 2-5. The following symbols are defined to streamline the notations throughout the dissertation: $h_1(t) \triangleq v_{cx}(t) - y_1(t) v_{cz}(t)$, $h_2(t) \triangleq v_{cy}(t) - y_2(t) v_{cz}(t)$, $p_1(t) \triangleq -y_1(t) y_2(t) \omega_1(t) + (1 + y_1^2(t))\omega_2(t) - y_2(t) \omega_3(t)$ and $p_2(t) \triangleq -(1 + y_2^2(t))\omega_1(t) + y_1(t) y_2(t) \omega_2(t) + y_1(t) \omega_3(t)$. The development in Chapters 3 and 4 uses the fact that in the generic camera-object relative motion state space dynamics, $v_{px}(t) = v_{py}(t) = v_{pz}(t) = 0$.

2.3 Assumptions

The following physically inspired assumptions are used in the development of the Chapters 3-7.

Assumption 2.1. *The relative Euclidean distance $x_3(t)$ between the camera and the feature points observed on the target is upper and lower bounded by some known positive constants (i.e., the object remains within some finite distance away from the camera).*

Assumption 2.2. *The camera velocities are assumed to be bounded, and the linear velocities are assumed to be differentiable with bounded accelerations.*

Remark 2.1. The states $y_1(t)$ and $y_2(t)$ represent pixel locations. From the finite size of the image, $y_1(t)$ and $y_2(t)$ are bounded by known constants as

$$\underline{y}_1 \leq y_1(t) \leq \bar{y}_1, \quad \underline{y}_2 \leq y_2(t) \leq \bar{y}_2.$$

The relative Euclidean distance $x_3(t)$ between the camera and the feature point is lower bounded by the camera focal length λ_m (in meters), and is not assumed to be upper bounded. Therefore, the state $y_3(t)$, an inverse of the state $x_3(t)$, can be upper and lower bounded as [2]

$$0 < \underline{y}_3 < y_3(t) \leq \frac{1}{\lambda_m} = \bar{y}_3.$$

Chapter 3

GLOBALLY EXPONENTIALLY STABLE OBSERVER FOR VISION-BASED RANGE ESTIMATION

The objective of the classic “structure from motion (SfM)” problem is to estimate the Euclidean coordinates of tracked feature points attached to an object (i.e., 3D structure) provided the relative motion between the camera and the object is known. In the motion model described in Chapter 3 the dynamics of the unknown state are nonlinear and the unknown state appears in the dynamics of the known states. In the previous work, the nonlinearities are mitigated using sliding mode techniques or the nonlinear part is considered as a perturbation term and stability is proven using a converse Lyapunov theorem or an immersion and invariance technique is used to find output injection by solving partial differential equations. In general, the observability condition for the existing results states that camera must be translating along at least one of the three directions and should not be translating parallel to the ray projected from a feature point at any instant of time. In this chapter, a globally exponentially stable reduced-order observer is designed. The contributions of this work is threefold. The observer is globally exponentially stable under sufficient observability and gain conditions. Second, the observer is proven to be exponentially convergent even under a relaxed observability condition which allows the camera motion to be zero along all three directions for sufficiently small duration of time. Finally, the observer is shown to be finite gain \mathcal{L}_p stable with respect to an exogenous disturbance input. Thus, the observer errors remain bounded even if the stationary object assumption is violated where the object motion is considered as an exogenous input. In comparison with the observer in [1], the gain condition is only a function of upper bounds on camera velocities and image size. Simulation and experimental results are provided to show the performance of the proposed observer. Comparison of the performance of proposed observer to the performance of observers in [2] and [1] is provided.

3.1 Vision-based Range Estimation

The objective of the range estimation problem (i.e., SfM) is to estimate the Euclidean coordinates of feature points in a static scene using a moving camera with known camera velocities $b(t)$ and $\omega(t)$. The projective transformation onto the image plane loses depth information, but it can be recovered from 2D point correspondences in the images. Once the Euclidean depth is recovered using Eq.s 2–3 and 2–5, the complete Euclidean coordinates can be computed.

3.1.1 Range Observer

In this section, a new nonlinear observer for range estimation is presented. The dynamics of the range, given by $\bar{m}(t)$, are represented using the perspective dynamic system in Eq. 2–12. All six velocities and linear accelerations of the camera are available as sensor measurements. Scenarios where the relative motion $\omega(t)$ and $b(t)$ are known include a camera attached to the end-effector of a robot manipulator, mobile robot, autonomous underwater vehicle (AUV), or micro air vehicle (MAV). Linear and angular camera velocity, and linear camera acceleration can be acquired using a wide array of sensor configurations utilizing an inertial measurement unit (IMU), global positioning system (GPS), or other sensors.

The state $y_3(t)$ contains depth information which is lost due to a perspective transformation. To obtain the range of a feature point $\bar{m}(t)$, it is necessary to scale the measured states $y_1(t)$ and $y_2(t)$ using the depth. Thus, the main motivation of the observer is to estimate the state $y_3(t)$. Let the estimates of the state $y_3(t)$ be defined as $\hat{y}_3(t)$. To quantify the depth estimation mismatch, an estimate error $e(t)$ is defined as

$$e \triangleq y_3 - \hat{y}_3. \quad (3-1)$$

To ensure the estimate $\hat{y}_3(t)$ is bounded, a locally Lipschitz projection law [92] is designed to update $\hat{y}_3(t)$ as

$$\dot{\hat{y}}_3(t) = proj(\hat{y}_3, \phi) = \begin{cases} \phi & \begin{cases} \text{if } \underline{y}_3 \leq \hat{y}_3(t) \leq \bar{y}_3 \text{ or} \\ \hat{y}_3(t) > \bar{y}_3 \text{ and } \phi(t) \leq 0 \text{ or} \\ \hat{y}_3(t) < \underline{y}_3 \text{ and } \phi(t) \geq 0 \end{cases} \\ \bar{\phi} & \text{if } \hat{y}_3(t) > \bar{y}_3 \text{ and } \phi(t) > 0 \\ \check{\phi} & \text{if } \hat{y}_3(t) < \underline{y}_3 \text{ and } \phi(t) < 0 \end{cases} \quad (3-2)$$

where $\phi(y_1, y_2, \hat{y}_3, v_c, \omega) \in \mathbb{R}$ is defined as

$$\begin{aligned} \phi &\triangleq \hat{y}_3^2 v_{cz} + (y_2 \omega_1 - y_1 \omega_2) \hat{y}_3 - k_3 (h_1^2 + h_2^2) \hat{y}_3 \\ &\quad + k_3 (-h_1 p_1 - h_2 p_2 + h_1 \dot{y}_1 + h_2 \dot{y}_2), \end{aligned} \quad (3-3)$$

where $h_1(t), h_2(t), p_1(t), p_2(t)$ are defined in Chapter 2, and $\bar{\phi}(t) \in \mathbb{R}$ and $\check{\phi}(t) \in \mathbb{R}$ are defined as

$$\bar{\phi} \triangleq \left[1 + \frac{\bar{y}_3 - \hat{y}_3}{\delta} \right] \phi, \quad \check{\phi} \triangleq \left[1 + \frac{\hat{y}_3 - \underline{y}_3}{\delta} \right] \phi. \quad (3-4)$$

The projection in Eq. 3-2 ensures that the estimate $\hat{y}_3 \in \Omega_\delta \forall t \geq 0$, where $\Omega_\delta = \{\hat{y}_3 \mid \underline{y}_3 - \delta \leq \hat{y}_3 \leq \bar{y}_3 + \delta\}$ for some known arbitrary constant $\delta > 0$. The signal $\phi(t)$ can be integrated to eliminate the computation of optical flow, i.e., \dot{y}_1 and \dot{y}_2 , and the signal \hat{y}_3 can be generated using

$$\hat{y}_3 = \alpha + \beta. \quad (3-5)$$

Instead of Eq. 3-3, in Eq. 3-5 the update law for the function $\alpha(y_1, y_2, \hat{y}_3, \omega, v_c, \dot{v}_c)$ is given by

$$\begin{aligned} \dot{\alpha} &= \hat{y}_3^2 v_{cz} + (y_2 \omega_1 - y_1 \omega_2) \hat{y}_3 \\ &\quad - k_3 (h_1^2 + h_2^2) \hat{y}_3 - k_3 h_1 p_1 - k_3 h_2 p_2 \\ &\quad - k_3 y_1 \dot{v}_{cx} - k_3 y_2 \dot{v}_{cy} + k_3 \dot{v}_{cz} \left(\frac{y_1^2 + y_2^2}{2} \right) \end{aligned} \quad (3-6)$$

and $\beta(y_1, y_2, v_c)$ is defined as

$$\beta \triangleq k_3 \left(v_{cx}y_1 + v_{cy}y_2 - v_{cz} \left(\frac{y_1^2 + y_2^2}{2} \right) \right) \quad (3-7)$$

where $k_3 \in \mathbb{R}^+$. The initial condition of the observer is selected as

$$\alpha(t_0) = \alpha_0$$

where α_0 is an arbitrary constant.

Assumption 3.1. *The subsequent development is based on the assumption that $h_1^2 + h_2^2 \geq \varepsilon > 0, \forall t \geq 0$ for a positive constant ε . This assumption is an observability condition for the observer in Eqs. 3-2-3-7, and is the same as obtained previously in the literature [1, 19, 23, 93]. The condition physically implies that $v_{cx}(t), v_{cy}(t), v_{cz}(t)$ are not equal to zero simultaneously and the motion of the camera should not be along the projected ray of the point being observed.*

3.1.2 Stability Analysis

Theorem 3.1. *The observer presented in Eqs. 3-2-3-7 is a globally exponentially stable observer provided Assumptions 2.2 and 3.1 are satisfied along with the sufficient condition*

$$k_3 \geq \frac{\frac{2\bar{v}_{cz}}{\lambda_m} + \delta\bar{v}_{cz} + \bar{y}_2\bar{\omega}_1 + \bar{y}_1\bar{\omega}_2}{\varepsilon} \quad (3-8)$$

where $\bar{v}_{cz}, \bar{\omega}_1$ and $\bar{\omega}_2$ are known upper bounds on $v_{cz}(t), \omega_1(t)$ and $\omega_2(t)$.

Proof. For three cases of projection law described by Eq. 3-2 the $e(t)$ error dynamics are given by

Case 1: $\underline{y}_3 \leq \hat{y}_3(t) \leq \bar{y}_3$ or $\hat{y}_3(t) > \bar{y}_3$ and $\phi(t) \leq 0$ or $\hat{y}_3(t) < \underline{y}_3$ and $\phi(t) \geq 0$

Using Eqs. 2-12 and 3-2-3-4, the error dynamics of $e(t)$ can be expressed as

$$\begin{aligned} \dot{e} &= \varsigma \triangleq (y_2\omega_1 - y_1\omega_2)e + (y_3 + \hat{y}_3)v_{cz}e \\ &\quad - k_3(h_1^2 + h_2^2)e. \end{aligned} \quad (3-9)$$

Case 2: $\hat{y}_3(t) > \bar{y}_3$ and $\phi(t) > 0$

Using Eqs. 2-12 and 3-2-3-4, the error dynamics of $e(t)$ can be expressed as

$$\dot{e} = \varsigma - \frac{\bar{y}_3 - \hat{y}_3}{\delta} \phi. \quad (3-10)$$

Case 3: $\hat{y}_3(t) < \underline{y}_3$ and $\phi(t) < 0$

Using Eqs. 2-12 and 3-2-3-4, the error dynamics of $e(t)$ can be expressed as

$$\dot{e} = \varsigma - \frac{\hat{y}_3 - \underline{y}_3}{\delta} \phi. \quad (3-11)$$

The stability of the proposed observer can be analyzed using Lyapunov-based stability analysis. Consider a domain $\mathcal{D} \subset \mathbb{R}$ containing $e(0)$ and a continuously differentiable, radially unbounded candidate Lyapunov function, $V(e) : \mathcal{D} \rightarrow \mathbb{R}$, defined as

$$V \triangleq \frac{1}{2} e^2. \quad (3-12)$$

The stability of the error system will be analyzed for all three cases of the projection law.

Case 1: Taking the derivative of $V(e)$ and utilizing Eq. 3-9 yields

$$\dot{V} = [(y_3 + \hat{y}_3) v_{cz} - y_2 \omega_1 + y_1 \omega_2 - k_3(h_1^2 + h_2^2)] e^2. \quad (3-13)$$

If k_3 satisfies the condition in Eq. 3-8, the bracketed term is strictly negative and the following expression is obtained

$$\dot{V} \leq -k_1 V \quad (3-14)$$

where $k_1 \in \mathbb{R}^+$.

Case 2: Taking the derivative of $V(e)$ and utilizing Eq. 3-10 yields

$$\begin{aligned} \dot{V} &= ((y_3 + \hat{y}_3) v_{cz} - y_2 \omega_1 + y_1 \omega_2) e^2 \\ &\quad - k_3(h_1^2 + h_2^2) e^2 - e \frac{\bar{y}_3 - \hat{y}_3}{\delta} \phi. \end{aligned} \quad (3-15)$$

where the last term on the right hand side of Eq. 3-15 is always negative, and hence, the inequality in Eq. 3-14 can be achieved.

Case 3: Taking the derivative of $V(e)$ and utilizing Eq. 3–11 yields

$$\begin{aligned}\dot{V} &= ((y_3 + \hat{y}_3) v_{cz} - y_2 \omega_1 + y_1 \omega_2) e^2 \\ &\quad - k_3 (h_1^2 + h_2^2) e^2 - e \frac{\hat{y}_3 - y_3}{\delta} \phi,\end{aligned}\tag{3–16}$$

where the last term on the right hand side of Eq. 3–16 is always negative, and hence, the inequality in Eq. 3–14 can be achieved.

For all three cases of projection the Gronwall-Bellman lemma [94] can be applied to Eq. 3–14 to yield

$$V(t) \leq V(0) \exp(-k_1 t).$$

Hence, from Eq. 6–17, the following upper bound for $e(t)$ can be obtained

$$\|e(t)\| \leq \gamma \|e(0)\| \exp(-k_1 t)\tag{3–17}$$

where $\gamma \in \mathbb{R}^+$.

From Eq. 3–17, $e(t) \in \mathcal{L}_\infty$.¹ Since $e(t) \in \mathcal{L}_\infty$, and using Remark 2.1, $y_3(t) \in \mathcal{L}_\infty$, thus $\hat{y}_3(t) \in \mathcal{L}_\infty$. From the boundedness of $y(t)$, $v_c(t)$ and $\omega(t)$, Eq. 3–8 can be used to prove that $k_3 \in \mathcal{L}_\infty$. Based on the fact that $e(t)$, $y(t)$, $\omega(t)$, $v_c(t)$, $k_3 \in \mathcal{L}_\infty$, standard linear analysis methods can be used to prove that $\dot{e}(t) \in \mathcal{L}_\infty$. Thus, $y_3(t)$ is exponentially estimated and Eqs. 2–2–2–5 can be used to recover the Euclidean coordinates $\bar{m}(t)$ of the feature point. \square

If the condition in Assumption 3.1 is not satisfied and the gain k_3 is chosen according to Eq. 3–8, the proposed observer is still exponentially convergent, provided the PE condition in [2] is satisfied.

¹ For a function $s(t) \in \mathbb{R}^n \forall n \in [1, \infty)$, $s(t) \in \mathcal{L}_\infty$ means the function $s(t)$ has a finite \mathcal{L}_∞ norm, i.e., $\|s(t)\|_{\mathcal{L}_\infty} = \sup_{t \geq 0} \|s(t)\|_2 < \infty$ where $\|\cdot\|_2$ denotes the 2-norm in \mathbb{R}^n .

Theorem 3.2. *The observer presented in Eqs.3-2-3-7 is a exponentially stable observer provided k_3 is chosen according to Eq. 3-8, Assumption 2.2 is satisfied, and the following PE condition is satisfied*

$$\int_t^{t+T} (h_1^2(\tau) + h_2^2(\tau)) d\tau \geq \rho > 0, \quad \forall t > t_0 \quad (3-18)$$

where $T, \rho \in \mathbb{R}^+$.

Proof. To examine the stability of the estimation error dynamics in Eq. 3-9 under the assumption that Eq. 3-18 is satisfied, consider the nominal system

$$\dot{e} = -k_3(h_1^2 + h_2^2)e. \quad (3-19)$$

Using Theorem 2.5.1 of [95] the error system in Eq. 3-19 is globally exponentially stable if the condition in Eq. 3-18 is satisfied. Since the nominal system in Eq. 3-19 is globally exponentially stable using 4.14 of [96] based on the Converse Lyapunov Theorem, there exists a function $\bar{V} : [0, \infty) \times \mathbb{R} \rightarrow \mathbb{R}$ that satisfies the inequalities

$$\begin{aligned} c_1 \|e\|^2 &\leq \bar{V}(t, e) \leq c_2 \|e\|^2, \\ \frac{\partial \bar{V}}{\partial t} + \frac{\partial \bar{V}}{\partial e} (-k_3(h_1^2 + h_2^2)e) &\leq -c_3 \|e\|^2, \\ \left\| \frac{\partial \bar{V}}{\partial e} \right\| &\leq c_4 \|e\| \end{aligned} \quad (3-20)$$

where $c_i \in \mathbb{R}^+, \forall i = \{1, \dots, 4\}$. After using Eq. 6-17 with the properties in Eq. 3-20 and substituting in the perturbed system Eq. 3-9, the following inequalities can be obtained

$$\begin{aligned} \dot{\bar{V}} &\leq \frac{\partial \bar{V}}{\partial t} + \frac{\partial \bar{V}}{\partial e} (-k_3(h_1^2 + h_2^2)e), \\ &\quad + \frac{\partial \bar{V}}{\partial e} (((y_3 + \hat{y}_3) v_{cz} - y_2 \omega_1 + y_1 \omega_2) e), \\ \dot{\bar{V}} &\leq -c_3 \|e\|^2 + c_4 \eta \|e\|^2, \end{aligned}$$

where $\eta = \frac{2\bar{v}_{cz}}{\lambda_m} + \delta \bar{v}_{cz} + \bar{y}_2 \bar{\omega}_1 + \bar{y}_1 \bar{\omega}_2$, and $\dot{\bar{V}}(t)$ can be upper bounded as

$$\dot{\bar{V}} \leq -(c_3 - \eta c_4) \|e\|^2.$$

Since k_3 is selected according to Eq. 3–8 with sufficiently small δ , c_3 satisfies $c_3 > \eta c_4$. Hence, the origin of the perturbed system Eq. 3–9 is exponentially stable. \square

Remark 3.1. As stated in [2], the PE condition physically implies that all the linear velocities should not be identically zero and that the camera should not be translating along the projected ray of any feature point during any small interval of time $[t, t + T]$. If all of the linear velocities are zero at any instant of time $h_1^2(t) + h_2^2(t) = 0$ and the stability of the observer in Eqs. 3–2–3–7 cannot be shown using Theorem 3.1, Theorem 3.2 ensures stability of system in such cases.

3.2 Stability Analysis in the Presence of Disturbances

In this section, the stability of the observer in Eqs. 3–2–3–7 is analyzed in the presence of an exogenous input such as a disturbance acting on the camera motion or a target object begins to move. The disturbance enters the system as

$$\dot{m} = \begin{bmatrix} 1 & 0 & 0 & 0 & -x_3 & x_2 \\ 0 & 1 & 0 & x_3 & 0 & -x_1 \\ 0 & 0 & 1 & -x_2 & x_1 & 0 \end{bmatrix} \begin{bmatrix} v_c + \Delta v_c \\ \omega + \Delta \omega \end{bmatrix}, \quad (3-21)$$

where $\Delta v_c(t)$, $\Delta \omega(t)$ represent the exogenous inputs such that $\Delta v_c(t)$, $\Delta \omega(t) \in \mathcal{L}_{pe}$ ² with $\sup_{0 \leq t \leq \tau} \|\Delta v_c(t)\| \leq r_b$ and $\sup_{0 \leq t \leq \tau} \|\Delta \omega(t)\| \leq r_\omega$ for some $r_b, r_\omega \in \mathbb{R}^+$. Using Eqs. 2–3 and 3–21, the dynamics of the unmeasurable state $y_3(t)$ can be expressed as

$$\dot{y}_3 = -y_3^2 v_{cz} - y_2 y_3 \omega_1 + y_1 y_3 \omega_2 + \Delta y_3 \quad (3-22)$$

where

$$\Delta y_3 = -y_3^2 \Delta v_{cz} - y_2 y_3 \Delta \omega_1 + y_1 y_3 \Delta \omega_2.$$

² The space $\mathcal{L}_{pe} = \{u | u_\tau \in \mathcal{L}_p, \forall \tau \in [0, \infty]\}$, and u_τ is a truncation of u defined by $u_\tau(t) = \begin{cases} u(t), & 0 \leq t \leq \tau \\ 0, & t > \tau \end{cases}$.

Theorem 3.3. *The observer presented in Eqs. 3-2-3-7 is finite-gain \mathcal{L}_p ³ stable where $p \in [1, \infty]$ with respect to the exogenous input $\begin{bmatrix} \Delta v_c^T & \Delta \omega^T \end{bmatrix}^T$ and \mathcal{L}_p gain less than or equal to $\frac{1}{k_1}$.*

Proof. Using Eqs. 3-22 and 3-2-3-7 the error system can be written as

$$\begin{aligned} \dot{e} &= (y_2\omega_1 - y_1\omega_2)e + (y_3 + \hat{y}_3)v_{cz}e \\ &\quad - k_3(h_1^2 + h_2^2)e + \Delta y_3 k_3. \end{aligned} \quad (3-23)$$

The error system in Eq. 3-23 can be expressed in the following form

$$\begin{aligned} \dot{e} &= f(e, u), \\ r &= h(e) \end{aligned}$$

where $u(t) = k_3\Delta y_3(t)$ is an exogenous disturbance/noise input, $r(t) = e(t)$. Let \mathbb{R} be a domain containing $e(t) = 0$ and $u(t) = 0$, the function $f : \mathbb{R} \times \mathbb{R} \rightarrow \mathbb{R}$ is linear and globally Lipschitz in $u(t)$, $h : \mathbb{R} \rightarrow \mathbb{R}$ is continuous in $e(t)$. Using Theorem 3.1, the unforced system

$$\dot{e} = f(e, 0)$$

is globally exponentially stable with the Lyapunov function in Eq. 6-17 which satisfies the following bounds

$$\begin{aligned} 0.5 \|e\|^2 &\leq V(e) \leq 0.5 \|e\|^2, \\ \frac{\partial V}{\partial t} + \frac{\partial V}{\partial e}(f(e, 0)) &\leq -k_1 \|e\|^2, \\ \left\| \frac{\partial V}{\partial e} \right\| &\leq \|e\|. \end{aligned} \quad (3-24)$$

³ A mapping $F : \mathcal{L}_e^m \rightarrow \mathcal{L}_e^n$ is finite-gain \mathcal{L} stable if there exist non-negative constants ϱ and χ such that $\|(Fu)\|_{\mathcal{L}} \leq \varrho \|u_\tau\|_{\mathcal{L}} + \chi$ for all $u \in \mathcal{L}_e^m$ and $\tau \in [0, \infty)$ where the extended space \mathcal{L}_e^m is defined as $\mathcal{L}_e^m = \{u \mid u_\tau \in \mathcal{L}^m, \forall \tau \in [0, \infty)\}$.

Since the function $f(e, u)$ is globally Lipschitz in $u(t)$, the following inequality is satisfied

$$\|f(e, u) - f(e, 0)\| \leq \|u\|. \quad (3-25)$$

Since Eqs. 3-24 and 3-25 are satisfied, using Theorem 5.1 of [96] the error system in Eq. 3-23 is finite gain \mathcal{L}_p stable where $p \in [1, \infty]$ with \mathcal{L}_p gain less than or equal to $\frac{1}{k_1}$ for each $e(0) \in \mathbb{R}$, i.e.,

$$\|e\|_{\mathcal{L}_p} \leq \frac{1}{k_1} \|u\|_{\mathcal{L}_p} + \|e_0\| \rho,$$

where

$$\rho = \begin{cases} 1, & \text{if } n = \infty \\ \left(\frac{1}{k_1 n}\right)^{1/n}, & \text{if } n \in [1, \infty) \end{cases}.$$

The velocities of the object denoted by b_O and ω_O can be assumed to be \mathcal{L}_{pe} disturbances acting on the system as shown in Eq. 3-21. Thus, Theorem 3.3 implies that even if the stationary object assumption is violated, the observer errors are bounded. The \mathcal{L}_p gain is the measure of accuracy of the estimates and gives an upper bound on the estimation errors. The \mathcal{L}_p gain can be reduced by increasing the gain k_3 which in turn reduces the constant k_1 (see Eqs. 6-19 and 3-14). □

3.3 Discussion

A comparison between the proposed observer with the I&I observer [1] and the observer in [2] is provided in Table 3-1 and the numbered list below.

1. The presented observer achieves *global* exponential estimation of the 3D Euclidean coordinates of feature points, which is a similar result achieved by the observer developed in [1]. The observer presented in [2] only achieves *local* exponential convergence of the estimation errors. Thus, the proposed observer and the observer in [1] can have arbitrary initial conditions as opposed to the initial conditions required by the observer presented in [2]. A limitation of the local nature of the result in [2] is illustrated in the subsequent simulations.

Table 3-1. Comparison of the presented observer with observers in [1] and [2].

Proposed observer	Observer via I&I [1]	Observer in [2]
Global exponential error convergence	Global exponential error convergence	Local exponential error convergence
Observability: $h_1^2(t) + h_2^2(t) \geq \varepsilon > 0,$ $\forall t \geq 0,$ stable if $\exists t : h_1^2(t) + h_2^2(t) = 0$	Observability: $h_1^2(t) + h_2^2(t) \geq \epsilon > 0,$ $\forall t \geq 0$ singular if $h_1^2(t) + h_2^2(t) = 0$ for any time t	Observability: $\nexists \bar{t} : \forall t > \bar{t},$ $h_1^2(t) + h_2^2(t) = 0$ stable if $\exists t : h_1^2(t) + h_2^2(t) = 0$
Requires camera velocities and linear accelerations	Requires camera velocities and linear accelerations	Requires only camera velocities
Reduced order	Reduced order	Full order

2. One of the advantages of the observer presented in [2] over the observer in [1], is the use of a less restrictive observability condition which enables the observer to be used for a larger set of camera motions. The observability condition of the proposed observer is the same as that in [1], but if the observability condition in [1] is not satisfied, the I&I observer becomes singular. The advantage of the proposed observer is that even if the observability condition in Assumption 3.1 is not satisfied, the observer is still locally exponentially stable and thus can encompass a larger set of camera motions. The limitations of the singularity issue with the observer in [1] is illustrated in the subsequent simulation section.

3. The proposed observer requires measurements of the camera linear acceleration along with camera velocities and image features, which are also required by the observer in [1]. Thus, the proposed observer and the observer in [1] are more sensitive to noisy input measurements compared to the observer in [2]. Improved steady-state performance is illustrated by the observer in [2] in the presence of noise in the subsequent simulation section.

4. The gain condition in [1] is a function of the image size, camera velocities and acceleration. On the contrary, the gain condition for the proposed observer is only a function of image size and camera velocities.

3.4 Simulations and Experiments

Simulations are conducted to evaluate the performance of the observer. The performance of the observer is compared with the observers in [2] and [1]. For each simulation the focal length of the camera is set to $\lambda_m = 30$ and the gains for the estimators are adjusted to achieve the best performance (i.e., the least estimation error). In contrast to the trial-and-error approach, methodological approaches such as [97–102] could be used to adjust the observer gains. For the first simulation, the initial location of the point on the target with respect to the initial camera frame is selected as $\bar{m}(t_0) = \begin{bmatrix} 10 & 5 & 0.5 \end{bmatrix}^T m$. The camera velocities are selected as

$$v_c = \begin{bmatrix} 0.3 & 0.4 + 0.1 \sin(\frac{\pi t}{4}) & -0.3 \end{bmatrix}^T \text{ m/s},$$

$$\omega = \begin{bmatrix} 0 & -\frac{\pi}{30} & 0 \end{bmatrix}^T \text{ rad/s}.$$

Additive white Gaussian noise with a signal-to-noise ratio (SNR) of 20dB is added to the image pixel measurements, and noise with zero mean and a variance of 0.01 is added to the velocity measurements. The velocity signal is differentiated using the “Derivative” block in Simulink to obtain a linear acceleration signal. The estimates are integrated with a step size of 0.01sec using the “ode4” Matlab command which uses a Runge-Kutta (R-K) integrator. The initial condition of the observer is set to $\alpha(t_0) = 5$ with $k_3 = 1.55 \times 10^{-3}$. For the observer in [1], the initial condition is chosen to be⁴ $\xi(t_0) = -0.9$ and the observer gain is set to 2.5×10^{-5} . The initial conditions and the observer gains for the observer in [2] are selected⁵ as $k_1 = k_2 = 200$, $k_3 = 0.1$ and $\hat{y}_1(t_0) = 600$, $\hat{y}_2(t_0) = 300$, $\hat{y}_3(t_0) = 50$. The initial conditions are selected so that the

⁴ The symbol $\xi(t)$ is taken from [1] and denotes an auxiliary state.

⁵ The symbols $k_1, k_2, k_3, \hat{y}_1(t), \hat{y}_2(t)$ are taken from [2]. The observer in [2] is a third order observer and $\hat{y}_1(t), \hat{y}_2(t)$ denotes the estimates of $y_1(t)$ and $y_2(t)$.

Table 3-2. Comparison of the RMS depth estimation errors.

	Proposed observer	Observer in [2]	Observer in [1]
Transient RMS error	0.3128	0.3477	0.3547
Steady-state RMS error	0.1717	0.0155	0.2150

initial value of the estimated depth is equal for all three observers. A comparison of the depth estimation performance of the observers is shown in Figure 3-1. As shown in Table 3-2, the root-mean square (RMS) of the depth estimation error is also compared for the transient and the steady-state response. The transient period is selected to be the first 0.2 sec. The proposed observer has the least transient RMS error, and the observer in [2] has the minimum steady-state RMS error.

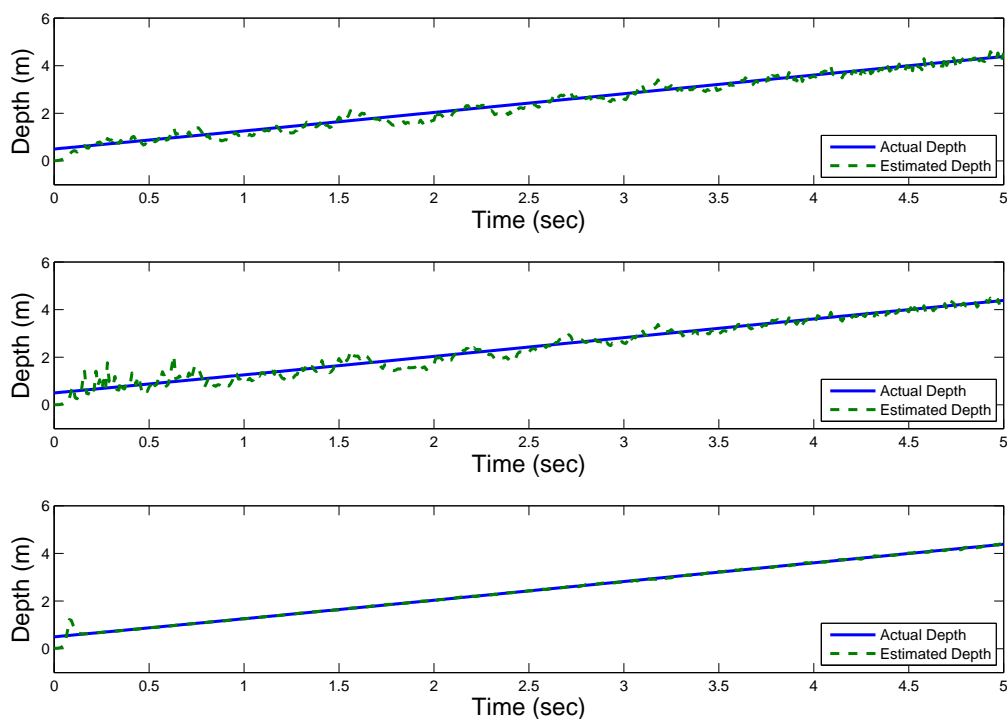


Figure 3-1. Comparison between the true and estimated depth in the presence of measurement noise A) top subplot shows the estimated depth using the proposed observer. B) middle subplot shows the estimated depth using the observer in [1]. C) bottom subplot shows the estimated depth using the observer in [2].

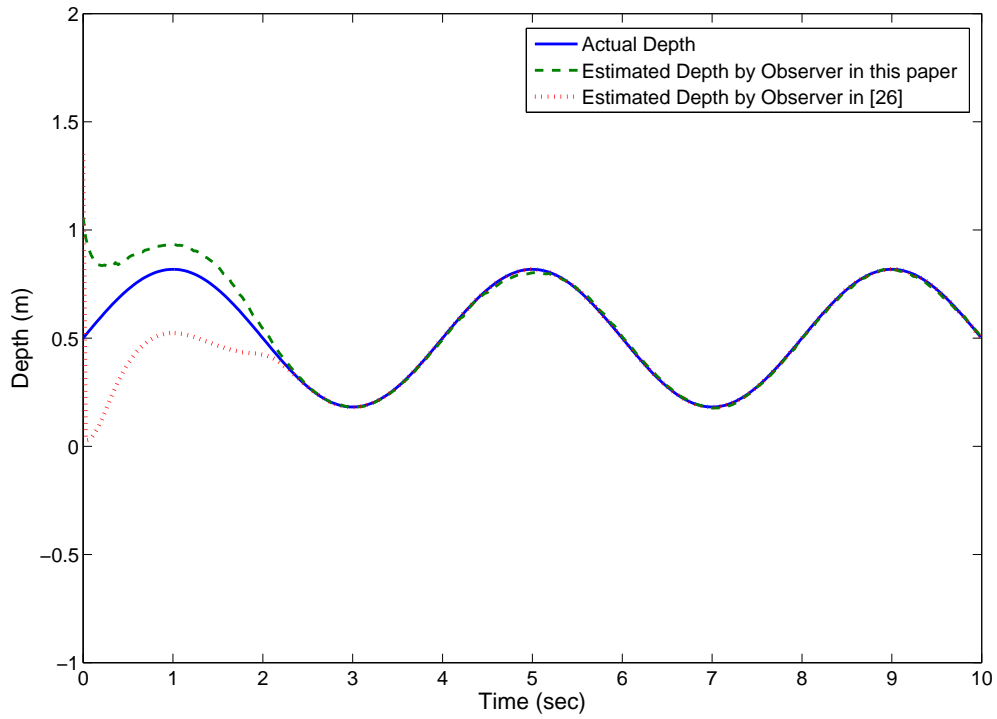


Figure 3-2. Comparison of the depth estimation using the proposed observer and the observer in [2] when camera motion does not satisfy Assumption 3.1.

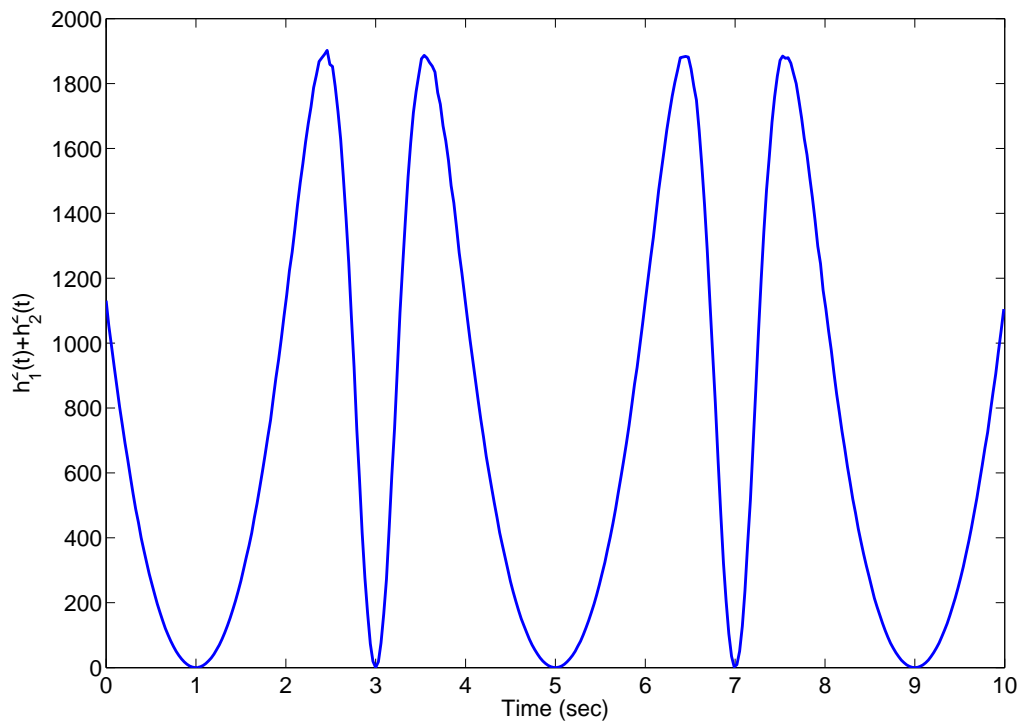


Figure 3-3. Evolution of the signal $h_1^2(t) + h_2^2(t)$ against time.

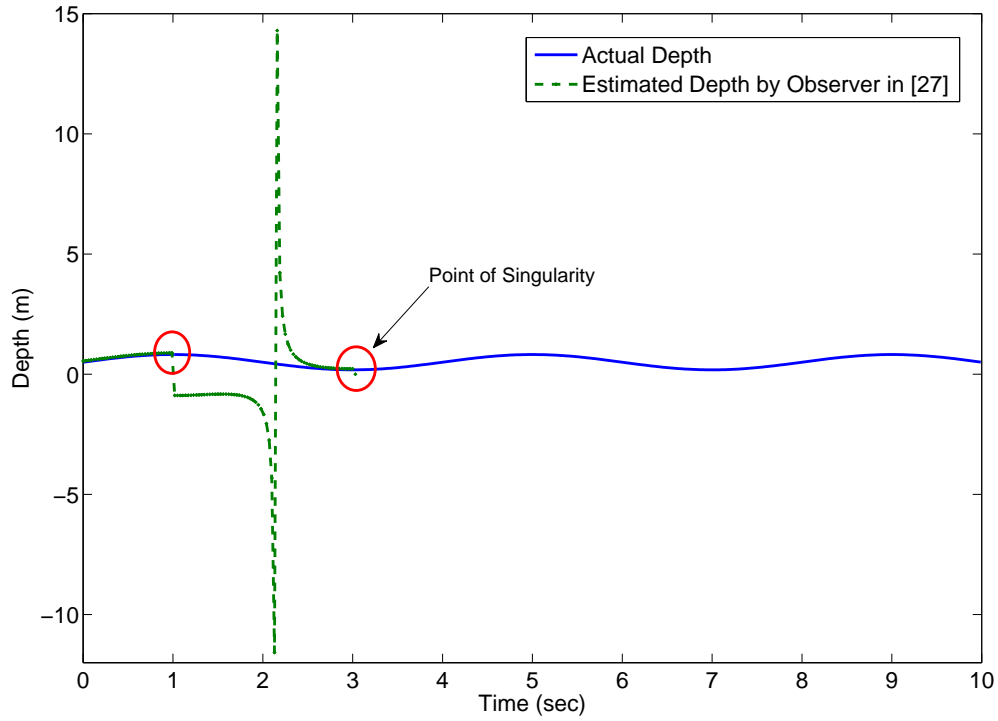


Figure 3-4. Depth estimation using the observer in [1].

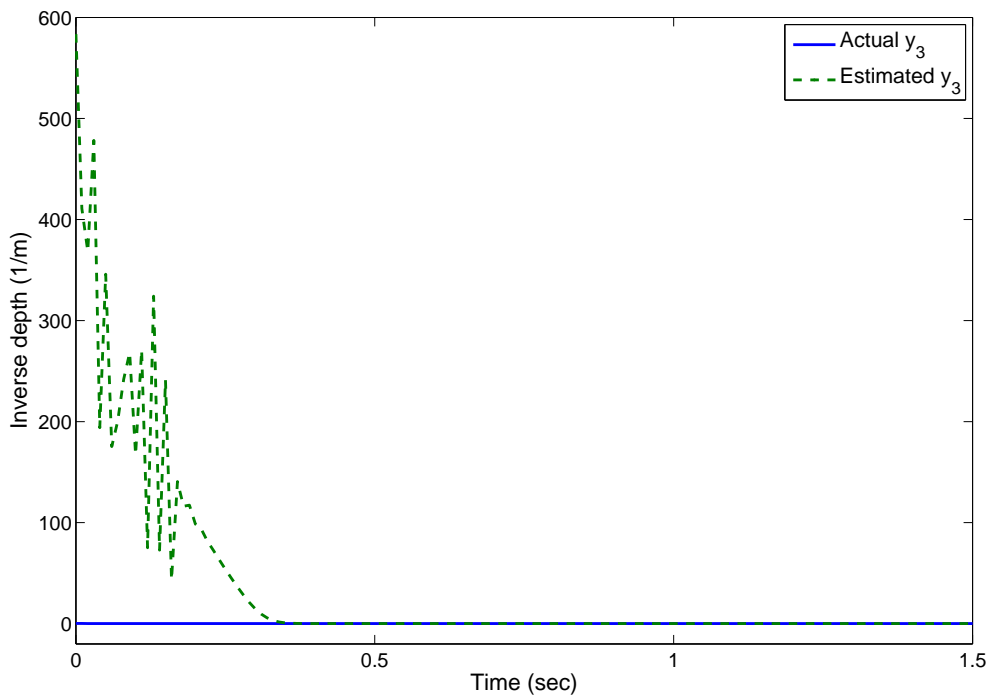


Figure 3-5. Estimation of $\hat{y}_3(t)$ starting from large initial condition $\alpha(t_0) = 300$ using the proposed observer.

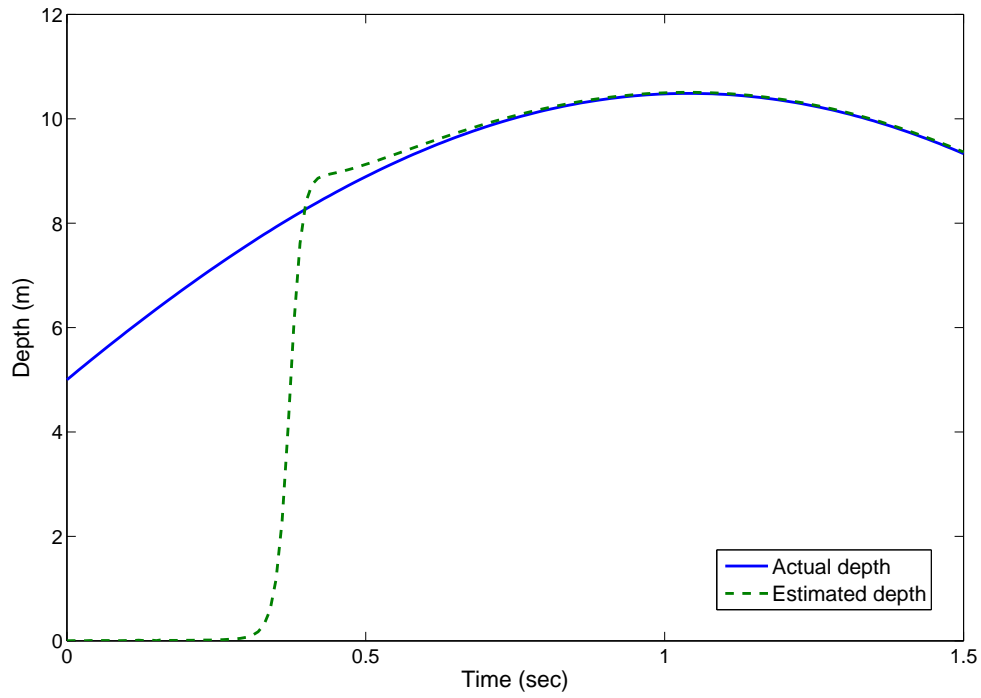


Figure 3-6. Depth estimation with large initial condition $\alpha(t_0) = 300$ using the proposed observer.

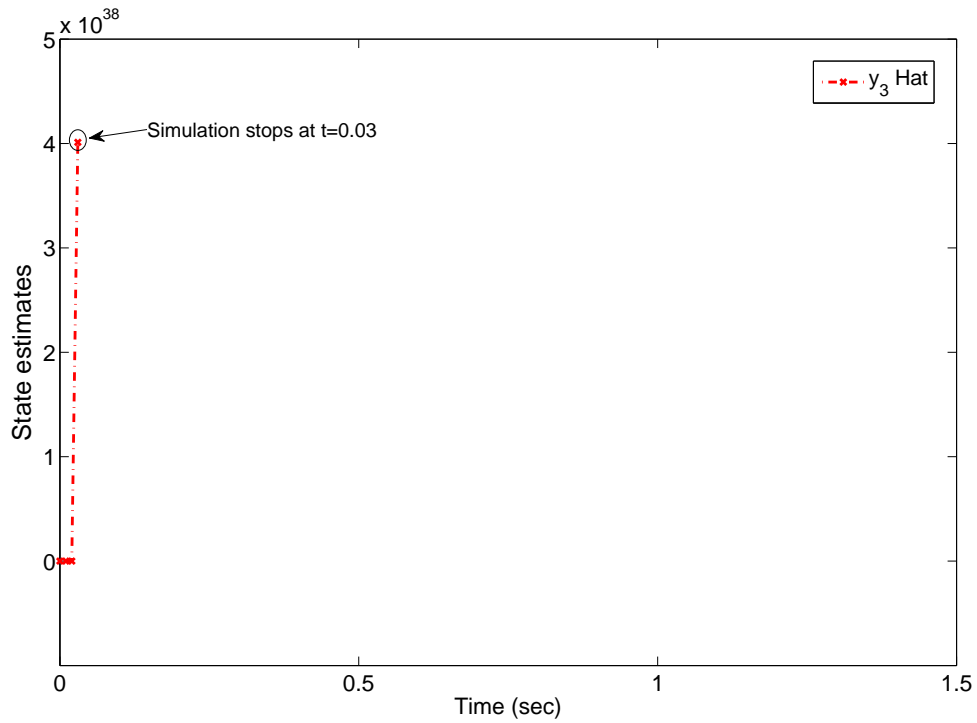


Figure 3-7. State estimation using the observer in [2] for large initial conditions. Since the state estimate is very large, simulation fails to integrate at $t = 0.03$.

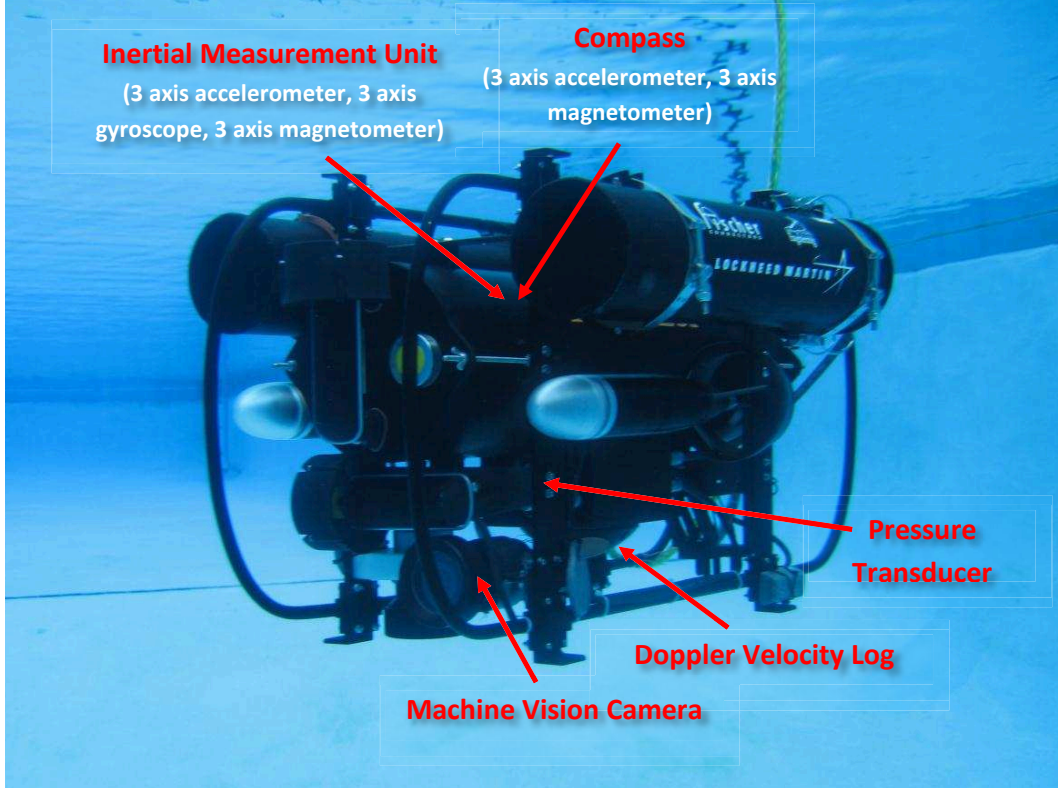


Figure 3-8. AUV experimental setup.

A second simulation is performed based on Discussion Point 2 of Section 3.3. The camera velocities for this simulation are selected as

$$v_c = \begin{bmatrix} 0 & 0 & 0.5 \cos(\pi t/2) \end{bmatrix}^T m/s,$$

$$\omega = \begin{bmatrix} 0 & 0 & 0 \end{bmatrix}^T rad/s$$

which violates the observability condition in Assumption 3.1 but satisfies the condition in Eq. 3-18. Again, the image pixel data is corrupted with the additive white Gaussian noise with an SNR of 20dB. Noise of zero mean and 0.01 variance is added to the camera velocity measurements. Using the Runge-Kutta integrator with a time step of 0.03sec, the state estimates are computed. Figure 3-2 shows the depth estimation performance of the proposed observer and the observer in [2] for the same initial conditions $\hat{y}_3(t_0)$. The proposed observer exhibits a better transient performance compared to the observer in [2].



Figure 3-9. An image frame displaying the tracked buoy target by the AUV.

Figure 3-3 shows the evolution of $h_1^2(t) + h_2^2(t)$. At $1sec$, $h_1^2(t) + h_2^2(t) = 0.1$ and at $3sec$, $h_1^2(t) + h_2^2(t) = 10e - 4$. In Figure 3-4, there is a peak in the depth estimate of [1] near $t = 1sec$. The response recovers from the peak at $t = 1sec$ but at $t = 3sec$ the observer in [1] becomes singular. The results in Figure 3-4 coincide with the theoretical prediction discussed in Point 2 of Section 3.3.

A third simulation is performed using camera velocities of

$$v_c = \begin{bmatrix} 0.3 & 0.4 + 0.1 \sin(\frac{\pi t}{4}) & -1 \end{bmatrix}^T m/s,$$

$$\omega = \begin{bmatrix} 0 & \frac{\pi}{3} & 0 \end{bmatrix}^T rad/s.$$

to demonstrate that for large initial conditions the proposed observer converges while the local observer in [2] is unstable. In [2], the domain of initial conditions is small for large $v_{cz}(t)$, $\omega_1(t)$ and $\omega_2(t)$. The initial relative position of the target point is

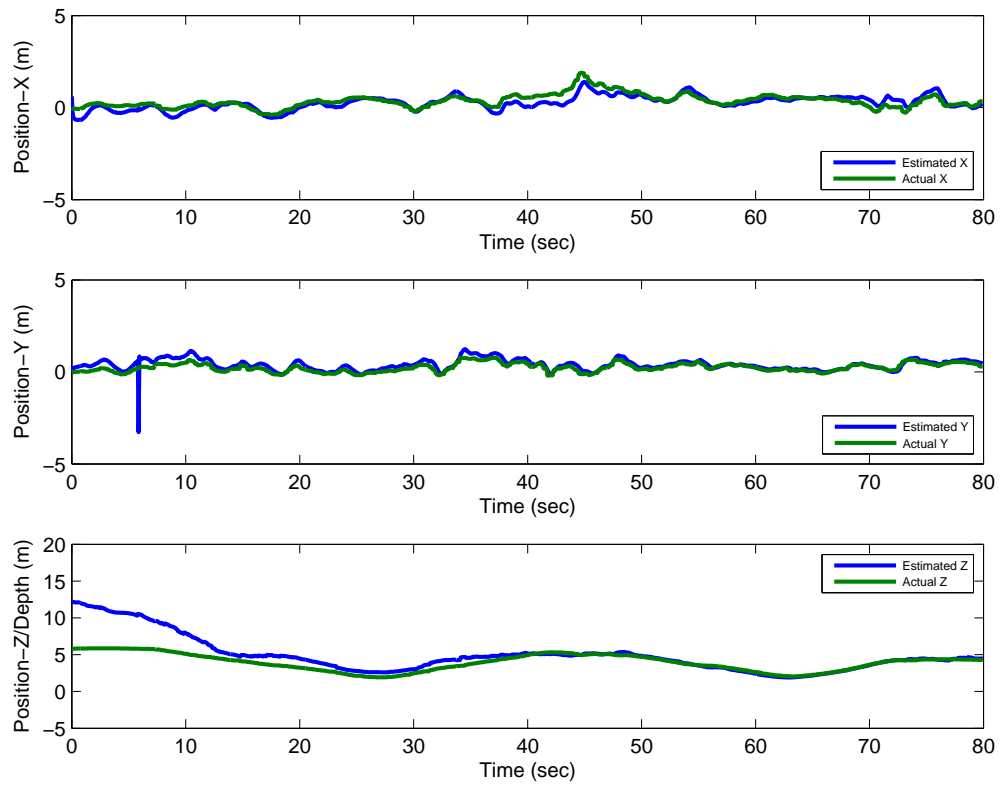


Figure 3-10. Comparison of the estimated and ground truth range of the buoy with respect to the underwater vehicle.

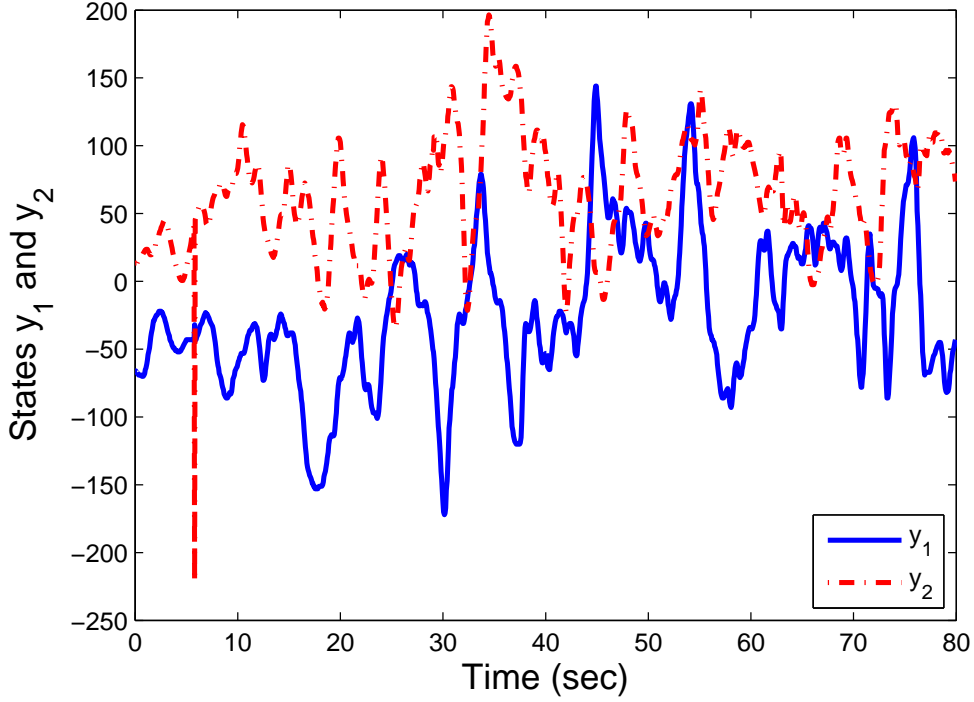


Figure 3-11. States $y_1(t)$ and $y_2(t)$ computed using image pixels.

$\bar{m}(t_0) = \begin{bmatrix} 10 & 5 & 5 \end{bmatrix}^T m$. The proposed observer is initialized to $\alpha(t_0) = 300$ and the gain is selected as $k_3 = 0.09$. For the observer in [2], the initial conditions and gains are set to $\hat{y}_1(t_0) = 60$, $\hat{y}_2(t_0) = 30$, $\hat{y}_3(t_0) = 144$ and $k_1 = k_2 = 12$, $k_3 = 10.2$. The observers are integrated using the Runge-Kutta integrator with a time step of 0.01sec . The state estimation results are shown in Figures 3-5-3-7. Since the states $y_1(t)$ and $y_2(t)$ are measurable, the initial conditions of $\hat{y}_1(t)$ and $\hat{y}_2(t)$ are set equal to the initial values of $y_1(t)$ and $y_2(t)$. The gains of the observer in [2] are tuned and the initial condition is progressively increased until the observer error converges. Convergence is observed for $\hat{y}_3(t_0) \leq 143$ but not for $\hat{y}_3(t_0) \geq 144$. For the proposed observer, the observer error converges even for an initial condition as large as $\alpha(t_0) = 300$. In this simulation a value of $\alpha(t_0) = 300$ corresponds to $\hat{y}_3(t_0) = 583.5$ for the proposed observer. The simulation demonstrates that the observer in [2] is unstable when the initial conditions are chosen outside a local domain.

Experiments are conducted to estimate the range of a 9-inch Mooring buoy floating in the middle of a water column as observed by a camera rigidly attached to an autonomous underwater vehicle (AUV). Figure 3-8 shows the AUV experimental platform. The AUV is equipped with a Matrix Vision mvBlueFox-120a color USB camera, a Doppler velocity log (DVL), a pressure transducer, a compass and an inertial measurement unit (IMU). Two computers running Microsoft Windows Server 2008 are used on the AUV. One computer is dedicated for running image processing algorithms and the other computer executes sensor data fusion, low level component communication and control, and mission planning. An unscented Kalman filter (UKF) is used to fuse the IMU, DVL and pressure transducer data at $100Hz$ to accurately estimate the position, orientation and velocity of the AUV with respect to an inertial frame by correcting the IMU bias. This position data is used to compare the results of the observer with a relative ground truth measurement of the AUV by rotating the localized AUV position into the camera fixed frame. The buoy is tracked in the video image of dimension 640×480 using a standard feature tracking algorithm as shown in Figure 3-9, and pixel data of the centroid of the buoy is recorded at $15Hz$. The camera is calibrated using a standard camera calibration algorithm [103] and is given by

$$A_c = \begin{bmatrix} 749.82231 & 0 & 321.05569 \\ 0 & 750.19507 & 292.41939 \\ 0 & 0 & 1 \end{bmatrix}.$$

The linear and angular velocity, and linear acceleration data obtained from the UKF is logged at the camera frame rate. Using the velocity, linear acceleration and pixel data obtained from the AUV sensors, the range of the buoy is estimated with respect to the camera. The initial condition is chosen as $\alpha(t_0) = 0.08$ and the observer gain is selected to be $k_3 = 2 \times 10e - 6$. The observer equations are integrated using a Runge-Kutta integrator with a time step of $\frac{1}{15}sec$. A comparison of the estimated range with the ground truth measurement is shown in Figure 3-10. In Figure 3-11, the feature tracking algorithm

fails for several frames near time $t = 6 \text{ sec}$. The range estimation algorithm shows robust performance even in the presence of feature tracking errors as illustrated in Figure 3-10.

3.5 Summary

A nonlinear observer is presented for the range estimation of feature points using a moving camera. The observer is globally exponentially stable provided an observability condition is satisfied. The observer is also shown to be exponentially stable under a relaxed observability condition. The observer requires velocity and linear acceleration measurements of the camera. The observer is shown to be robust against external disturbances acting on the camera motion and pixel noise. Simulation results and data from an AUV experiment demonstrate the performance of the observer.

Chapter 4
STRUCTURE AND MOTION USING A SINGLE KNOWN CAMERA LINEAR
VELOCITY

In this chapter, a solution to the SaM estimation is presented when only one of the linear camera velocities of the camera can be measured. The angular velocity of the camera is estimated by decomposing the homography estimated from two images. A robust derivative estimator is used for the angular velocity estimation. In the state dynamics, the unknown time-varying linear velocities is multiplied by an unknown state poses a problem of multiplicative time-varying uncertainties. In this work a strategy is presented to segregate the multiplicative uncertainties, and then to develop a reduced order nonlinear observer to address the SaM problem where the structure (i.e., the properly scaled relative Euclidean coordinates of tracked feature points), the time-varying angular velocities, and two unknown time-varying linear velocities are estimated. The result exploits an uncertain locally Lipschitz model of the unknown linear velocities of the camera. A persistency of excitation (PE) condition is formulated, which provides an observability condition that can be physically interpreted as the known camera linear velocity should not be zero over any small interval of time, and the camera should not be moving along the projected ray of a point being tracked. A Lyapunov-based analysis is provided that indicates the SaM observer errors are globally asymptotically regulated provided the PE condition is satisfied. By developing a reduced order observer to segregate and estimate the multiplicative uncertainties, new applications can be addressed including: range and velocity estimation using a camera fixed to a moving vehicle where only the forward velocity/acceleration of the vehicle is known, range and velocity estimation using an unmanned air vehicle (UAV) using only a forward velocity/acceleration sensors, etc.

4.1 Structure and Motion Estimation

4.1.1 Estimation with a Known Linear Velocity

In this section, an estimator is designed for the perspective dynamic system in Eq. 2–12, where the angular velocity is considered unknown and only one of the linear velocities (i.e., v_{cz})¹ and respective acceleration (i.e., \dot{v}_{cz}) is available. Moreover, an uncertain dynamic model of the linear velocity $v_c(t)$ is assumed to be available as [3, 21]

$$\dot{v}_{ci}(t) = q(v_{ci}, t)v_{ci}, \forall i = \{x, y\} \quad (4-1)$$

where $q(v_{ci}, t) \in \mathbb{R}$ is a known locally Lipschitz function of unknown states.

To facilitate the design and analysis of the subsequent observer, a new state $u(t) \in \mathcal{U} \subset \mathbb{R}^2 \triangleq \begin{bmatrix} u_1(t) = y_3 v_{cx}, u_2(t) = y_3 v_{cy} \end{bmatrix}^T$, is defined where \mathcal{U} is a closed and bounded set. After utilizing Eqs. 2–12 and 4–1, the dynamics for $u_1(t)$, $u_2(t)$ can be expressed as

$$\dot{u}_i = y_3 v_{cz} u_i + (y_2 \omega_1 - y_1 \omega_2) u_i + q(v_{ci}) u_i, \forall i = \{1, 2\}. \quad (4-2)$$

From Eqs. 2–12 and 4–2 the dynamics of the known states $y_1(t)$, $y_2(t)$ and the unknown state $\theta(t) = \begin{bmatrix} y_3 & u_1 & u_2 \end{bmatrix}^T$ are

$$\begin{bmatrix} \dot{y}_1 \\ \dot{y}_2 \end{bmatrix} = \begin{bmatrix} -y_1 v_{cz} & 1 & 0 \\ -y_2 v_{cz} & 0 & 1 \end{bmatrix} \begin{bmatrix} y_3 \\ u_1 \\ u_2 \end{bmatrix} + \begin{bmatrix} -y_1 y_2 \omega_1 + (1 + y_1^2) \omega_2 - y_2 \omega_3 \\ -(1 + y_2^2) \omega_1 + y_1 y_2 \omega_2 + y_1 \omega_3 \end{bmatrix} \quad (4-3)$$

and

$$\begin{bmatrix} \dot{y}_3 \\ \dot{u}_1 \\ \dot{u}_2 \end{bmatrix} = g(\theta, \omega, y_1, y_2, v_{cz}) = \begin{bmatrix} y_3^2 v_{cz} + (y_2 \omega_1 - y_1 \omega_2) y_3 \\ y_3 v_{cz} u_1 + (y_2 \omega_1 - y_1 \omega_2) u_1 + q(b_1) u_1 \\ y_3 v_{cz} u_2 + (y_2 \omega_1 - y_1 \omega_2) u_2 + q(b_2) u_2 \end{bmatrix}. \quad (4-4)$$

¹ An observer can be developed with any of the three linear velocities known. In this chapter, $v_{cz}(t)$ is assumed to be known w.l.o.g.

Let

$$J(y, v_{cz}) = \begin{bmatrix} -y_1 v_{cz} & 1 & 0 \\ -y_2 v_{cz} & 0 & 1 \end{bmatrix},$$

and

$$\Psi(y, \omega) = \begin{bmatrix} -y_1 y_2 \omega_1 + (1 + y_1^2) \omega_2 - y_2 \omega_3 \\ -(1 + y_2^2) \omega_1 + y_1 y_2 \omega_2 + y_1 \omega_3 \end{bmatrix}.$$

Since $y_1(t)$ and $y_2(t)$ are measurable, from Eqs. 2–2 and 2–5 the Euclidean structure $\bar{m}(t)$ can be estimated once the state $y_3(t)$ is determined. Since the dynamics of the outputs $y_1(t)$, $y_2(t)$ are affine in the unknown state $\theta(t)$, a reduced order observer can be developed based on this relationship for the unknown state $\theta(t)$. The subsequent development is based on the strategy of constructing the estimates $\hat{\theta}(t) \triangleq \begin{bmatrix} \hat{y}_3 & \hat{u}_1 & \hat{u}_2 \end{bmatrix}^T \in \mathbb{R}^3$. To quantify the SaM estimation objective, an estimation error $\tilde{\theta}(t) = \begin{bmatrix} \tilde{\theta}_1 & \tilde{\theta}_2 & \tilde{\theta}_3 \end{bmatrix}^T \in \mathbb{R}^3$ is defined as

$$\tilde{\theta}(t) \triangleq \begin{bmatrix} y_3 - \hat{y}_3 & u_1 - \hat{u}_1 & u_2 - \hat{u}_2 \end{bmatrix}^T. \quad (4-5)$$

Assumption 4.1. *The function $q(v_{ci}, t) \forall i = \{x, y\}$ is locally Lipschitz where $q(v_{cx}) - q(\hat{v}_{cx}) = \lambda_1(v_{cx} - \hat{v}_{cx})$ and $q(v_{cy}) - q(\hat{v}_{cy}) = \lambda_2(v_{cy} - \hat{v}_{cy})$ where λ_1 and λ_2 are Lipschitz constants.*

Remark 4.1. The linear velocity model in Eq. 4–1 (and in the results in [3, 21]) is restricted to motions that are satisfied by Assumption 4.1; yet, various classes of trajectories satisfy this assumption (e.g., straight line trajectories, circles, some periodic trajectories, etc.).

Assumption 4.2. *The function $J(y_1, y_2, v_{cz})$ defined in Eq. 4–3 satisfies the persistency of excitation condition, i.e., $\exists \gamma, \delta > 0 : \int_t^{t+\delta} J^T(y_1(\tau), y_2(\tau), v_{cz}(\tau)) J(y_1(\tau), y_2(\tau), v_{cz}(\tau)) d\tau \geq \gamma I \quad \forall t \geq 0$.*

Remark 4.2. Assumption 4.2 is violated iff $\exists t_1 | \forall t > t_1, v_{cz}(t) = 0$ or $y_1(t) = c_1, y_2(t) = c_2$. That is, Assumption 4.2 is valid unless there exists a time t_1 such that for all $t > t_1$ the camera translates along the projected ray of an observed feature point.

Assumption 4.3. *The linear camera velocities $v_c(t)$ are upper and lower bounded by constants.*

Remark 4.3. The following bounds can be developed using Assumption 2.1, Remark 2.1 and the definitions of $u_1(t)$ and $u_2(t)$

$$u_{1 \min} \leq u_1 \leq u_{1 \max}, \quad u_{2 \min} \leq u_2 \leq u_{2 \max}.$$

4.1.1.1 Step I: Angular velocity estimation

Solutions are available in literature that can be used to determine the relative angular velocity between the camera and a target [16]. To quantify the rotation mismatch between \mathcal{F}_c^* and \mathcal{F}_c , a rotation error vector $e_\omega(t) \in \mathbb{R}^3$ is defined by the angle-axis representation as

$$e_\omega \triangleq u_\omega(t)\theta_\omega(t) \tag{4-6}$$

where $u_\omega(t) \in \mathbb{R}^3$ represents a unit rotation axis, and $\theta_\omega(t) \in \mathbb{R}$ denotes the rotation angle about $u_\omega(t)$ that is assumed to be confined to region $-\pi < \theta_\omega(t) < \pi$. The angle $\theta_\omega(t)$ and axis $u_\omega(t)$ can be computed using the rotation matrix $\bar{R}(t)$ obtained by decomposing the Homography matrix $H(t)$ given by the relation in Eq. 2-4. Taking time derivative of Eq. 4-6 yields

$$\dot{e}_\omega = L_\omega \omega \tag{4-7}$$

where $L_\omega(t) \in R^{3 \times 3}$ denotes an invertible Jacobian matrix [16]. A robust integral of the sign of the error (RISE)-based observer $\hat{e}_\omega(t) \in \mathbb{R}^3$ is generated in [16] as

$$\begin{aligned} \dot{\hat{e}}_\omega &= (K_\omega + I_{3 \times 3})\tilde{e}_\omega(t) + \int_{t_0}^t (K_\omega + I_{3 \times 3})\tilde{e}_\omega d\tau + v \\ \dot{v} &= \rho_\omega \text{sgn}(\tilde{e}_\omega) \end{aligned} \tag{4-8}$$

where $K_\omega, \rho_\omega \in \mathbb{R}^{3 \times 3}$ are positive constant diagonal gain matrices, and $\tilde{e}_\omega(t) \in \mathbb{R}^3$ quantifies the observer error as $\tilde{e}_\omega(t) \triangleq e_\omega - \hat{e}_\omega$. A Lyapunov-based stability analysis is

provided in [16] that proves

$$\dot{\hat{e}}_\omega(t) - \dot{e}_\omega(t) \rightarrow 0 \quad \text{as} \quad t \rightarrow \infty \quad (4-9)$$

and that all closed-loop signals are bounded. Based on Eqs. 4-7 and 4-9, the angular velocity can be determined as

$$\hat{\omega}(t) = L_\omega^{-1} \dot{\hat{e}}_\omega(t) \quad \text{as} \quad t \rightarrow \infty. \quad (4-10)$$

An angular velocity estimation error $\tilde{\omega}(t) \in \mathbb{R}^3 \triangleq \begin{bmatrix} \tilde{\omega}_1(t) & \tilde{\omega}_2(t) & \tilde{\omega}_3(t) \end{bmatrix}^T$ is defined as $\tilde{\omega}_i(t) = \omega_i(t) - \hat{\omega}_i(t)$, $\forall i = \{1, 2, 3\}$. As shown in [16], the angular velocity estimator given by Eq. 4-8 is asymptotically stable; thus, the angular velocity estimation error $\|\tilde{\omega}(t)\| \rightarrow 0$ as $t \rightarrow \infty$.

4.1.1.2 Step II: Structure estimation

A reduced order observer for $\theta(t)$ is designed as

$$\begin{bmatrix} \hat{y}_3 \\ \hat{u}_1 \\ \hat{u}_2 \end{bmatrix} = \begin{bmatrix} \bar{y}_3 \\ \bar{u}_1 \\ \bar{u}_2 \end{bmatrix} + \Gamma \begin{bmatrix} -\frac{v_{cz}(y_1^2 + y_2^2)}{2} \\ y_1 \\ y_2 \end{bmatrix} \quad (4-11)$$

where the state vector $\begin{bmatrix} \bar{y}_3 & \bar{u}_1 & \bar{u}_2 \end{bmatrix}^T$ is updated using the following update law

$$\begin{aligned} \begin{bmatrix} \dot{\bar{y}}_3 \\ \dot{\bar{u}}_1 \\ \dot{\bar{u}}_2 \end{bmatrix} &= \underbrace{\begin{bmatrix} \hat{y}_3^2 v_{cz} + (y_2 \hat{\omega}_1 - y_1 \hat{\omega}_2) \hat{y}_3 \\ \hat{y}_3 v_{cz} \hat{u}_1 + (y_2 \hat{\omega}_1 - y_1 \hat{\omega}_2) \hat{u}_1 + q(\hat{v}_{cx}) \hat{u}_1 \\ \hat{y}_3 v_{cz} \hat{u}_2 + (y_2 \hat{\omega}_1 - y_1 \hat{\omega}_2) \hat{u}_2 + q(\hat{v}_{cy}) \hat{u}_2 \end{bmatrix}}_{g(\hat{\theta}, \hat{\omega}, y_1, y_2, b_3)} - \Gamma J^T \begin{bmatrix} -y_1 v_{cz} & 1 & 0 \\ -y_2 v_{cz} & 0 & 1 \end{bmatrix} \begin{bmatrix} \hat{y}_3 \\ \hat{u}_1 \\ \hat{u}_2 \end{bmatrix} \\ &+ \underbrace{\begin{bmatrix} -y_1 y_2 \hat{\omega}_1 + (1 + y_1^2) \hat{\omega}_2 - y_2 \hat{\omega}_3 \\ -(1 + y_2^2) \hat{\omega}_1 + y_1 y_2 \hat{\omega}_2 + y_1 \hat{\omega}_3 \end{bmatrix}}_{\Psi(y, \hat{\omega})} + \Gamma \begin{bmatrix} \frac{\dot{v}_{cz}(y_1^2 + y_2^2)}{2} \\ 0 \\ 0 \end{bmatrix}. \end{aligned} \quad (4-12)$$

In Eq. 4–12, $\Gamma \in \mathbb{R}^{3 \times 3}$, $\hat{\omega}_i(t)$ are given by Eq. 4–10, and $J(y, v_{cz})$ is defined in Eq. 4–3. Differentiating Eq. 4–5 and using Eqs. 4–3, 4–4, 4–11 and 4–12 yields the following closed-loop observer error dynamics

$$\begin{aligned} \begin{bmatrix} \dot{\tilde{\theta}}_1 \\ \dot{\tilde{\theta}}_2 \\ \dot{\tilde{\theta}}_3 \end{bmatrix} &= \begin{bmatrix} (y_3 + \hat{y}_3)v_{cz}\tilde{\theta}_1 + (y_2\omega_1 - y_1\omega_2)\tilde{\theta}_1 \\ y_3v_{cz}\tilde{\theta}_2 + v_{cz}\hat{u}_1\tilde{\theta}_1 + (y_2\hat{\omega}_1 - y_1\hat{\omega}_2)\tilde{\theta}_2 + q(v_{cx})\tilde{\theta}_2 \\ y_3v_{cz}\tilde{\theta}_3 + v_{cz}\hat{u}_2\tilde{\theta}_1 + (y_2\hat{\omega}_1 - y_1\hat{\omega}_2)\tilde{\theta}_3 + q(v_{cy})\tilde{\theta}_3 \\ + (y_2\tilde{\omega}_1 - y_1\tilde{\omega}_2)\hat{y}_3 \\ + (y_2\tilde{\omega}_1 - y_1\tilde{\omega}_2)\hat{u}_1 + \lambda_1(v_{cx} - \hat{v}_{cx})\hat{u}_1 \\ + (y_2\tilde{\omega}_1 - y_1\tilde{\omega}_2)\hat{u}_2 + \lambda_2(v_{cy} - \hat{v}_{cy})\hat{u}_2 \end{bmatrix} \\ &+ \Gamma J^T \left(\begin{bmatrix} -y_1b_3 & 1 & 0 \\ -y_2b_3 & 0 & 1 \end{bmatrix} \begin{bmatrix} \hat{y}_3 \\ \hat{u}_1 \\ \hat{u}_2 \end{bmatrix} - \begin{bmatrix} \dot{y}_1 \\ \dot{y}_2 \end{bmatrix} \right) \\ &+ \begin{bmatrix} -y_1y_2\hat{\omega}_1 + (1 + y_1^2)\hat{\omega}_2 - y_2\hat{\omega}_3 \\ -(1 + y_2^2)\hat{\omega}_1 + y_1y_2\hat{\omega}_2 + y_1\hat{\omega}_3 \end{bmatrix} \end{aligned}$$

Using the output dynamics from Eq. 4–3, the error dynamics can be rewritten as

$$\dot{\tilde{\theta}} = g(\theta, \omega, y_1, y_2, v_{cz}) - g(\hat{\theta}, \hat{\omega}, y_1, y_2, v_{cz}) - \Gamma J^T \left(J\tilde{\theta} + \Psi(y, \tilde{\omega}) \right). \quad (4-13)$$

Using Assumption 4.2, and locally Lipschitz property of $g(\cdot)$, following relationship can be developed

$$\left\| g(\theta, \omega, y_1, y_2, v_{cz}) - g(\hat{\theta}, \hat{\omega}, y_1, y_2, v_{cz}) \right\| \leq \rho \left(\left\| \tilde{\theta} \right\| + \left\| \tilde{\omega} \right\| \right) \quad (4-14)$$

where $\rho \in \mathbb{R}^+$. The results from the angular velocity estimator in Section 4.1.1.1 prove that $\tilde{\omega}_1, \tilde{\omega}_2, \tilde{\omega}_3 \rightarrow 0$ therefore, $\Psi(\cdot) \rightarrow 0$ as $t \rightarrow \infty$.

4.1.2 Stability Analysis

Theorem 4.1. *If Assumptions 4.1–4.3 are satisfied, the reduced order observer in Eqs. 4–11 and 4–12 asymptotically estimates $\theta(t)$ in the sense that $\left\| \tilde{\theta}(t) \right\| \rightarrow 0$ as $t \rightarrow \infty$.*

Proof. The stability of the error system in Eq. 4-13 can be proved using a converse Lyapunov theorem [96]. Consider the nominal system

$$\dot{\tilde{\theta}} = f(\tilde{\theta}) = -\Gamma J^T J \tilde{\theta}. \quad (4-15)$$

Using Theorem 2.5.1 of [95] the error system in Eq. 4-15 is globally exponentially stable if Assumption 4.2 is satisfied. Hence, $\tilde{\theta}(t)$ satisfies the inequality $\|\tilde{\theta}(t)\| \leq \|\tilde{\theta}(t_0)\| \alpha_1 e^{-\alpha_2(t-t_0)}$, where $\alpha_1, \alpha_2 \in \mathbb{R}^+$, and α_2 is directly proportional to Γ and inversely proportional to δ [3, 95]. Consider a set $\mathcal{D} = \{\tilde{\theta}(t) \in \mathbb{R}^3 \mid \|\tilde{\theta}(t)\| < \infty\}$. Using a converse Lyapunov theorem there exists a function $V : [0, \infty) \times \mathcal{D} \rightarrow \mathbb{R}$ that satisfies

$$\begin{aligned} c_1 \|\tilde{\theta}(t)\|^2 &\leq V(t, \tilde{\theta}) \leq c_2 \|\tilde{\theta}(t)\|^2, \\ \frac{\partial V}{\partial t} + \frac{\partial V}{\partial \tilde{\theta}}(-\Gamma J^T J \tilde{\theta}) &\leq -c_3 \|\tilde{\theta}(t)\|^2, \\ \left\| \frac{\partial V}{\partial \tilde{\theta}} \right\| &\leq c_4 \|\tilde{\theta}(t)\| \end{aligned} \quad (4-16)$$

for some positive constants c_1, c_2, c_3, c_4 . Using $V(t, \tilde{\theta})$ as a Lyapunov function candidate for the perturbed system in Eq. 4-13, the derivative of $V(t, \tilde{\theta})$ along the trajectories of Eq. 4-13 is given by

$$\begin{aligned} \dot{V}(t, \tilde{\theta}) &= \frac{\partial V}{\partial t} + \frac{\partial V}{\partial \tilde{\theta}}(-\Gamma J^T J \tilde{\theta}) + \frac{\partial V}{\partial \tilde{\theta}}(g(\theta, \omega, y_1, y_2, v_{cz}) - g(\hat{\theta}, \hat{\omega}, y_1, y_2, v_{cz})) \\ &\quad + \frac{\partial V}{\partial \tilde{\theta}}(-\Gamma J^T \Psi(y, \tilde{\omega})). \end{aligned}$$

Using the bounds in Eq. 4-16 the following inequality is developed

$$\dot{V}(t, \tilde{\theta}) \leq -(c_3 - c_4 \rho) \|\tilde{\theta}\|^2 + c_4 d \|\tilde{\theta}\| \quad (4-17)$$

where ρ is introduced in Eq. 4-14 and $d(t) = \|\Gamma\| \|J^T\| \|\Psi(y, \tilde{\omega})\| + \rho c_4 \|\tilde{\omega}\|$ where $d(t) \rightarrow 0$ as $t \rightarrow \infty$. Using Theorem 4.14 of [96] the estimates of c_3 and c_4 are given by²

$$c_3 = \frac{1}{2}, \quad c_4 = \frac{2\alpha_1}{(\alpha_2 - L)} \left[1 - e^{-\frac{(\alpha_2 - L) \ln(2\alpha_1^2)}{2\alpha_2}} \right]$$

where $L \in \mathbb{R}^+$ is an upper bound on the norm of Jacobian matrix $\frac{\partial f(\tilde{\theta})}{\partial \tilde{\theta}}$, where $f(\tilde{\theta})$

is defined in Eq. 4-15. Since α_2 is directly proportional to the gain Γ , the inequality $c_3 - c_4\rho = \frac{1}{2} - \frac{2\alpha_1\rho}{(\alpha_2 - L)} \left[1 - e^{-\frac{(\alpha_2 - L) \ln(2\alpha_1^2)}{2\alpha_2}} \right] > 0$ can be achieved by choosing the gain Γ sufficiently large. Using Eqs. 4-16, 4-17, and based on the development in Section 9.3 of [96], the following bound is obtained

$$\|\tilde{\theta}(t)\| \leq \sqrt{\frac{c_2}{c_1}} e^{\frac{c_4}{2c_1}} \|\tilde{\theta}(t_0)\| e^{-\beta(t-t_0)} + \frac{c_4}{2c_1} e^{\frac{c_4}{2c_1}} \int_0^t e^{-\beta(t-\tau)} d(\tau) d\tau \quad (4-18)$$

where a constant convergence rate $\beta > 0$ can be increased by increasing c_3 . From Eq.

4-18, $\|\tilde{\theta}(t)\| \in \mathcal{L}_\infty$, thus $\tilde{\theta}_1(t), \tilde{\theta}_2(t), \tilde{\theta}_3(t) \in \mathcal{L}_\infty$. Since $\tilde{\theta}_1(t), \tilde{\theta}_2(t), \tilde{\theta}_3(t) \in \mathcal{L}_\infty$,

and the fact that $\theta_1(t), \theta_2(t), \theta_3(t) \in \mathcal{L}_\infty$ can be used to conclude that $\hat{\theta}_1(t), \hat{\theta}_2(t),$

$\hat{\theta}_3(t) \in \mathcal{L}_\infty$. Using the result from Section 4.1.1.1 that $\|\tilde{\omega}(t)\| \rightarrow 0$ as $t \rightarrow \infty$, the

function $\|\Psi(y, \tilde{\omega})\| \rightarrow 0$ as $t \rightarrow \infty$. Hence, $d(t) \rightarrow 0$ as $t \rightarrow \infty$ and $d(t) \in \mathcal{L}_\infty$. Since

$d(t) \rightarrow 0$ as $t \rightarrow \infty$ and $d(t) \in \mathcal{L}_\infty$, by the Lebesgue dominated convergence theorem [104]

$\lim_{t \rightarrow \infty} \int_0^t e^{-\beta(t-\tau)} d(\tau) d\tau = \int_0^t e^{-\beta\sigma} \lim_{t \rightarrow \infty} d(\tau - \sigma) d\sigma = \frac{\lim_{t \rightarrow \infty} d(t)}{\beta} = 0$ [see Theorem

3.3.2.33 of [105]]. Lemma 9.6.3 of [96] can now be invoked to show that $\|\tilde{\theta}(t)\| \rightarrow 0$ as

$t \rightarrow \infty$. Hence, the reduced order estimator in Eqs. 4-11 and 4-12 identifies the structure

of observed feature points and unknown camera motion asymptotically. Since $y_3(t), u_1(t),$

and $u_2(t)$ can be estimated, the motion parameters $b_1(t)$ and $b_2(t)$ can be recovered based

on the definition of $u(t)$. □

² Note that $\lim_{\alpha_2 \rightarrow L} c_4 = \lim_{\alpha_2 \rightarrow L} \left(\frac{1 - e^{-\frac{(\alpha_2 - L) \ln(2\alpha_1^2)}{2\alpha_2}}}{(\alpha_2 - L)} \right) = 0$.

4.2 Simulation

In this addendum, a numerical solution is presented to illustrate the performance of the proposed estimation in estimating depth of a feature point and linear, and angular velocities of the camera. The time varying angular motion of the camera is selected as

$$\omega = \begin{bmatrix} 0.01 \sin(\frac{t}{2}) & 0.01 \sin(\frac{t}{2}) & 0 \end{bmatrix}^T .$$

The linear velocities in the X and Y directions are updated using the equation

$$\dot{v}_c(t) = \begin{bmatrix} -v_{cx}^2(t) & -v_{cy}^2(t) \end{bmatrix}^T$$

which is of the form described by (7) in the chapter. The linear velocity in Z direction measured using a sensor is chosen as

$$v_{cz}(t) = \cos(2t).$$

The initial linear velocity in the X and Y directions are chosen as

$$v_c(t_0) = \begin{bmatrix} 1 & 1 \end{bmatrix}^T ,$$

and the initial Euclidean coordinates of the first point are chosen as

$$\bar{m}(t_0) = \begin{bmatrix} 10 & 10 & 100 \end{bmatrix}^T .$$

The camera motion induces a motion of the feature points in the image frame. The camera calibration matrix is arbitrarily chosen to be

$$A_c = \begin{bmatrix} 800 & 0 & 300 \\ 0 & 800 & 200 \\ 0 & 0 & 1 \end{bmatrix} .$$

Points are tracked in the image while the camera is moving. Image coordinates of the first point and linear velocity $v_{cz}(t)$ of the camera are fed back to the estimator. The states of

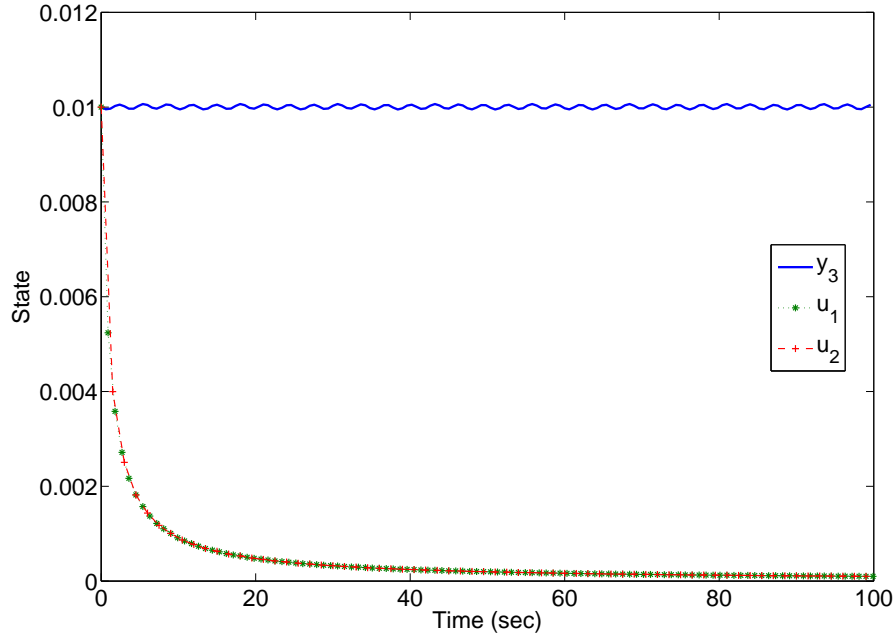


Figure 4-1. State $[y_3 \ u_1 \ u_2]^T$.

the estimator are initialized to

$$\bar{y}_3(t_0) = 0.1, \quad \bar{u}_1(t_0) = 0.1, \quad \bar{u}_2(t_0) = 0.1.$$

The estimator gain is chosen as

$$\Gamma = \begin{bmatrix} 3.6 & 0 & 0 \\ 0 & 0.44 & 0 \\ 0 & 0 & 0.44 \end{bmatrix}.$$

A measurement noise with mean zero and variance 0.1 is added using Matlab's 'randn()' command to the image point vector p defined in (4) and linear velocity in Z direction $v_{cz}(t)$. The state vector $\theta(t) = [y_3(t), u_1(t), u_2(t)]$ is shown in Fig. 4-1. The state estimated by an observer in (18) and (19) is shown in Fig. 4-2. In Fig. 4-3, an asymptotic convergence of the estimation error is shown in the presence of noisy measurement inputs.

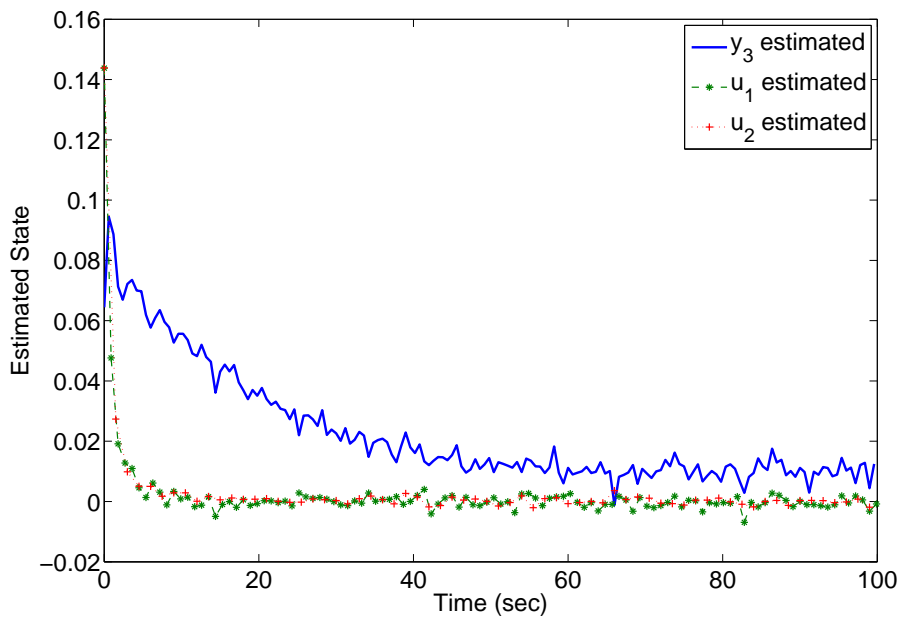


Figure 4-2. State $\begin{bmatrix} y_3 & u_1 & u_2 \end{bmatrix}^T$.

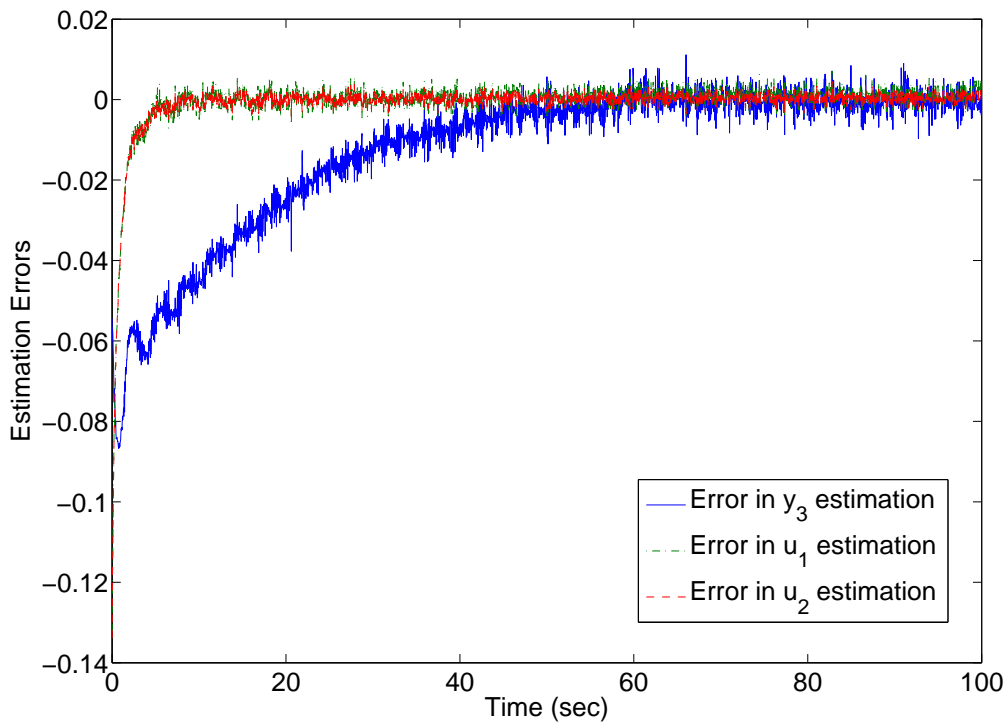


Figure 4-3. State $\begin{bmatrix} y_3 & u_1 & u_2 \end{bmatrix}^T$.

4.3 Summary

A reduced order observer is developed for the estimation of the structure (i.e. range to the target and Euclidean coordinates of the feature points) of a stationary target with respect to a moving camera, along with two unknown time-varying linear velocities and the angular velocity. The angular velocity is estimated using Homography relationships between two camera views. The observer requires the image coordinates of the points, a single linear camera velocity, and the corresponding linear camera acceleration in any one of the three camera coordinate axes. Under a physically motivated PE condition, asymptotic convergence of the observer is guaranteed. However, future efforts could potentially eliminate the need for any model of the vehicle trajectory (even if uncertain as in this result) and eliminate the need for an acceleration measurement.

Chapter 5
A LYAPUNOV-BASED OBSERVER FOR A CLASS OF NONLINEAR SYSTEMS
WITH APPLICATION TO IMAGE-BASED STRUCTURE AND MOTION
ESTIMATION

In this chapter, an online solution is presented to answer the question: *Given observations of point correspondences in every image of a video stream with known camera motion, is it possible to recover the Euclidean structure and motion (i.e. linear and angular velocities) of independently moving objects observed by the moving camera?* A nonlinear observer is developed to estimate the structure and motion of the object viewed by a moving camera. The observer algorithm uses camera velocities and the feature point data obtained from an image sequence. The proposed method has several advantages over the existing methods. There are no requirements of minimum number of point correspondences or number of views. The nonlinear observer processes the data in every image as it arrives, and thus, can perform real-time computation of the structure and motion of a moving object. A stability analysis of the proposed observer is presented which guarantees convergence of the observer, provided an observability condition based on the persistency of excitation (PE) of the camera motion is satisfied.

5.1 Nonlinear Observer

5.1.1 System Dynamics

Consider a class of nonlinear systems described by the following dynamics

$$\begin{aligned} \dot{y} &= f(y, u) + J(y, u)x, \\ \dot{x} &= g(y, x, u) + d(t) \end{aligned} \tag{5-1}$$

where $y(t) \in \mathcal{Y} \subset \mathbb{R}^{n_1}$ is the measured state, $x(t) \in \mathcal{X} \subset \mathbb{R}^{n_2}$ is the unmeasured state, $u(t) \in \mathcal{U} \subset \mathbb{R}^m$ is the input, $d(t) \in \mathcal{D} \subset \mathbb{R}^{n_2}$ is an external disturbance, $J : \mathbb{R}^{n_1} \times \mathbb{R}^m \rightarrow \mathbb{R}^{n_1 \times n_2}$ is a known function of inputs and outputs, and $f : \mathbb{R}^{n_1} \times \mathbb{R}^m \rightarrow \mathbb{R}^{n_1}$ and $g : \mathbb{R}^{n_1} \times \mathbb{R}^{n_2} \times \mathbb{R}^m \rightarrow \mathbb{R}^{n_2}$ are known nonlinear functions. The sets \mathcal{Y} , \mathcal{X} , \mathcal{U} and \mathcal{D} are compact sets. The system satisfies the following assumptions.

Assumption 1: The functions $g(y, x, u)$ and $\dot{g}(y, x, u)$ are bounded for all $y \in \mathcal{Y}$, $x \in \mathcal{X}$ and $u \in \mathcal{U}$, and is locally Lipschitz with respect to x in the sense that $\exists \gamma \in \mathbb{R}^+$: $\|g(y, x_1, u) - g(y, x_2, u)\| \leq \gamma \|x_1 - x_2\|$, where $x_1, x_2 \in \Omega$ and Ω is a compact subset of \mathbb{R}^{n_2} .

Assumption 2: The unknown time-varying disturbance satisfies the properties: $\dot{d}(t) \in \mathcal{L}_\infty$ and $d(t) \in \mathcal{L}_2 \cap \mathcal{L}_\infty$ [106, 107].

Assumption 3: The functions $J(y, u)$, $\dot{J}(y, u)$, $\ddot{J}(y, u)$ are bounded for all $y \in \mathcal{Y}$ and $u \in \mathcal{U}$.

Assumption 4: There exists $\beta_1, \varepsilon \in \mathbb{R}^+$ such that the inequality¹

$$\int_t^{t+\varepsilon} J^T(y(\sigma), u(\sigma))J(y(\sigma), u(\sigma))d\sigma \geq \beta_1 I_{n_2}$$

is satisfied for all $t \geq 0$. This is the well-known persistence of excitation (P.E.) condition [95].

5.1.2 State Estimator

A state estimator is developed for the system in Eq. 5-1 under Assumptions 1-4. To quantify the estimation objective, errors denoted by $e_1(y, t) \in \mathbb{R}^{n_1}$ and $e_2(x, t) \in \mathbb{R}^{n_2}$ are defined as

$$e_1 \triangleq y - \hat{y}, \quad e_2 \triangleq x - \hat{x} \tag{5-2}$$

where $\hat{y}(t) \in \mathbb{R}^{n_1}$ and $\hat{x}(t) \in \mathbb{R}^{n_2}$ are the estimates of $y(t)$ and $x(t)$. To facilitate the stability analysis, a filtered error $r(e_1, \dot{e}_1) \in \mathbb{R}^{n_1}$ is defined as

$$r \triangleq \dot{e}_1 + \alpha e_1 \tag{5-3}$$

¹ For any two matrices \mathcal{X} and \mathcal{Y} , the expression $\mathcal{X} \geq (>) \mathcal{Y}$ means the matrix $\mathcal{X} - \mathcal{Y}$ is positive semi-definite (positive definite). The subscript of the Identity matrix I defines the dimension of I .

where $\alpha \in \mathbb{R}^+$ is a tuning parameter. Based on the structure of Eq. 5-1, a full-order continuous nonlinear observer is designed as

$$\begin{aligned}\dot{\hat{y}} &= f(y, u) + (\alpha + \beta)e_1 + v, \\ \dot{\hat{x}} &= g(y, \hat{x}, u) + \Gamma J^T(y, u)(v - \alpha e_1) - \Gamma J^T(y, u)J(y, u)\hat{x}\end{aligned}\quad (5-4)$$

where $\Gamma \in \mathbb{R}^{n_2 \times n_2}$ is a gain matrix, $v(e_1) \in \mathbb{R}^{n_1}$ is the generalized solution to

$$\dot{v} = \beta \alpha e_1 + \rho \operatorname{sgn}(e_1), \quad v(0) = 0 \quad (5-5)$$

where $\beta, \rho \in \mathbb{R}^{n_1 \times n_1}$ are diagonal gain matrices, and $\operatorname{sgn}(e_1) = \begin{bmatrix} \operatorname{sgn}(e_{11}) & \dots & \operatorname{sgn}(e_{1n_1}) \end{bmatrix}^T$.

The closed-loop error dynamics for $e_1(y, t)$ and $e_2(x, t)$ are determined by differentiating Eq. 5-2 and using Eqs. 5-1 and 5-4 as

$$\dot{e}_1 = Jx - (\alpha + \beta)e_1 - v, \quad (5-6)$$

$$\dot{e}_2 = g(y, x, u) - g(y, \hat{x}, u) - \Gamma J^T(v - \alpha e_1) + \Gamma J^T J \hat{x} + d. \quad (5-7)$$

The closed-loop dynamics for $r(e_1, \dot{e}_1)$ are determined by differentiating Eq. 5-3 and using Eq. 5-6 as

$$\dot{r} = J\dot{x} + \dot{J}x - \beta \dot{e}_1 - \dot{v}. \quad (5-8)$$

Let $\chi_1(y, u, x, \dot{x}) \triangleq J(y, u)\dot{x}(t) + \dot{J}(y, u)x(t)$. From Eq. 5-1 and Assumption 1-3, $\dot{x}(t), \ddot{x}(t) \in \mathcal{L}_\infty$; these facts, along with Assumption 3, indicate that

$$\|\chi_1(y, u, x, \dot{x})\| \leq \zeta_1, \quad \|\dot{\chi}_1(y, u, x, \dot{x})\| \leq \zeta_2 \quad (5-9)$$

where $\zeta_1, \zeta_2 \in \mathbb{R}^+$ are known constants. Utilizing Eq. 5-5, the expression in Eq. 5-8 can be written as

$$\dot{r} = \chi_1 - \beta r - \rho \operatorname{sgn}(e_1). \quad (5-10)$$

5.1.3 Stability Analysis

Stability of the observer in Eq. 5–4 is analyzed by first studying the stability of the $e_1(t)$ dynamics. Since $\chi_1(y, u, x, \dot{x})$ satisfies the bounds in Eq. 5–9, $\chi_1(y, u, x, \dot{x})$ can be considered as a time-varying bounded disturbance. The robust term $v(t)$ is used to compensate for the disturbance $\chi_1(y, u, x, \dot{x})$ and asymptotically stabilize $e_1(t)$ and $r(t)$. Hence in Eq. 5–6, the signal $v(t)$ identifies the term $J(y, u)x(t)$ and can be used to stabilize the $\dot{e}_2(t)$ dynamics in Eq. 5–7. The main result of the paper follows in Theorem 1 which proves $\|e_2(t)\| \rightarrow 0$ as $t \rightarrow \infty$ using tools from converse Lyapunov theory. To facilitate the proof for Theorem 1, the following Lemma is established.

Lemma 5.1. *The error system in Eq. 5–6 is globally asymptotically stable in the sense that*

$$\|e_1(t)\| \rightarrow 0 \quad \text{as } t \rightarrow \infty$$

provided Assumptions 1-3 and following sufficient conditions are satisfied

$$\rho > \zeta_1 + \frac{1}{\alpha}\zeta_2, \quad \beta > \frac{1}{2}, \quad \alpha > \frac{1}{2}. \quad (5-11)$$

Proof. Let $\psi(r, e, P) \in \mathbb{R}^{2n_1+1}$ be defined as

$$\psi \triangleq \begin{bmatrix} r^T & e_1^T & \sqrt{P} \end{bmatrix}^T \quad (5-12)$$

such that \mathbb{R}^{2n_1+1} contains $\psi(r, e, P) = 0$. In Eq. 5–12, the auxiliary function $P(e_1, r, \chi_1, t) \in \mathbb{R}$ is a generalized solution to the differential equation

$$\dot{P} = -L, \quad P(0) = \rho \sum_{i=1}^{n_1} e_{1i}(0) - e_1^T(0)\chi_1(0) \quad (5-13)$$

where the function $L(e_1, r, \chi_1) \in \mathbb{R}$ is defined as

$$L \triangleq r^T(\chi_1 - \rho \text{sgn}(e_1)). \quad (5-14)$$

Provided the sufficient conditions in Eq. 5–11 are satisfied, $P(e_1, r, \chi_1, t) \geq 0$ as shown in the Appendix. Let $V(\psi) : \mathbb{R}^{2n_1+1} \rightarrow \mathbb{R}$ be a Lipschitz, regular positive definite function

defined as

$$V \triangleq \frac{1}{2}r^T r + \frac{1}{2}e_1^T e_1 + P \quad (5-15)$$

which satisfies the following inequalities

$$\frac{1}{2} \|\psi\|^2 = U_2(\psi) \leq V \leq U_1(\psi) = \|\psi\|^2. \quad (5-16)$$

The closed-loop system in Eqs. 5-3, 5-8, and 5-13 can be described by $\dot{\psi} = F(\psi, t)$, where $F(\psi, t) \in \mathbb{R}^{2n_1+1}$. The right-hand side of the closed-loop system $F(\psi, t)$ is discontinuous in the set $\{(\psi, t) | e_1 = 0\}$. As shown in [108, 109], a unique generalized solution can be established in the Filippov's sense by studying a differential inclusion $\dot{\psi} \in F(\psi, t)$, where $\psi(r, e, P)$ is absolutely continuous (i.e., differentiable almost everywhere (a.e.)) and $F(\cdot)$ is Lebesgue measurable and locally bounded. Under Filippov's framework, generalized Lyapunov stability theory can be used to establish strong stability of the closed-loop system in Eqs. 5-3, 5-8, and 5-13 (see [110-112] for further details). Since $V(\psi)$ is Lipschitz and regular, and $\psi(r, e, P)$ is absolutely continuous, Theorem 2.2 of [112] can be invoked to conclude that $V(\psi)$ is absolutely continuous, $\dot{V}(\psi)$ exists a.e., and $\dot{V}(\psi) \in^{a.e.} \check{V}(\psi)$ where

$$\check{V}(\psi) = \bigcap_{\xi \in \partial V(\psi)} \xi^T K \begin{bmatrix} \dot{r} & \dot{e}_1 & \frac{1}{2}P^{-\frac{1}{2}}\dot{P} \end{bmatrix}^T \quad (5-17)$$

where $\partial V(\psi)$ is the generalized gradient of $V(\psi)$ [111], and $K[\cdot]$ is defined in [110, 112].

Since $V(\psi)$ is Lipschitz and regular, Eq. 5-17 can be simplified as [110]

$$\begin{aligned} \check{V}(\psi) &= \nabla V^T K \begin{bmatrix} \dot{r} & \dot{e}_1 & \frac{1}{2}P^{-\frac{1}{2}}\dot{P} \end{bmatrix}^T \\ &= \begin{bmatrix} r & e_1 & 2\sqrt{P} \end{bmatrix} K \begin{bmatrix} \dot{r} & \dot{e}_1 & \frac{1}{2}P^{-\frac{1}{2}}\dot{P} \end{bmatrix}^T. \end{aligned}$$

Utilizing Eqs. 5–3, 5–8, and 5–13, and using Property 2, 5, and 7 of $K[\cdot]$ given in Theorem 1 of [110] yields

$$\begin{aligned}\dot{\check{V}} &\subset r^T (\chi_1 - \beta r - \rho K [\text{sgn}(e_1)]) + e_1^T r - \alpha e_1^T e_1 - r^T (\chi_1 - \rho K [\text{sgn}(e_1)]) \\ &= -\beta r^T r + e_1^T r - \alpha e_1^T e_1\end{aligned}$$

where $(r^T - r^T)_i \text{SGN}(e_{1i}) = 0$ and $K[\text{sgn}(e_1)] = \text{SGN}(e_1)$ are used [110], where $\text{SGN}(\cdot)$ is defined such that $\text{SGN}(e_{1i}) = -1$ if $e_{1i} < 0$, $[-1, 1]$ if $e_{1i} = 0$, and 1 if $e_{1i} > 0$. Using Young's inequality to show that $\|e_1\| \|r\| \leq \frac{1}{2} \|e_1\|^2 + \frac{1}{2} \|r\|^2$, the following inequality is obtained

$$\dot{\check{V}} \leq -(\beta - \frac{1}{2}) \|r\|^2 - (\alpha - \frac{1}{2}) \|e_1\|^2$$

where the symbol \leq means every element of $\dot{\check{V}}(\psi)$ is less than or equal to the right hand side [112]. Choosing $\alpha > \frac{1}{2}$ and $\beta > \frac{1}{2}$, the following upper bound can be established

$$\dot{\check{V}} \leq -\bar{\beta} \|r\|^2 - \bar{\alpha} \|e_1\|^2 = -U(\psi) \quad (5-18)$$

where $\bar{\beta} \triangleq \beta - \frac{1}{2}$, $\bar{\alpha} \triangleq \alpha - \frac{1}{2}$. The result in Eq. 5–18 indicates that

$$\dot{V}(\psi) \leq -U(\psi) \quad \forall \dot{V}(\psi) \in^{a.e.} \dot{\check{V}}(\psi). \quad (5-19)$$

The inequalities in Eqs. 5–16 and 5–19, indicate that $V(\psi) \in \mathcal{L}_\infty$; thus $r(t), e_1(t) \in \mathcal{L}_\infty$, and from $y(t) \in \mathcal{L}_\infty, \hat{y}(t) \in \mathcal{L}_\infty$. Since $r(t)$ and $e_1(t) \in \mathcal{L}_\infty$, Eq. 5–3 can be used to show that $\dot{e}_1(t) \in \mathcal{L}_\infty$, and Eqs. 5–5, 5–8, and Assumption 1 can be used to show that $\dot{v}(t), \dot{r}(t) \in \mathcal{L}_\infty$. Since $r(t), e_1(t) \in \mathcal{L}_\infty$, Eq. 5–10 can be used to prove that $r(t)$ is uniformly continuous. From Eq. 5–19 and the fact that $V(\psi) \in \mathcal{L}_\infty, r(t), e_1(t) \in \mathcal{L}_2$. Since $\dot{e}_1(t) \in \mathcal{L}_\infty, e_1(t) \in \mathcal{L}_\infty \cap \mathcal{L}_2, \dot{r}(t) \in \mathcal{L}_\infty$, and $r(t) \in \mathcal{L}_\infty \cap \mathcal{L}_2$, Barbalat's lemma can be invoked to prove that

$$\|r(t)\| \rightarrow 0 \text{ and } \|e_1(t)\| \rightarrow 0 \text{ as } t \rightarrow \infty. \quad (5-20)$$

□

Theorem 5.1. *Given the dynamics in Eq. 5-1 with inputs $u(t)$ and output $y(t)$, the observer in Eq. 5-4 asymptotically estimates the state $x(t)$ in the sense that*

$$\|e_2(t)\| \rightarrow 0 \quad \text{as } t \rightarrow \infty$$

provided Assumptions 1-4 are satisfied.

Proof. Substituting $v(t)$ from the $\dot{e}_1(t)$ dynamics into the $\dot{e}_2(t)$ dynamics in Eq. 5-7 yields

$$\dot{e}_2 = g - \hat{g} - \Gamma J^T J e_2 - \Gamma J^T (-r - \beta e_1) + d. \quad (5-21)$$

Since $g(y, x, u)$ is locally Lipschitz, the Mean Value Theorem (MVT) can be invoked to yield

$$g(y, x, u) - g(y, \hat{x}, u) = \Lambda(y, \hat{x}, u) e_2(t), \quad (5-22)$$

where $\Lambda(y, \hat{x}, u)$ is bounded for all time t as

$$\bar{\Lambda} = \sup_t \|\Lambda(y, \hat{x}, u)\|. \quad (5-23)$$

The $\dot{e}_2(t)$ dynamics in Eq. 5-21 can be written as

$$\dot{e}_2 = -\Gamma J^T J e_2 + \Lambda e_2 + \Gamma J^T r + \Gamma J^T \beta e_1 + d. \quad (5-24)$$

The nominal system

$$\dot{e}_2 = \bar{f}(e_2) = -\Gamma J^T J e_2 \quad (5-25)$$

is globally exponentially stable if Assumption 4 is satisfied using Theorem 2.5.1 of [95].

Hence, trajectories of the nominal system in Eq. 5-25 satisfy the inequality:

$$\|e_2(t)\| \leq k \|e_2(0)\| e^{-\lambda(t-t_0)}, \quad \forall t \geq t_0 \geq 0$$

where $k, \lambda \in \mathbb{R}$ are positive constants. Using the converse Lyapunov theorem there exists a Lyapunov function $\bar{V}_1 : [0, \infty) \times \mathbb{R}^{n_2} \rightarrow \mathbb{R}$ that satisfies

$$\begin{aligned} c_{11} \|e_2\|^2 &\leq \bar{V}_1(t, e_2) \leq c_{21} \|e_2\|^2, \\ \dot{\bar{V}}_1(t, e_2) &= \frac{\partial \bar{V}_1}{\partial t} + \frac{\partial \bar{V}_1}{\partial e_2} (-\Gamma J^T J e_2) \leq -c_{31} \|e_2\|^2, \\ \left\| \frac{\partial \bar{V}_1}{\partial e_2} \right\| &\leq c_{41} \|e_2\|, \end{aligned} \tag{5-26}$$

where $c_{11}, c_{21}, c_{31}, c_{41} \in \mathbb{R}^+$. Taking the time derivative of $\bar{V}_1(t, e_2)$ along the trajectories of the system

$$\dot{e}_2 = -\Gamma J^T J e_2 + \Lambda e_2 \tag{5-27}$$

the following expression is obtained

$$\begin{aligned} \dot{\bar{V}}_1(t, e_2) &= \frac{\partial \bar{V}_1}{\partial t} + \frac{\partial \bar{V}_1}{\partial e_2} (-\Gamma J^T J e_2 + \Lambda e_2) \\ &\leq -c_{31} \|e_2\|^2 + c_{41} \bar{\Lambda} \|e_2\|^2 \\ &= -(c_{31} - c_{41} \bar{\Lambda}) \|e_2\|^2. \end{aligned} \tag{5-28}$$

Using Theorem 4.14 of [96], the estimates for c_{31} and c_{41} are given by

$$c_{31} = \frac{1}{2}, \quad c_{41} = \frac{2\alpha_1}{(\alpha_2 - L)} \left[1 - e^{-\frac{(\alpha_2 - L) \ln(2\alpha_1^2)}{2\alpha_2}} \right]$$

where $\alpha_1, \alpha_2 \in \mathbb{R}^+$ and $L \in \mathbb{R}^+$ is an upper bound on the norm of the Jacobian matrix

$$\frac{\partial \bar{f}(e_2)}{\partial e_2}, \text{ where } \bar{f}(e_2) \text{ is defined in Eq. 5-25. Note that } \lim_{\alpha_2 \rightarrow L} c_{41} = \lim_{\alpha_2 \rightarrow L} \left(\frac{1 - e^{-\frac{(\alpha_2 - L) \ln(2\alpha_1^2)}{2\alpha_2}}}{(\alpha_2 - L)} \right) =$$

0. Since α_2 is directly proportional to the gain Γ [95], the inequality $c_{31} - c_{41} \bar{\Lambda} > 0$ can be achieved by choosing the gain Γ sufficiently large. Using the upper bounds in Eq. 5-26 and the inequality in Eq. 5-28, the error system in Eq. 5-27 is globally exponentially

stable. Hence, there exists a Lyapunov function $\bar{V}_2 : [0, \infty) \times \mathbb{R}^{n_2} \rightarrow \mathbb{R}$ that satisfies

$$\begin{aligned} c_{12} \|e_2\|^2 &\leq \bar{V}_2(t, e_2) \leq c_{22} \|e_2\|^2, \\ \dot{\bar{V}}_2(t, e_2) &= \frac{\partial \bar{V}_2}{\partial t} + \frac{\partial \bar{V}_2}{\partial e_2} (-\Gamma J^T J e_2 + \Lambda e_2) \leq -c_{32} \|e_2\|^2, \\ \left\| \frac{\partial \bar{V}_2}{\partial e_2} \right\| &\leq c_{42} \|e_2\| \end{aligned} \quad (5-29)$$

where $c_{12}, c_{22}, c_{32}, c_{42} \in \mathbb{R}^+$. Taking the time derivative of $\bar{V}_2(t, e_2)$ along the trajectories of the error system in Eq. 5-24, the following expression is obtained:

$$\begin{aligned} \dot{\bar{V}}_2 &= \frac{\partial \bar{V}_2}{\partial t} + \frac{\partial \bar{V}_2}{\partial e_2} (-\Gamma J^T J e_2 + \Lambda e_2 + \Gamma J^T r + \Gamma J^T \beta e_1 + d) \\ &\leq -c_{32} \|e_2\|^2 + c_{42} \|e_2\| \|\Gamma J^T (r + \beta e_1)\| + c_{42} \|e_2\| \|d\| \\ &\leq -c_{32} \|e_2\|^2 + c_{42} \varsigma_1 \|e_2\| \|r\| + c_{42} \varsigma_2 \|e_2\| \|e_1\| + c_{42} \|e_2\| \|d\| \end{aligned}$$

where the fact that the matrix $J(y, u)$ is norm bounded is used so that $\|\Gamma J^T\| \leq \varsigma_1$ and $\|\Gamma J^T \beta\| \leq \varsigma_2$ for constants $\varsigma_1, \varsigma_2 \in \mathbb{R}^+$. Completing the squares, the following inequality can be obtained

$$\dot{\bar{V}}_2 \leq -\gamma_1 \|e_2\|^2 + \gamma_2 \quad (5-30)$$

where $\gamma_1 \triangleq c_{32} - \xi_1 - \xi_2 > 0$, $\gamma_2(t) \triangleq \frac{c_{42}^2 \varsigma_1^2 \|r(t)\|^2 + \varsigma_2^2 \|e_1(t)\|^2}{4\xi_1} + \frac{c_{42}^2 \|d(t)\|^2}{4\xi_2}$ and $\gamma_1, \gamma_2(t), \xi_1, \xi_2 \in \mathbb{R}^+$.

Using the bounds on $\bar{V}_2(t, e_2)$ in Eq. 5-29, the inequality in Eq. 6-19 can be expressed as

$$\dot{\bar{V}}_2 \leq -\frac{\gamma_1}{c_{22}} \bar{V}_2 + \bar{\gamma}_2 \quad (5-31)$$

where $\bar{\gamma}_2 \triangleq \max(\gamma_2)$. From Eqs. 5-29 and 5-31, $\bar{V}_2(t, e_2)$ decreases along the trajectories of Eq. 5-24 until the solution reaches a compact set $\Omega_c \triangleq \left\{ e_2(t) \mid \|e_2(t)\| \leq \sqrt{\frac{\bar{\gamma}_2}{\gamma_1}} \right\}$. Hence, all solutions of the closed-loop system Eq. 5-24 converge to the compact ball Ω_c and all signals of the closed-loop system Eq. 5-24 are uniformly ultimately bounded. Since $e_2(t) \in \mathcal{L}_\infty$, using Eq. 5-29, $\bar{V}_2(t, e_2) \in \mathcal{L}_\infty$. Integrating Eq. 6-19, following inequality can

be obtained

$$\int_{t_0}^t \gamma_1 \|e_2(\tau)\|^2 d\tau \leq \bar{V}_2(t_0) + \frac{c_{42}^2}{4\zeta_1} \left(\zeta_1^2 \int_{t_0}^t \|r(\tau)\|^2 d\tau + \zeta_2^2 \int_{t_0}^t \|e_1(\tau)\|^2 d\tau \right) \quad (5-32)$$

$$+ \frac{c_{42}^2}{4\zeta_2} \int_{t_0}^t \|d(\tau)\|^2 d\tau$$

Using Assumption 2 and the fact that $r(t), e_1(t) \in \mathcal{L}_2$ (from Eq. 5-19), it can be concluded that

$$\int_{t_0}^t \|e_2(\tau)\|^2 d\tau < \infty.$$

Hence, $e_2(t) \in \mathcal{L}_2 \cap \mathcal{L}_\infty$. Since all signals on the right hand side of Eq. 5-24 are bounded, $\dot{e}_2(t) \in \mathcal{L}_\infty$. Thus, Barbalat's lemma can be invoked to prove that $\|e_2(t)\| \rightarrow 0$ as $t \rightarrow \infty$. □

5.2 Application to Structure and Motion Problem

In this section, the nonlinear observer developed in Section 5.1 is applied to a well known machine vision problem called ‘structure and motion from motion’. In contrast to the traditional ‘structure from motion’ problem where the objective is to estimate structure of a stationary object, the SaMfM problem solves the structure and motion estimation of the object moving with unknown velocities. In the following, the estimation objective is described and a physical plant model is provided which can be transformed into a state space model of the form given in Eq. 5-1 under some assumptions. An observer is developed by following the guidelines presented in Section 5.1.2. The performance of the observer is demonstrated via a numerical simulation.

5.2.1 Structure and Motion from Motion (SaMfM) Objective

The objective of SaMfM is to recover the structure (i.e. Euclidean coordinates) and motion (i.e. Euclidean linear and angular velocities) of moving objects observed by a moving camera, assuming all camera velocities are known. The object can be tracked as a

single point or a collection of multiple points, where the range (i.e., $\frac{1}{x_3(t)}$) and the motion of each point are estimated.

5.2.2 State Dynamics Formulation

The camera-object relative motion model developed in Chapter 2 is used for the subsequent technical development in this chapter. Some assumptions are made on the moving object's velocities to facilitate the development.

The states defined in Eq. 2–3 contain unknown structure information of the object. To facilitate the observer design, states are defined in this section to incorporate unknown structure and velocity information. Specifically, an auxiliary state vector

$p(t) = \begin{bmatrix} p_1(t) & p_2(t) & p_3(t) \end{bmatrix}^T \in \mathbb{R}^3$ is defined as

$$p \triangleq \begin{bmatrix} v_{px}y_3(t) & v_{py}y_3(t) & v_{pz}y_3(t) \end{bmatrix}^T \quad (5-33)$$

which incorporates the unknown object velocity information. To recover the 3D structure, the state $y_3(t)$ should be estimated because it contains range information. Since, the states $y_1(t), y_2(t)$ can be measured from the images, the estimated state $y_3(t)$ can be used to scale $y_1(t)$ and $y_2(t)$, and thus $\bar{m}(t)$, i.e. the 3D structure can be recovered. To recover velocity information, the state $p(t)$ must be estimated. Once $y_3(t)$ and $p(t)$ are estimated, velocity information can be recovered by scaling the estimated $p(t)$ by the estimated $y_3(t)$. Using Eqs. 2–3 and 2–8, the dynamics of the state vector $y(t)$ are expressed as

$$\begin{aligned} \dot{y}_1 &= \Omega_1 + (v_{cx} - y_1v_{cz})y_3 - p_1 + y_1p_3, \\ \dot{y}_2 &= \Omega_2 + (v_{cy} - y_2v_{cz})y_3 - p_2 + y_2p_3, \\ \dot{y}_3 &= -v_{cz}y_3^2 - (y_2\omega_1 - y_1\omega_2)y_3 + v_{pz}y_3^2 \end{aligned} \quad (5-34)$$

where $\Omega_1(t) \in \mathbb{R}$ and $\Omega_2(t) \in \mathbb{R}$ are defined as

$$\begin{aligned} \Omega_1(t) &\triangleq -y_1y_2\omega_1 + (1 + y_1^2)\omega_2 - y_2\omega_3, \\ \Omega_2(t) &\triangleq -(1 + y_2^2)\omega_1 + y_1y_2\omega_2 + y_1\omega_3. \end{aligned}$$

Differentiating Eq. 5–33 and using Eq. 5–34, the dynamics of the state $p(t)$ can be represented by the following set of differential equations

$$\begin{aligned}\dot{p}_1 &= y_3 \dot{v}_{px} - v_{cz} p_1 y_3 - (y_2 \omega_1 - y_1 \omega_2) p_1 + p_3 p_1, \\ \dot{p}_2 &= y_3 \dot{v}_{py} - v_{cz} p_2 y_3 - (y_2 \omega_1 - y_1 \omega_2) p_2 + p_3 p_2, \\ \dot{p}_3 &= y_3 \dot{v}_{pz} - v_{cz} p_3 y_3 - (y_2 \omega_1 - y_1 \omega_2) p_3 + p_3^2.\end{aligned}\tag{5–35}$$

By defining the vector $z(t) \in \mathbb{R}^2$ and the vector $\theta(t) \in \mathbb{R}^4$ as

$$\begin{aligned}z(t) &\triangleq \begin{bmatrix} y_1 & y_2 \end{bmatrix}^T, \\ \theta(t) &\triangleq \begin{bmatrix} y_3 & p_1 & p_2 & p_3 \end{bmatrix}^T\end{aligned}$$

the state dynamics in Eqs. 5–34 and 5–35 can be expressed as

$$\begin{aligned}\dot{z} &= \Omega(z, u) + J(z, u)\theta, \\ \dot{\theta} &= g(z, \theta, u) + d(t)\end{aligned}\tag{5–36}$$

where $\Omega(t) = \begin{bmatrix} \Omega_1(t) & \Omega_2(t) \end{bmatrix}^T$, $u(t) = \begin{bmatrix} v_c(t) & \omega(t) \end{bmatrix}^T$, $d(t) = y_3(t) \dot{v}_p(t)$, and the functions $J(z, u) \in \mathbb{R}^{2 \times 4}$ and $g(z, \theta, u) \in \mathbb{R}^4$ are given by

$$J = \begin{bmatrix} (v_{cx} - y_1 v_{cz}) & -1 & 0 & y_1 \\ (v_{cy} - y_2 v_{cz}) & 0 & -1 & y_2 \end{bmatrix},\tag{5–37}$$

and

$$g = \begin{bmatrix} -v_{cz} y_3^2 - (y_2 \omega_1 - y_1 \omega_2) y_3 + p_3 y_3 \\ -v_{cz} p_1 y_3 - (y_2 \omega_1 - y_1 \omega_2) p_1 + p_3 p_1 \\ -v_{cz} p_2 y_3 - (y_2 \omega_1 - y_1 \omega_2) p_2 + p_3 p_2 \\ -v_{cz} p_3 y_3 - (y_2 \omega_1 - y_1 \omega_2) p_3 + p_3^2 \end{bmatrix}.\tag{5–38}$$

Assumption 5.1. *The velocity of object expressed in the camera reference frame satisfies $\dot{v}_p(t) \in \mathcal{L}_2 \cap \mathcal{L}_\infty$ and $\ddot{v}_p(t) \in \mathcal{L}_\infty$.*

Assumption 5.2. The camera velocities $\omega(t), v_c(t)$ and the point velocity $v_p(t)$ belongs to class C^2 with bounded derivatives.

Assumption 5.3. There exists $\bar{\beta}_2, \bar{\varepsilon} \in \mathbb{R}^+$ such that the inequality

$$\int_t^{t+\bar{\varepsilon}} J^T(z(\tau), u(\tau))J(z(\tau), u(\tau))d\tau \geq \bar{\beta}_2 I_4 \quad \forall t \geq 0.$$

Remark 5.1. Assumption 5.5 indicates that the linear velocity of the moving object $v_p(t)$, measured in the camera reference frame, can be time-varying but converges to a constant.

Assumption 5.5 holds for a special case of $v_p(t) = c$, where c is a constant.

Remark 5.2. Based on Assumptions 5.5 and 5.6, Eqs. 5-33, 5-34 and 5-35 the following inequalities can be developed

$$\|\chi_1(t)\| = \left\| J(z, u)\dot{\theta}(t) + \dot{J}(z, u)\theta(t) \right\| \leq \bar{\xi}_3 \quad \|\dot{\chi}_1(t)\| \leq \bar{\xi}_4$$

where $\bar{\xi}_3, \bar{\xi}_4 \in \mathbb{R}^+$ denote known bounding constants.

Remark 5.3. (Observability Condition) Even though the rank of $J^T(z, u)J(z, u)$ can be at most 2, the integration of $J^T(z, u)J(z, u)$ can achieve full rank [3, 95, 113, 114].

The condition in Assumption 5.5-5.7 fail if the camera is translating parallel to the ray projected by the moving object on the camera, i.e., $y_1(t), y_2(t) = 0$ or if the camera is not translating in any direction, i.e., $v_{cx} = v_{cy} = v_{cz} = 0 \forall t \geq 0$.

5.2.3 Structure and Motion Observer

Based on the work presented in Section 5.1.2, an observer is designed to estimate $\theta(t)$ which contains unknown depth and unknown velocity information of the moving object. Let $\hat{z}(t) \in \mathbb{R}^2$ and $\hat{\theta}(t) \in \mathbb{R}^4$ denote the estimates of $z(t)$ and $\theta(t)$. Based on the structure of Eq. 5-36 and the observer design in Eq. 5-4, a full-order continuous nonlinear observer is designed as

$$\begin{aligned} \dot{\hat{z}} &= \Omega(z, u) + (\alpha + \beta)e_1 + v, \\ \dot{\hat{\theta}} &= g(z, \hat{\theta}, u) + \Gamma J^T(z, u)(v - \alpha e_1) - \Gamma J^T J \hat{\theta} \end{aligned} \quad (5-39)$$

where $\Gamma \in \mathbb{R}^{4 \times 4}$ is a gain matrix, $\alpha, \beta \in \mathbb{R}^+$ are tuning parameters, the signal $v(t) \in \mathbb{R}^2$ is a generalized solution to

$$\dot{v} = \beta \alpha e_1 + \rho \operatorname{sgn}(e_1), \quad v(0) = 0 \quad (5-40)$$

where $\rho \in \mathbb{R}^{2 \times 2}$, $\operatorname{sgn}(e_1) = \begin{bmatrix} \operatorname{sgn}(e_{11}) & \operatorname{sgn}(e_{12}) \end{bmatrix}^T$, and $e_1(t) \in \mathbb{R}^2$ is the output estimation error defined as

$$e_1 \triangleq y - \hat{y}.$$

If Assumptions 5 and 6 are satisfied, Assumptions 1-4 are satisfied by the dynamic system in Eq. 5-36. Based on the stability analysis presented in Section 7.1.3, $\hat{\theta}(t) \rightarrow \theta(t)$ as $t \rightarrow \infty$.

5.2.4 Conditions on the Moving Object Trajectory

In this section, physical constraints on the trajectory of the moving target due to Assumption 5 are discussed. According to Assumption 2, the time-varying disturbance, $d(t) = y_3(t) \dot{v}_p(t) \in \mathcal{L}_2 \cap \mathcal{L}_\infty$ and $\dot{d}(t) = \dot{y}_3 \dot{v}_p + y_3 \ddot{v}_p \in \mathcal{L}_\infty$. Using Remark 1, Assumption 5, Assumption 6 and Eq. 5-34, $y_3 \dot{v}_p(t) \in \mathcal{L}_\infty$ and $\dot{y}_3 \dot{v}_p + y_3 \ddot{v}_p \in \mathcal{L}_\infty$. For $y_3(t) \dot{v}_p(t) \in \mathcal{L}_2$,

$$\lim_{t \rightarrow \infty} \int_0^t \|y_3(\tau) \dot{v}_p(\tau)\|^2 d\tau < \infty. \quad (5-41)$$

Using $\|y_3(t) \dot{v}_p(t)\|^2 \leq \|y_3(t)\|^2 \|\dot{v}_p(t)\|^2$, the following norm inequality can be developed

$$\lim_{t \rightarrow \infty} \int_0^t \|y_3(\tau) \dot{v}_p(\tau)\|^2 d\tau \leq (\sup_{t \geq 0} \|y_3(t)\|^2) \left(\lim_{t \rightarrow \infty} \int_0^t \|\dot{v}_p(\tau)\|^2 d\tau \right).$$

Using Remark 1, $y_3(t) \in \mathcal{L}_\infty$ hence, $\sup_{t \geq 0} \|y_3(t)\|^2 < \infty$. From Assumption 5, $\dot{v}_p(t) \in \mathcal{L}_2$; thus, Eq. 6-10 is satisfied.

According to Remark 2, one of the cases for which Assumption 5 is satisfied is when the object velocity, $v_p(t)$, is constant, i.e.,

$$\bar{R} \bar{v}_p = c \quad (5-42)$$

where $c \in \mathbb{R}^3$ is a vector of constants. The expression in Eq. 5-42 can be interpreted in two ways:

Case 1: The rotation matrix between the current camera coordinate frame and the inertial coordinate frame, $\bar{R}(t)$, and the velocity of the moving object in the inertial coordinate frame, $\bar{v}_p(t)$, do not change with time. The rotation matrix $\bar{R}(t)$ is a constant matrix if the angular velocities of the camera are zero. Hence, if the camera exhibits only translational motion and the object velocity is constant in the inertial coordinate frame then the expression in Eq. 5-42 holds.

Case 2: The time derivative of the equality in Eq. 5-42 is zero, i.e., $\dot{\bar{R}}(t) \bar{v}_p(t) + \bar{R}(t) \dot{\bar{v}}_p(t) = 0$. Using $\dot{\bar{R}}(t) = [\omega(t)]_{\times} \bar{R}(t)$, the following ordinary differential equation (ODE) can be developed

$$\dot{\bar{v}}_p = -\bar{R}^T [\omega]_{\times} \bar{R} \bar{v}_p.$$

Based on the fact that $\bar{R}^T(t) [\omega(t)]_{\times} \bar{R}(t) = [\bar{R}^T(t) \omega(t)]_{\times}$, the following ODE is obtained

$$\dot{\bar{v}}_p = -[\bar{R}^T \omega]_{\times} \bar{v}_p. \quad (5-43)$$

Since $\bar{R}^T(t) \omega(t) = \omega(t)$, the ODE for object velocity can be expressed as

$$\dot{\bar{v}}_p = -[\omega]_{\times} \bar{v}_p. \quad (5-44)$$

For a special case of constant camera angular velocity, ω , the ODE in Eq. 5-44 has an analytical solution given by

$$\bar{v}_p(t) = e^{-[\omega]_{\times} t} \bar{v}_p(t_0). \quad (5-45)$$

Using Rodrigues' formula for a matrix exponential, Eq. 5-45 can be transformed into

$$\bar{v}_p(t) = \left(I + \frac{[\bar{\omega}]_{\times}}{\|\bar{\omega}\|} \sin(\|\bar{\omega}\|) + \frac{[\bar{\omega}]_{\times}^2}{\|\bar{\omega}\|^2} (1 - \cos(\|\bar{\omega}\|)) \right) \bar{v}_p(t_0) \quad (5-46)$$

where $\bar{\omega}(t) \triangleq -\omega t$. For time varying object linear velocity, $\bar{v}_p(t)$, and the constant camera angular velocity, ω , which in combination satisfies the equation Eq. 5-46, the object linear velocity $v_p(t)$ satisfies the Assumption 5. Hence, the observer in Section 5.1 can be used for the class of object linear velocity and camera angular velocity for which Eq. 5-46 is satisfied.

For the case of time-varying camera angular velocity, an analytical solution to Eq. 5-46 is a wide open problem in literature. For $\bar{v}_p(t)$ and $\omega(t)$ satisfying the ODE in Eq. 5-44, Assumption 5 is satisfied and the observer in Eq. 5-39 can be used to achieve asymptotic range and motion estimation.

5.3 Simulation

The performance of the observer in Eq. 5-39 is tested using a numerical simulation in Matlab. The results are compared with the observer in [3]. The camera calibration matrix is selected as

$$A = \begin{bmatrix} 720 & 0 & 320 \\ 0 & 720 & 240 \\ 0 & 0 & 1 \end{bmatrix}.$$

The velocities of the camera are selected as

$$\begin{aligned} v_c(t) &= \begin{bmatrix} -3\sin(t/5) + 2 & 2\cos(t/10) + 1 & 5\sin(t/2) + 0.5 \end{bmatrix}^T \text{ m/s}, \\ \omega(t) &= \begin{bmatrix} -0.01\sin(t/5) & 0.01\cos(t/2) & 0 \end{bmatrix}^T \text{ rad/s} \end{aligned}$$

and the time-varying object velocity $\bar{v}_p(t)$, expressed in the inertial frame, is shown in Fig. 5-1. The equivalent object velocity expressed in the camera reference frame is

$$v_p(t) = \begin{bmatrix} -2 & -1 & -1 \end{bmatrix}^T \text{ m/s}.$$

The initial relative range between the camera and the object is $m(t_0) = \begin{bmatrix} 4 & 4 & 50 \end{bmatrix}^T \text{ m}$. The estimates are integrated using a fourth order Runge-Kutta integrator with a time step of 0.01sec. For the proposed observer, the initial conditions and observer gains are selected

as² $\hat{z}(t_0) = \begin{bmatrix} \frac{4}{50} & \frac{4}{50} \end{bmatrix}^T$, $\hat{\theta}(t_0) = \begin{bmatrix} 0.015 & -0.02 & -0.01 & -0.01 \end{bmatrix}^T$, $\alpha = 70$, $\beta = 80$, $\rho = \text{diag} \left\{ \begin{bmatrix} 0.05 & 0.05 \end{bmatrix}^T \right\}$,³ and $\Gamma = \text{diag} \left\{ \begin{bmatrix} 0.091 & 0.095 & 0.2 & 0.165 \end{bmatrix}^T \right\}$. The initial conditions for the observer in [3] are selected exactly the same as for the proposed observer and the observer gains are selected as⁴ $\alpha_1 = \alpha_2 = 5$, $\delta_1 = \delta_2 = 0.01$, and $\Gamma = \text{diag} \left\{ \begin{bmatrix} 0.091 & 0.095 & 0.2 & 0.165 \end{bmatrix}^T \right\}$. The errors in the estimation of $\theta(t)$ using the proposed observer and the observer in [3] are shown in Figs. 5-2 and 5-3. From Fig. 5-3, it is determined that the estimation errors converge to a small ball around the origin (a UUB result). The proposed observer shows an improved transient performance over the observer in [3]. In Fig. 5-4, a comparison of the estimated and actual 3D relative position of the target is presented.

In the second simulation, the camera velocities are selected to be the same as the first simulation and the object velocity, $v_p(t)$, is selected as

$$v_p(t) = \begin{bmatrix} -2e^{-0.01t} & -1\sin(0.001t) & -1 \end{bmatrix}^T \text{ m/s.}$$

The object velocity, $v_p(t)$, is slowly time-varying and satisfies Assumption 5.5. The initial conditions are chosen the same as the first simulation. The Γ gain is selected as $\Gamma = \text{diag} \left\{ \begin{bmatrix} 0.090 & 0.23 & 0.2 & 0.215 \end{bmatrix}^T \right\}$. The object velocity in the inertial frame is shown in Fig. 5-5. The observer shows robust performance even in the presence of time-varying object velocities, $v_p(t)$ as seen in the state estimation errors in Fig. 5-6, and the estimated and actual position comparison in Fig. 5-7.

² Since $z(t)$ is measurable from the image, the initial conditions of $\hat{z}(t)$ are selected equal to $z(t_0)$.

³ $\text{diag} \{ \cdot \}$ represents a diagonal matrix constructor.

⁴ The symbols $\alpha_1, \alpha_2, \delta_1, \delta_2$ are introduced in [3].

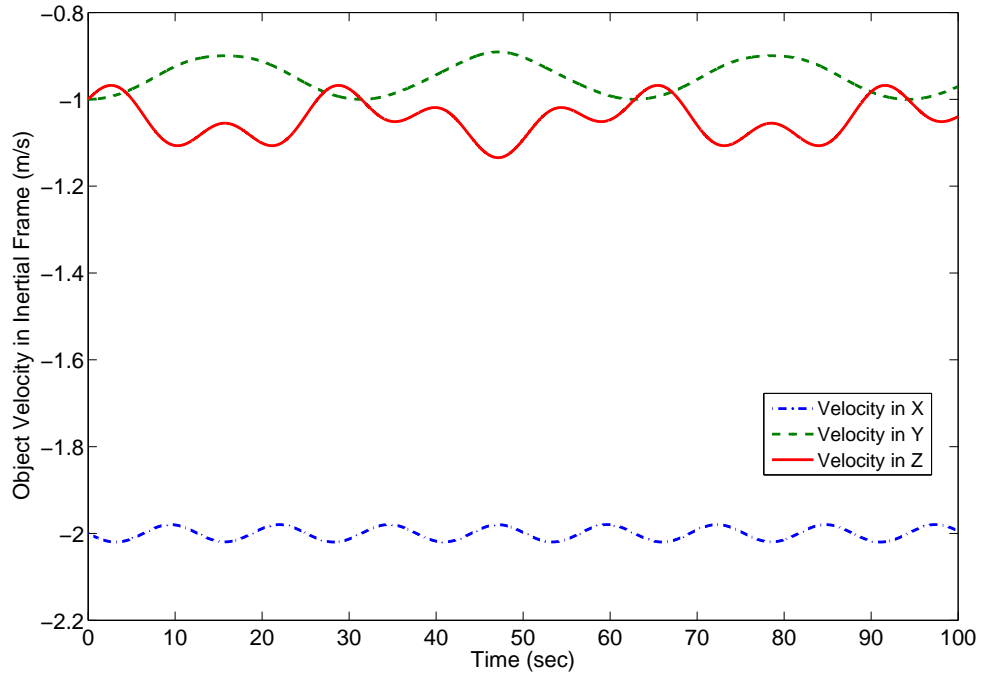


Figure 5-1. The velocity of the moving object measured in the inertial reference frame.

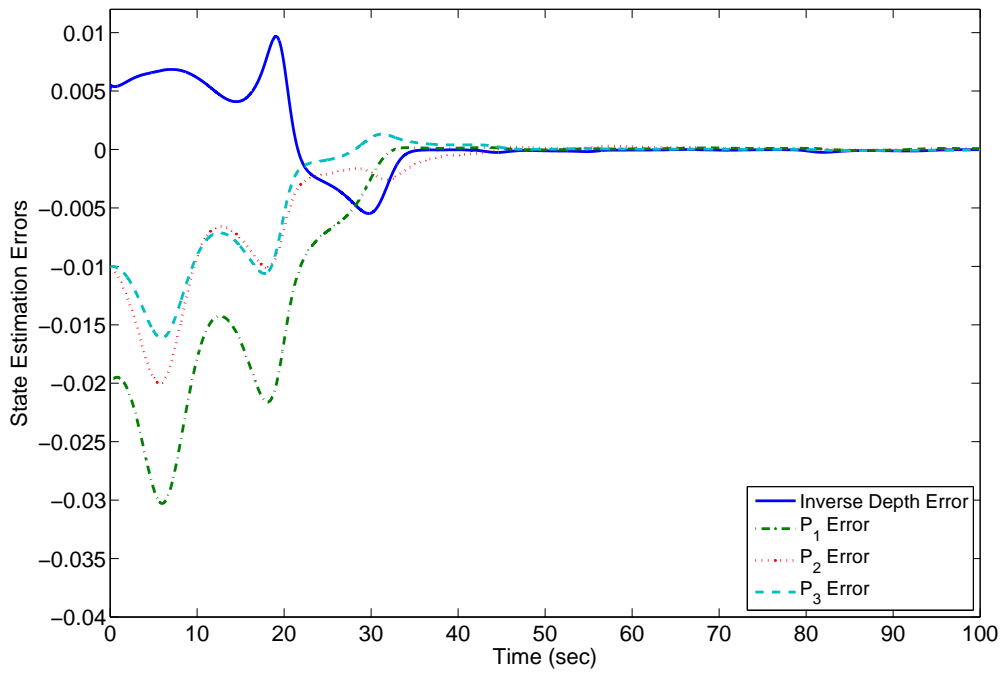


Figure 5-2. State estimation errors using the proposed observer.

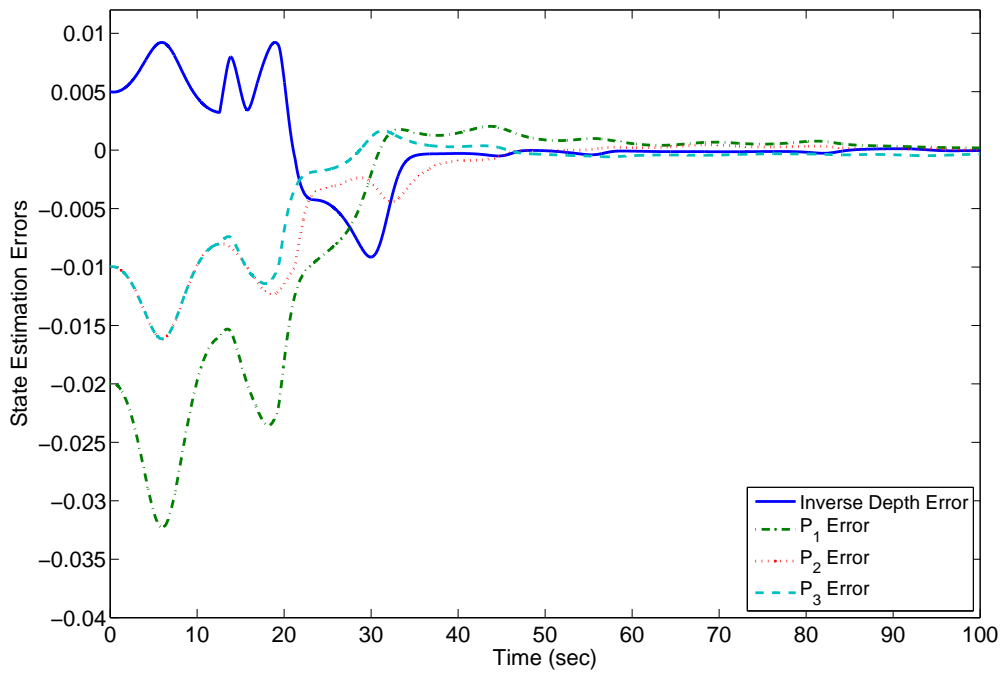


Figure 5-3. State estimation errors using the observer in [3].

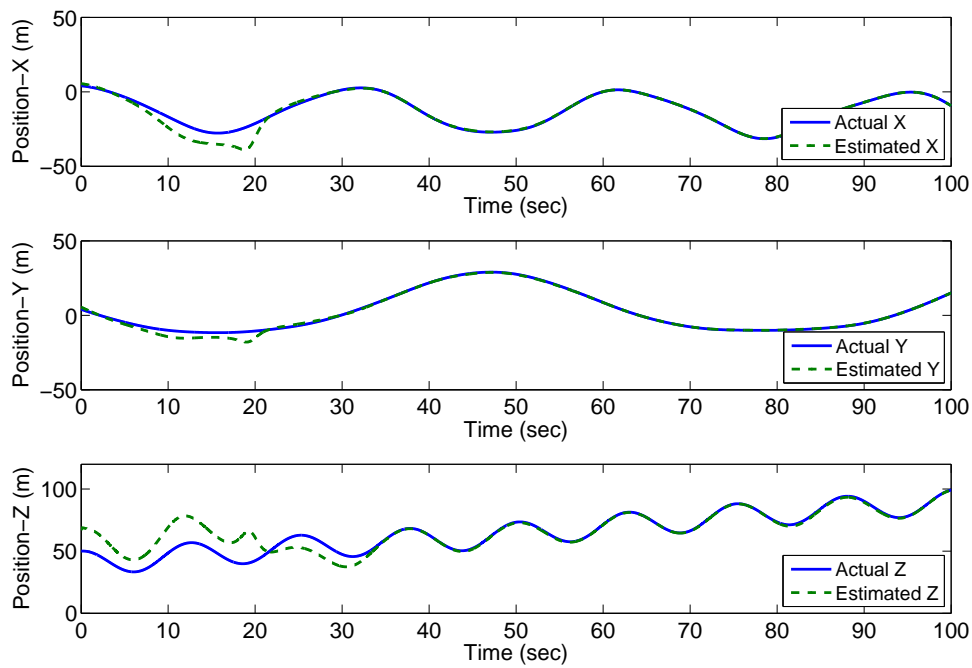


Figure 5-4. Comparison of the actual and estimated 3D relative position of the object and the camera.

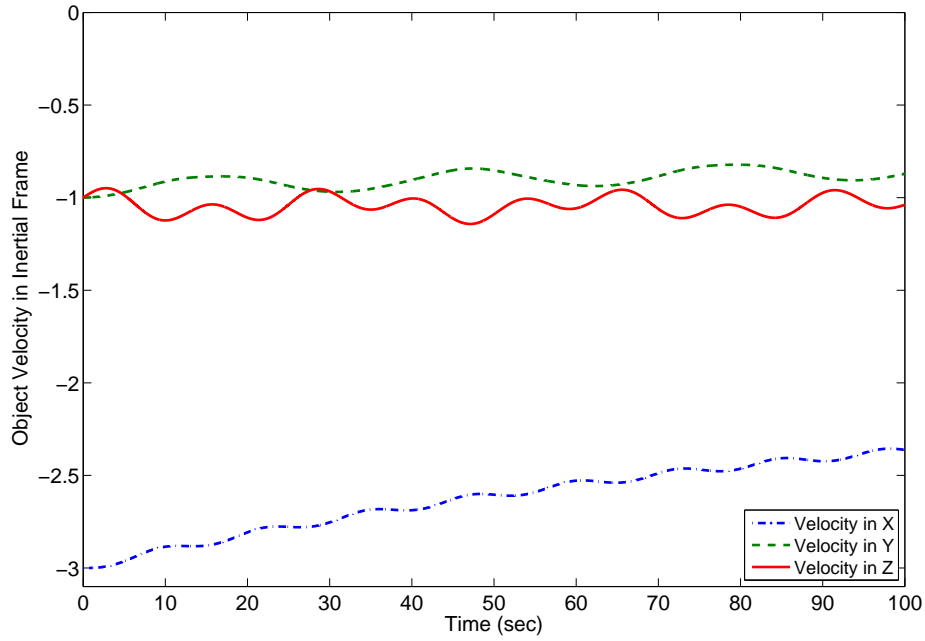


Figure 5-5. The velocity of the moving object measured in the inertial reference frame.

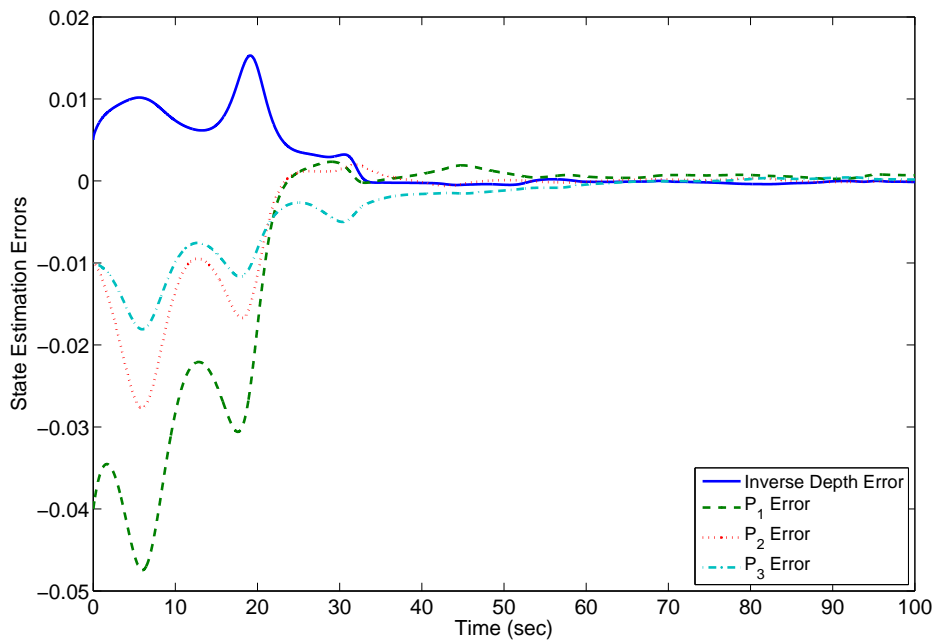


Figure 5-6. State estimation errors for time varying velocity, $v_p(t)$, using the proposed observer.

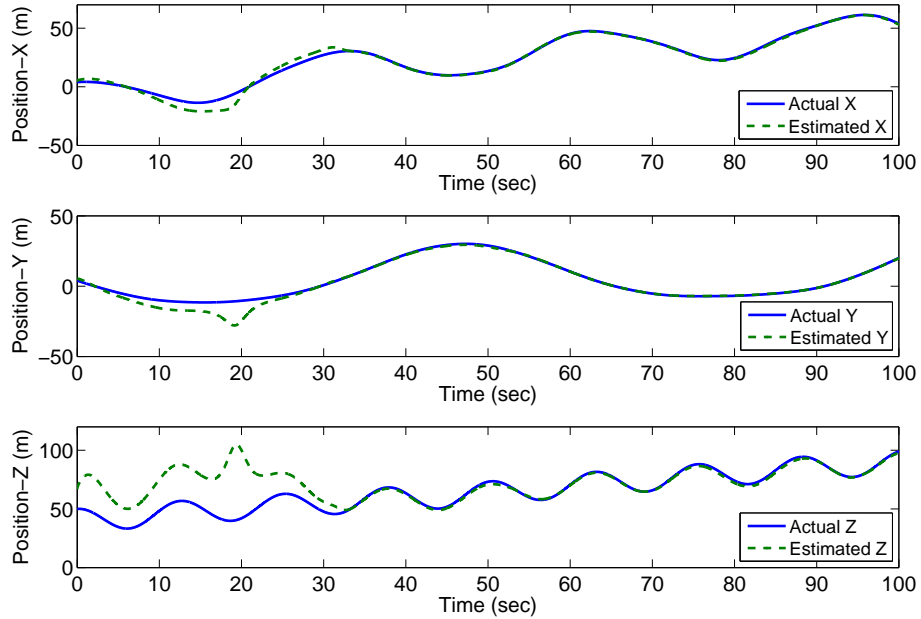


Figure 5-7. Comparison of the actual and estimated 3D relative position of the object and the camera for time-varying object velocity $v_p(t)$.

5.4 Summary

An observer for a class of nonlinear systems is designed. The design is based on an identifier approach where the unmeasurable part of the state is identified using a robust identifier from the output dynamics and the identifier is used to stabilize the error dynamics of the unmeasurable part of the state. It is shown that the observer design improves upon existing solutions to the problem presented in [3] by proving asymptotic estimation error convergence even in the presence of external disturbances. An application of the observer to the structure and motion problem in machine vision is presented. The observer has some advantages over both existing batch solutions and online solutions. New insight on moving object trajectories are developed for online structure and motion estimation when the object is moving.

Chapter 6
 LYAPUNOV-BASED UNKNOWN INPUT OBSERVER FOR A CLASS OF
 NONLINEAR SYSTEMS

In this chapter, a nonlinear UIO is developed for a general class of multi-input multi-output (MIMO) nonlinear systems. Based on the existence of a solution to the Riccati equation, necessary and sufficient existence conditions are derived. The conditions provide guidelines for choosing the observer gain matrix K based on the Lipschitz constant of the nonlinearity present in the dynamics. An algorithm for choosing K based on the Eigenvalue placement is suggested in [52]. In this chapter, K is obtained by solving an LMI feasibility problem.

6.1 Nonlinear Unknown Input Observer

6.1.1 Nonlinear Dynamics

Consider a general class of MIMO nonlinear systems expressed as

$$\begin{aligned} \dot{x} &= f(x, u) + g(y, u) + Dd \\ y &= Cx \end{aligned} \tag{6-1}$$

where $x(t) \in \mathbb{R}^n$ is the state of the system, $u(t) \in \mathbb{R}^m$ is the known control input, $d(t) \in \mathbb{R}^q$ is an unknown input, $y(t) \in \mathbb{R}^p$ is the output of the system¹, $C \in \mathbb{R}^{p \times n}$ is full row rank, $D \in \mathbb{R}^{n \times q}$ is full column rank², $g : \mathbb{R}^p \times \mathbb{R}^m \rightarrow \mathbb{R}^n$ is nonlinear in $y(t)$ and $u(t)$, $f : \mathbb{R}^n \times \mathbb{R}^m \rightarrow \mathbb{R}^n$ is nonlinear in $x(t)$ and $u(t)$, and satisfies the Lipschitz condition $\|f(x, u) - f(\hat{x}, u)\| \leq \gamma_1 \|x - \hat{x}\|$ where $\gamma_1 \in \mathbb{R}^+$, and $\hat{x}(t) \in \mathbb{R}^n$ is an estimate of the unknown state $x(t)$.

¹ It is assumed that $p \geq q$. This is a standard condition present in the UIO literature (cf. [59–70, 72–76, 78]).

² This condition is not restrictive since if $\text{rank}(D) = q_1 < q$ then D can be written as $D = D_1 D_2$ where $\text{rank}(D_1) = q_1$ and the new disturbance $\bar{d}(t) = D_2 d(t)$ [60].

The system in Eq. 7-1 can be written as

$$\begin{aligned}\dot{x} &= Ax + \bar{f}(x, u) + g(y, u) + Dd \\ y &= Cx\end{aligned}\tag{6-2}$$

where $A \in \mathbb{R}^{n \times n}$, and $\bar{f}(x, u) = f(x, u) - Ax$. The auxiliary function $\bar{f}(x, u)$ satisfies the Lipschitz condition [115, 116]

$$\|f(x, u) - f(\hat{x}, u) - A(x - \hat{x})\| \leq (\gamma_1 + \gamma_2) \|x - \hat{x}\|\tag{6-3}$$

where $\gamma_2 \in \mathbb{R}^+$.

6.1.2 UIO Design

The UIO objective is to design an asymptotically converging state observer to estimate $x(t)$ in the presence of an unknown input $d(t)$. To quantify this objective an estimation error is defined as

$$e(t) \triangleq \hat{x}(t) - x(t).\tag{6-4}$$

Based on Eq. 7-8 and the subsequent stability analysis, the UIO for the system in Eq. 7-2 is designed as

$$\begin{aligned}\dot{z} &= Nz + Ly + M\bar{f}(\hat{x}, u) + Mg(y, u) \\ \hat{x} &= z - Ey\end{aligned}\tag{6-5}$$

where $z(t) \in \mathbb{R}^n$ and $N \in \mathbb{R}^{n \times n}$, $L \in \mathbb{R}^{n \times p}$, $M \in \mathbb{R}^{n \times n}$ are designed as [66]³

$$\begin{aligned}M &= I_n + EC \\ N &= MA - KC \\ L &= K(I_p + CE) - MAE\end{aligned}\tag{6-6}$$

³ The subscript of the Identity matrix I defines the dimension of I .

where $E \in \mathbb{R}^{n \times p}$ is subsequently designed, and $K \in \mathbb{R}^{n \times p}$ is a gain matrix which satisfies the inequality

$$Q \triangleq N^T P + PN + (\gamma_1 + \gamma_2)^2 P M M^T P + I_n < 0 \quad (6-7)$$

where $P \in \mathbb{R}^{n \times n}$ is a positive definite, symmetric matrix. Using Eq. 7-4, the equality

$$NM + LC - MA = 0_{n \times n} \quad (6-8)$$

is satisfied, where $0_{i \times j}$ denotes a zero matrix of the dimensions $i \times j$. If E is selected so that

$$E = F + YG \quad (6-9)$$

where $Y \in \mathbb{R}^{n \times p}$ can be chosen arbitrarily, and F and G are given by

$$F \triangleq -D(CD)^\dagger, \quad G \triangleq (I_p - (CD)(CD)^\dagger)$$

then $ECD = -D$ and the following equality is satisfied:

$$MD = (I_n + EC)D = 0_{n \times q}. \quad (6-10)$$

Note that the generalized pseudo inverse of the matrix CD , defined as

$$(CD)^\dagger = \left((CD)^T (CD) \right)^{-1} (CD)^T$$

exists provided $\text{rank}(CD) = q$. Substituting Eq. 7-3 into Eq. 7-8, taking the time derivative of the result, and using Eqs. 7-2 and 7-3 yields

$$\dot{e} = Nz + Ly + M\bar{f}(\hat{x}, u) - (I_n + EC)Ax - (I_n + EC)\bar{f}(x, u) - (I_n + EC)Dd \quad (6-11)$$

Using Eqs. 7-8 and 7-4, and the conditions in Eqs. 6-8 and 6-10 the error system in Eq. 7-9 can be written as

$$\dot{e} = Ne + M(\bar{f}(\hat{x}, u) - \bar{f}(x, u)). \quad (6-12)$$

6.1.3 Necessary and Sufficient Condition

Lemma 6.1 provides a condition on the gain matrix K for the inequality in Eq. 7-5 to hold. The result of Lemma 6.1 is used in Theorem 6.1 to develop a necessary and sufficient condition for the existence of the observer presented in Section 6.1.2.

Lemma 6.1. *The matrix inequality in Eq. 7-5 is satisfied if the pair (MA, C) is observable, K is selected so that $MA - KC$ is Hurwitz⁴, and the following condition is satisfied*

$$\min_{\omega \in \mathbb{R}^+} \sigma_{\min}(MA - KC - j\omega I_n) > \sqrt{\gamma_3}(\gamma_1 + \gamma_2) \quad (6-13)$$

where $\sigma_{\min}(\cdot)$ denotes the minimum singular value of a matrix, and $\gamma_3 \triangleq \lambda_{\max}(MM^T)$.

Proof. The proof of this theorem is inspired by the work in [52] which developed necessary and sufficient conditions for an observer design for nonlinear systems with known inputs. The development of the proof is based on the conditions for the existence of a solution to the algebraic Riccati equation (ARE). Consider a Hamiltonian matrix H , defined as

$$H = \begin{bmatrix} \bar{A} & R \\ -Q & -\bar{A}^T \end{bmatrix}$$

where \bar{A} , Q and R are real matrices, Q and R are symmetric. If the Hamiltonian, has no imaginary eigenvalues, R is either positive semi-definite or negative semi-definite and the pair (\bar{A}, R) is stabilizable, then there exists a symmetric solution to the ARE

$$\bar{A}^T X + X\bar{A} + XRX + Q = 0_{n \times n}.$$

Consider a Hamiltonian matrix, \bar{H} , defined as

⁴ As pointed out in [52], stability of the matrix $MA - KC$ is not sufficient for the error system of the form (7-10) to be stable.

$$\bar{H} = \begin{bmatrix} MA - KC & (\gamma_1 + \gamma_2)^2 MM^T \\ -\varepsilon I_n - I_n & -(MA - KC)^T \end{bmatrix}$$

associated with the ARE

$$(MA - KC)^T P + P(MA - KC) + (\gamma_1 + \gamma_2)^2 P M M^T P + I_n + \varepsilon I_n = 0_{n \times n} \quad (6-14)$$

where $\varepsilon \in \mathbb{R}^+$ is a small constant. Since (MA, C) is observable, the matrix K can be selected so that $MA - KC$ is Hurwitz, and hence the pair $(MA - KC, (\gamma_1 + \gamma_2)^2 MM^T)$ is stabilizable. If \bar{H} has no eigenvalues on the imaginary axis then there exists a symmetric positive definite solution to the ARE in Eq. 6-14. In the following, it is proven that if the condition in Eq. 7-11 is satisfied then the eigenvalues of \bar{H} do not lie on the imaginary axis. The proof is given by contradiction.

Consider the characteristic equation of \bar{H} as

$$\det \begin{bmatrix} \lambda I_n - (MA - KC) & -(\gamma_1 + \gamma_2)^2 MM^T \\ \varepsilon I_n + I_n & \lambda I_n + (MA - KC)^T \end{bmatrix} = 0$$

where $\lambda \in \mathbb{C}$ denotes an eigenvalue of \bar{H} . Using the fact that for any two real matrices \check{A} and \check{B} , if $\det(\check{B}) = 1$, then $\det(\check{A}) = \det(\check{A}) \det(\check{B}) = \det(\check{A}\check{B})$, the characteristic equation can be written as

$$\det \begin{bmatrix} \lambda I_n - (MA - KC) & -(\gamma_1 + \gamma_2)^2 MM^T \\ \varepsilon I_n + I_n & \lambda I_n + (MA - KC)^T \end{bmatrix} \begin{bmatrix} I_n & -\frac{1}{1+\varepsilon} [\lambda I_n + (MA - KC)^T] \\ 0 & I_n \end{bmatrix} = 0.$$

Let the eigenvalues of \bar{H} be on the imaginary axis i.e., $\lambda = j\omega$, then the characteristic equation becomes

$$\det \left[[j\omega I_n - (MA - KC)] \begin{bmatrix} j\omega I_n + (MA - KC)^T \end{bmatrix} + (1 + \varepsilon) (\gamma_1 + \gamma_2)^2 MM^T \right] = 0.$$

Using $(MA - KC - j\omega I_n)^* = j\omega I_n + (MA - KC)^T$, the characteristic equation is transformed into following equality,

$$\det [(MA - KC - j\omega I_n)(MA - KC - j\omega I_n)^* - (1 + \varepsilon)(\gamma_1 + \gamma_2)^2 MM^T] = 0. \quad (6-15)$$

Now, it is shown that if Eq. 7-11 is true then the equality in Eq. 6-15 cannot be satisfied which proves that \bar{H} cannot have eigenvalues on the imaginary axis.

Since the singular values of a matrix are continuous functions of the elements of the matrix, $\sigma_{\min}(MA - KC - j\omega I_n)$ is a continuous function of $\omega \in \mathbb{R}^+$ and $\sigma_{\min}(MA - KC - j\omega I_n) \rightarrow \infty$ as $\omega \rightarrow \infty$. Hence, there exists a finite $\omega \in \mathbb{R}^+$ for which $\sigma_{\min}(MA - KC - j\omega I_n)$ has a minimum [52,104]. That is, $\exists \omega_1 : \min_{\omega \in \mathbb{R}^+} \sigma_{\min}(MA - KC - j\omega I_n) = \sigma_{\min}(MA - KC - j\omega_1 I_n) = \gamma_{\min}$. Using Eq. 7-11 $\gamma_{\min} = \sigma_{\min}(MA - KC - j\omega_1 I_n) > \sqrt{\gamma_3}(\gamma_1 + \gamma_2)$ and the following inequality holds:

$$(MA - KC - j\omega I_n)(MA - KC - j\omega I_n)^* \geq \gamma_{\min}^2 I_n \quad \forall \omega$$

⁵ where $\gamma_{\min} \in \mathbb{R}^+$, and $(\cdot)^*$ denotes the complex conjugate transpose of a matrix. By choosing ε such that $\gamma_{\min}^2 I_n > (\gamma_1 + \gamma_2)^2 (1 + \varepsilon) \gamma_3 I_n \geq (\gamma_1 + \gamma_2)^2 (1 + \varepsilon) (MM^T)$, the following inequality can be obtained:

$$(MA - KC - j\omega I_n)(MA - KC - j\omega I_n)^* - (1 + \varepsilon)(\gamma_1 + \gamma_2)^2 MM^T > 0_{n \times n}. \quad (6-16)$$

which contradicts the conclusion of Eq. 6-15 that $(MA - KC - j\omega I_n)(MA - KC - j\omega I_n)^* - (1 + \varepsilon)(\gamma_1 + \gamma_2)^2 MM^T$ is a singular matrix. Hence, if Eq. 7-11 holds, then \bar{H} can not have eigenvalues on the imaginary axis. Thus, a symmetric solution to Eq. 6-14 exists and Eq. 7-5 is satisfied. \square

⁵ For any two matrices \mathcal{X} and \mathcal{Y} , the expression $\mathcal{X} \geq (>) \mathcal{Y}$ means the matrix $\mathcal{X} - \mathcal{Y}$ is positive semi-definite (positive definite).

Theorem 6.1. *The nonlinear UIO in Eq. 7-3 is exponentially stable such that $\exists \xi, \zeta \in \mathbb{R}^+$*

$$\|e(t)\| \leq \zeta \|e(t_0)\| \exp(-\xi t)$$

iff $\text{rank}(CD) = q$ and the condition in Eq. 7-11 is satisfied.

Proof. (Sufficiency) If $\text{rank}(CD) = q$ then the solution to Eq. 6-10 exists. For proving the sufficiency of the condition in Eq. 7-11, consider a Lyapunov candidate function

$V(e) : \mathbb{R}^n \rightarrow \mathbb{R}$ defined as

$$V = e^T P e. \quad (6-17)$$

The Lyapunov function satisfies

$$\lambda_{\min}(P) \|e\|^2 \leq V \leq \lambda_{\max}(P) \|e\|^2 \quad (6-18)$$

where λ_{\min} and λ_{\max} are the minimum and maximum eigenvalues of the matrix P . Taking the time derivative of Eq. 6-17 along the trajectories of Eq. 7-10 yields

$$\begin{aligned} \dot{V} &= e^T (N^T P + P N) e + 2e^T P M (\bar{f}(\hat{x}, u) - \bar{f}(x, u)) \\ \dot{V} &\leq e^T (N^T P + P N) e + 2 \|e^T P M\| \|f(\hat{x}, u) - f(x, u) - A(x - \hat{x})\| \\ \dot{V} &\leq e^T (N^T P + P N) e + 2 \|e^T P M\| \gamma_1 \|e\| + 2 \|e^T P M\| \gamma_2 \|e\|. \end{aligned}$$

Using the norm inequality

$$2\gamma_i \|e^T P M\| \|e\| \leq \gamma_i^2 \|e^T P M\|^2 + \|e\|^2, \quad \forall i = \{1, 2\},$$

the upper bound on \dot{V} is given by

$$\begin{aligned} \dot{V} &\leq e^T (N^T P + P N) e + (\gamma_1 + \gamma_2)^2 e^T P M M^T P e + e^T e \\ \dot{V} &\leq e^T (N^T P + P N + (\gamma_1 + \gamma_2)^2 P M M^T P + I_n) e \\ \dot{V} &\leq e^T Q e. \end{aligned} \quad (6-19)$$

If the condition in Eq. 7–11 is satisfied, then Lemma 6.1 can be invoked to conclude $Q < 0$ and hence $\dot{V} < 0$. Using Eqs. 6–17–6–19 the upper bounds for $V(e)$ and $e(t)$ can be developed as

$$V(e) \leq V(e(0)) \exp(-\xi t)$$

where $\xi = \frac{\lambda_{max}(Q)}{\lambda_{min}(P)}$ and

$$\|e(t)\| \leq \zeta \|e(0)\| \exp(-\xi t)$$

where $\zeta = \frac{\lambda_{max}(P)}{\lambda_{min}(P)}$.

(Necessity) If $rank(CD) < q$ then a solution to Eq. 6–10 does not exist and the UIO in Eq. 7–3 cannot be designed. The necessity of the condition in Eq. 7–11, is proven with the help of following proposition. If the observer gain K is chosen such that

$$\min_{\omega \in \mathbb{R}^+} \sigma_{min}(MA - KC - j\omega I_n) \leq \sqrt{\gamma_3}(\gamma_1 + \gamma_2) \quad (6-20)$$

then there exists at least one matrix $V \in \mathbb{R}^{n \times n}$ such that $M\bar{f}(x, u) = Vx$ has the Lipschitz constant $\sqrt{\gamma_3}(\gamma_1 + \gamma_2)$, and the error dynamics in Eq. 7–10 are unstable. The proof of this proposition follows the proof of Theorem 3 in [52]. Consider $\bar{\omega}_1 \in \mathbb{R}^+$ such that

$$\sigma_{min}(MA - KC - j\bar{\omega}_1 I_n) < \bar{\gamma} \quad (6-21)$$

where $\bar{\gamma} \in \mathbb{R}^+$ and satisfies $\bar{\gamma} < \sqrt{\gamma_3}(\gamma_1 + \gamma_2)$. Choose $\bar{\varepsilon} > 0$ such that $\bar{\gamma} + \bar{\varepsilon} < \sqrt{\gamma_3}(\gamma_1 + \gamma_2)$. Since Eq. 6–21 holds, $\exists W \in \mathbb{R}^{n \times n} : \|W\|_2 < \bar{\gamma}$,⁶ and $(MA - KC - j\bar{\omega}_1 I_n + W)$ is singular. Let

$$V = W + \bar{\varepsilon} I_n \quad (6-22)$$

thus, $\|V\|_2 \leq \|W\|_2 + \|\bar{\varepsilon} I_n\|_2 < \sqrt{\gamma_3}(\gamma_1 + \gamma_2)$. Since $(MA - KC - j\bar{\omega}_1 I_n + W)$ is singular, using Eq. 6–22 $(MA - KC + V - \bar{\varepsilon} I_n - j\bar{\omega}_1 I_n)$ is singular and the matrix $MA - KC + V$ has at least one eigenvalue with a positive real-part, viz., $\bar{\varepsilon} + j\bar{\omega}_1$. Hence, if the condition

⁶ The norm $\|\cdot\|_2$ denotes the maximum singular value.

in Eq. 7-11 is not satisfied, then the error dynamics $\dot{e} = (MA - KC)e + Ve$ are not asymptotically stable. □

6.1.4 Conditions for Choosing Matrix A

In this section, conditions on choosing A are provided based on the necessary and sufficient observer existence conditions. The existence conditions for the UIO in Eq. 7-3 can be summarized as follows:

1. (MA, C) is observable,
2. ⁷ $rank(CD) = rank(D) = q$,
3. $MA - KC$ is Hurwitz, and
4. Eq. 7-11 holds.

Hence, matrix A should be chosen such that (MA, C) is observable. Since $rank(CD) = rank(D) = q$, it is proven subsequently that the observability of the pair (MA, C) is equivalent to the following rank condition [66, 72]

$$rank \begin{bmatrix} \lambda I_n - A & D \\ C & 0_{p \times q} \end{bmatrix} = n + q, \quad \forall \lambda \in \mathbb{C}. \quad (6-23)$$

Thus, A in Eq. 7-2 should be selected so that Eq. 7-12 is satisfied. The condition in Eq. 7-12 facilitates the selection of A based on the system matrices and hence circumvents the computation of M for checking the observability of (MA, C) . Another criteria on the selection of A is to minimize the Lipschitz constant in Eq. 6-3.

In the following, Theorem 6.2 proves the relationship between Eq. 7-12 and the observability of the pair (MA, C) and uses the result proved in Lemma 6.2.

⁷ Since $rank(CD) = \min\{rank(C), rank(D)\}$ and by assumption $rank(C) = p, p \geq q$, the rank of D must be q for rank of CD to be q .

Lemma 6.2. *If $\text{rank}(CD) = \text{rank}(D) = q$, D^\dagger denotes a left inverse of matrix D , then⁸ $\text{Ker}(D^\dagger) \cap \text{Ker}(M) = \phi$, where ϕ is a null set, and if $\text{rank}(M) = n - q$ then*

$$\text{rank} \begin{bmatrix} M \\ D^\dagger \end{bmatrix} = n.$$

Proof. From Eq. 6–10 $MD = 0_{n \times q}$, hence, $\text{Ker}(M) = \text{Im}(D)$. Also, $\text{Ker}(D^\dagger) = \text{Ker}(D^T)$ and $\text{Ker}(D^T) = (\text{Im}(D))^\perp$ [117]. Hence, $\text{Ker}(D^\dagger) \cap \text{Ker}(M) = (\text{Im}(D))^\perp \cap \text{Im}(D) = \phi$. Using the fact that the null spaces of M and D^\dagger do not have any common

elements, $\begin{bmatrix} M \\ D^\dagger \end{bmatrix} h = \begin{bmatrix} Mh \\ D^\dagger h \end{bmatrix} \neq 0_{n+q} \forall h \in \mathbb{R}^n$, where 0_{n+q} is a zero vector of dimension $n + q$, and $\dim \left(\text{Ker} \begin{bmatrix} M \\ D^\dagger \end{bmatrix} \right) = 0$. Using $\text{rank} \begin{bmatrix} M \\ D^\dagger \end{bmatrix} + \dim \left(\text{Ker} \begin{bmatrix} M \\ D^\dagger \end{bmatrix} \right) = n$, [117]

it can be concluded that $\text{rank} \begin{bmatrix} M \\ D^\dagger \end{bmatrix} = n$. □

Theorem 6.2. [66] *Assume $\text{rank}(CD) = \text{rank}(D) = q$, and $\text{rank}(M) = n - q$. The pair (MA, C) is observable iff Eq. 7–12 holds.*

Proof. The rank condition $\text{rank}(CD) = \text{rank}(D) = q$ is obtained as a necessary and sufficient condition for the existence of an unknown input observer for linear systems in [60, 62, 66, 72]. Using the Popov-Bellman-Hautus (PBH) test of observability, the pair (MA, C) is observable iff

$$\text{rank} \begin{bmatrix} \lambda I_n - MA \\ C \end{bmatrix} = n \quad \forall \lambda \in \mathcal{C}. \quad (6-24)$$

⁸ $\text{Ker}(\cdot)$ denotes a kernel of a null space of a matrix and $\text{Im}(\cdot)$ denotes an image space of a matrix.

Consider the following matrix rank properties

Property 1: $\text{rank}(\tilde{A}\tilde{B}) = \text{rank}\tilde{B}$ if $\tilde{A} \in \mathbb{R}^{l \times r}$ with $\text{rank } r$ and $\tilde{B} \in \mathbb{R}^{r \times s}$,

Property 2: $\text{rank}(\tilde{A}\tilde{B}) = \text{rank}\tilde{A}$ if $\tilde{B} \in \mathbb{R}^{l \times r}$ with $\text{rank } l$ and $\tilde{A} \in \mathbb{R}^{s \times l}$.

Using Eqs. 7-4, 6-24 and the Property 1, following equality is obtained

$$\begin{aligned} \text{rank} \begin{bmatrix} \lambda M - MA \\ C \end{bmatrix} &= \text{rank} \begin{bmatrix} I_n & \lambda E \\ 0_{p \times n} & I_p \end{bmatrix} \begin{bmatrix} \lambda I_n - MA \\ C \end{bmatrix} \\ &= \text{rank} \begin{bmatrix} \lambda I_n - MA \\ C \end{bmatrix} = n \quad \forall \lambda \in \mathcal{C}. \end{aligned}$$

Given matrices $S \in \mathbb{R}^{(n+q+p) \times (n+p)}$ and $T \in \mathbb{R}^{(n+q) \times (n+q)}$ as

$$S = \begin{bmatrix} M & 0_{n \times p} \\ D^\dagger & 0_{q \times p} \\ 0_{p \times p} & I_p \end{bmatrix}, \quad T = \begin{bmatrix} I_n & 0_{n \times q} \\ -(\lambda D^\dagger - D^\dagger A) & I_q \end{bmatrix}$$

the result in Lemma 6.2 shows that S is full column rank (i.e., $\text{rank}(S) = n + p$), and T is full row rank matrix (i.e., $\text{rank}(T) = n + q$). Using Properties 1 and 2, the following rank condition can be obtained

$$\begin{aligned} \text{rank} \begin{bmatrix} \lambda I_n - A & D \\ C & 0_{p \times q} \end{bmatrix} &= \text{rank} \left(S \begin{bmatrix} \lambda I_n - A & D \\ C & 0_{p \times q} \end{bmatrix} T \right) = \text{rank} \begin{bmatrix} \lambda M - MA & 0_{n \times q} \\ 0_{q \times n} & I_q \\ C & 0_{p \times q} \end{bmatrix} \\ &= q + \text{rank} \begin{bmatrix} \lambda M - MA \\ C \end{bmatrix} \quad \forall \lambda \in \mathcal{C}, \end{aligned}$$

which implies that $\text{rank} \begin{bmatrix} \lambda M - MA \\ C \end{bmatrix} = n$. Hence, if $\text{rank}(M) = n - q$, the observability of (MA, C) and Eq. 7-12 are equivalent. \square

Remark 6.1. The condition in Eq. 7-12 implies that the pair (C, A, D) has no invariant zeros. For a LTI system with unknown inputs, Eq. 7-12 implies observability [72]. In [72], it is mentioned that system observability is not sufficient for the existence of an UIO for LTI systems. The condition $\text{rank}(CD) = \text{rank}(D) = q$ is also required for the existence of the observer. The condition $\text{rank}(CD) = \text{rank}(D) = q$ and Eq. 7-12 are defined as the strong* detectability⁹ condition and are necessary and sufficient conditions for the existence of UIO for LTI systems. For a general nonlinear system, necessary and sufficient UIO existence conditions are unknown and is an open problem in the literature.

6.1.5 LMI Formulation

In the following section, the condition in Eq. 7-5 is reformulated as an LMI feasibility problem. The matrices P , K and Y should be selected such that the sufficient condition for the observer error stability in Eq. 7-5 is satisfied. Substituting N and M from Eq. 7-4 into Eq. 7-5 yields

$$\begin{aligned} & (MA - KC)^T P + P(MA - KC) + I \\ & + (\gamma_1 + \gamma_2)^2 P(I + EC)(I + EC)^T P < 0. \end{aligned} \quad (6-25)$$

After using Eq. 6-9, the inequality in Eq. 6-25 can be expressed as

$$\begin{aligned} & A^T(I + FC)^T P + P(I + FC)A + A^T C^T G^T P_Y^T \\ & + P_Y G C A - C^T P_K^T - P_K C + I \\ & + (\gamma_1 + \gamma_2)^2 (P + PFC + P_Y GC)(P + PFC + P_Y GC)^T < 0 \end{aligned} \quad (6-26)$$

where $P_Y = PY$ and $P_K = PK$. For the observer synthesis, the matrices Y , K and $P > 0$ should be computed such that the matrix inequality in Eq. 7-5 is satisfied. Since

⁹ The notion of 'strong* detectability' is introduced in [72] to distinguish from a strong detectability condition which implies minimum-phase condition for linear systems with unknown inputs.

$P > 0$, P^{-1} exists, and Y and K can be computed using $Y = P^{-1}P_Y$, and $K = P^{-1}P_K$. Using Schur's complement, the inequality in Eq. 6–26 can be transformed into the matrix inequality

$$\begin{bmatrix} P_1 & \beta R \\ \beta R^T & -I \end{bmatrix} < 0 \quad (6-27)$$

where

$$P_1 = A^T (I + FC)^T P + P (I + FC) A + A^T C^T G^T P_Y^T + P_Y G C A - C^T P_K^T - P_K C + I,$$

$$R = P + PFC + P_Y GC,$$

$$\beta = \gamma_1 + \gamma_2.$$

The matrix inequality in Eq. 6–27 is an LMI in variables P , P_Y , and P_K . The LMI feasibility problem can be solved using standard LMI algorithms [118] and is a problem of finding P , P_Y and P_K such that β is maximized. Maximizing β is equivalent to maximizing γ_1 which means the observer can be designed for nonlinear functions with a larger Lipschitz constant. If the LMI in Eq. 6–27 is feasible, then a solution to Eq. 7–5 exists. Hence, the LMI feasibility problem is a sufficient condition for the stability of the observer. Alternatively, a sufficient numerical algorithm is presented in [52] to compute K such that Eq. 7–11 is satisfied. The algorithm is based on the eigenvalue placement approach and is a sufficient condition for Eq. 7–11 to be satisfied.

6.2 Summary

An UIO for a class of nonlinear systems is developed. Necessary and sufficient conditions for the existence of the UIO are developed and computation of the observer gain is achieved via an LMI formulation. The necessary and sufficient conditions developed for the existence of developed UIO extend the necessary and sufficient conditions of UIOs for LTI systems and the existence conditions of nonlinear observer for Lipschitz nonlinear systems with known inputs.

Chapter 7
APPLICATION OF THE UNKNOWN INPUT OBSERVER TO THE STRUCTURE
ESTIMATION

In this chapter, the unknown input observer developed in Chapter 6 is applied to the structure and motion estimation problem with a moving object. The developed causal algorithm requires less restrictive assumptions on the object's motion than existing approaches. The object is assumed to be moving on a ground plane with arbitrary velocities observed by a downward looking camera with arbitrary linear motion. No assumptions are made on the minimum number of points or minimum number of views required to estimate the structure. Feature point data and camera velocity data from each image frame is required. Simulation results are presented to show the effectiveness of the proposed approach.

7.1 Structure and Motion Estimation

7.1.1 Structure and Motion from Motion (SaMfM) Objective

The objective of SaMfM is to recover the structure (i.e., Euclidean coordinates with a scaling factor) and motion (i.e., velocities) of moving objects observed by a moving camera, assuming that all camera velocities are known. In this chapter, an observer is presented which estimates the structure of the moving object with respect to the moving camera. It is assumed that one or more feature points on the object are tracked in each image frame and camera velocities are recorded using sensors such as an IMU. The camera is assumed to be internally calibrated. Estimating the structure of an object is equivalent to estimating the state $x(t)$ in each image frame. Based on the definition of the state in Eq. 2-3, the structure of the moving object can be estimated by scaling $\hat{x}_1(t)$ and $\hat{x}_2(t)$ by $\hat{x}_3(t)$.

7.1.2 Nonlinear Unknown Input Observer

Consider the following system

$$\begin{aligned}\dot{x} &= f(x, u) + g(y, u) + Dd \\ y &= Cx\end{aligned}\tag{7-1}$$

where $x(t) \in \mathbb{R}^3$ is a state of the system, $u(t) \in \mathbb{R}^6$ is a measurable control input, $d(t) \in \mathbb{R}$ is an unmeasurable input, $y(t) \in \mathbb{R}^2$ is output of the system, the function $f(x, u)$ is nonlinear in $x(t)$ and $u(t)$ and satisfies the Lipschitz condition $\|f(x, u) - f(\hat{x}, u)\| \leq \gamma_1 \|x - \hat{x}\|$ where $\gamma_1 \in \mathbb{R}^+$. The system in Eq. 2-12 can be represented in the form of Eq. 7-1 with

$$\begin{aligned}f(x, u) &= \begin{bmatrix} (v_{cx} - y_1 v_{cz})x_3 \\ (v_{cy} - y_2 v_{cz})x_3 \\ -x_3^2 v_{cz} - y_2 x_3 \omega_1 + y_1 x_3 \omega_2 \end{bmatrix}, \\ g(y, u) &= \begin{bmatrix} -y_1 y_2 \omega_1 + (1 + y_1^2) \omega_2 - y_2 \omega_3 \\ -(1 + y_2^2) \omega_1 + y_1 y_2 \omega_2 + y_1 \omega_3 \\ 0 \end{bmatrix},\end{aligned}$$

and $C = \begin{bmatrix} 1 & 0 & 0 \\ 0 & 1 & 0 \end{bmatrix}$ is full row rank, $D \in \mathbb{R}^{3 \times 1}$ is full column rank, and $q = 1$.

The system in (7-1) can be written in the following form

$$\begin{aligned}\dot{x} &= Ax + \bar{f}(x, u) + g(y, u) + Dd \\ y &= Cx\end{aligned}\tag{7-2}$$

where $A \in \mathbb{R}^{3 \times 3}$, and $\bar{f}(x, u) = f(x, u) - Ax$. The function $\bar{f}(x, u)$ satisfies the Lipschitz condition $\|f(x, u) - f(\hat{x}, u) - A(x - \hat{x})\| \leq (\gamma_1 + \gamma_2) \|x - \hat{x}\|$, where $\gamma_2 \in \mathbb{R}^+$. An exponentially converging state observer is designed to estimate $x(t)$ in the presence of an unknown input $d(t)$ (i.e., the moving object's velocity).

An unknown input reduced order state observer for the system in Eq. 7-2 is designed as

$$\begin{aligned}\dot{z} &= Nz + Ly + M\bar{f}(\hat{x}, u) + Mg(y, u) \\ \hat{x} &= z - Ey\end{aligned}\tag{7-3}$$

where $\hat{x}(t) \in \mathbb{R}^3$ is an estimate of the unknown state $x(t)$, $z(t) \in \mathbb{R}^3$ is an auxiliary signal, the matrices $N \in \mathbb{R}^{3 \times 3}$, $L \in \mathbb{R}^{3 \times 2}$, $E \in \mathbb{R}^{3 \times 2}$, $M \in \mathbb{R}^{3 \times 3}$ are designed as [66]

$$\begin{aligned}M &= I_3 + EC \\ N &= MA - KC \\ L &= K(I + CE) - MAE\end{aligned}\tag{7-4}$$

where E is subsequently designed and $K \in \mathbb{R}^{3 \times 2}$ is a gain matrix which satisfies the inequality

$$Q \triangleq N^T P + PN + (\gamma_1 + \gamma_2)^2 PMM^T P + I_3 < 0\tag{7-5}$$

where $P \in \mathbb{R}^{n \times n}$ is a positive definite, symmetric matrix. Using Eq. 7-4 the equality $NM + LC - MA = 0_{3 \times 3}$ is satisfied, and if E is selected as

$$E = F + YG\tag{7-6}$$

where $Y \in \mathbb{R}^{3 \times 2}$ can be chosen arbitrarily, and F and G are given by

$$F \triangleq -D(CD)^\dagger, \quad G \triangleq (I_2 - (CD)(CD)^\dagger)$$

then $ECD = -D$, and the following equality is satisfied:

$$MD = (I_3 + EC)D = 0_{3 \times 1}.\tag{7-7}$$

Since $\text{rank}(CD) = 1$, the generalized pseudo inverse of the matrix CD exists and is given by

$$(CD)^\dagger = \left((CD)^T (CD) \right)^{-1} (CD)^T.$$

To quantify the estimation objective an estimation error is defined as

$$e(t) \triangleq \hat{x}(t) - x(t) = z - Ey - x. \quad (7-8)$$

Taking the time derivative of the estimation error and using Eqs. 7-2 and 7-3 yields

$$\begin{aligned} \dot{e} &= \dot{z} - (I + EC)\dot{x}, \\ \dot{e} &= Nz + Ly + M\bar{f}(\hat{x}, u) - (I + EC)Ax \\ &\quad - (I + EC)\bar{f}(x, u) - (I + EC)Dd. \end{aligned} \quad (7-9)$$

Using Eqs. 7-4 and 7-8, the error system in Eq. 7-9 can be written as

$$\begin{aligned} \dot{e} &= Ne + (NM + LC - MA)x \\ &\quad + M(\bar{f}(\hat{x}, u) - \bar{f}(x, u)) - MDd. \end{aligned}$$

Using Eq. 7-7 and $NM + LC - MA = 0$, the error dynamics can be written as

$$\dot{e} = Ne + M(\bar{f}(\hat{x}, u) - \bar{f}(x, u)). \quad (7-10)$$

7.1.3 Stability Analysis

Theorem 7.1. *The nonlinear unknown input observer in Eq. 7-3 is exponentially stable iff*

$$\min_{\omega \in \mathbb{R}^+} \sigma_{\min}(MA - KC - j\omega I_3) > \sqrt{\gamma_3}(\gamma_1 + \gamma_2) \quad (7-11)$$

where $\sigma_{\min}(\cdot)$ denotes the minimum singular value of a matrix, and $\gamma_3 \triangleq \lambda_{\max}(MM^T)$.

Proof. The proof follows directly from the proof of Theorem 6.1. □

7.1.4 Conditions for Stability

The SaMfM observer developed in this chapter follows the same existence conditions developed in Chapter 6. In this section, conditions specific to the SaMfM dynamics are developed. The inequality in Eq. 7-5 is satisfied if the pair (MA, C) is observable [66] and the condition in Eq. 7-11 is satisfied. If the pair (MA, C) is observable then the gain matrix K can be selected so that $N = MA - KC$ is Hurwitz. Since $\text{rank}(CD) = \text{rank}(D) = 1$ the condition

$$\text{rank} \begin{bmatrix} sI_n - A & D \\ C & 0 \end{bmatrix} = 4, \quad \forall s \in \mathbb{C} \quad (7-12)$$

implies that the pair (MA, C) is observable [66].

7.1.5 Conditions on Object Trajectories

The dynamics in Eq. 2-12 cannot be transformed into the form of Eq. 7-1 because of the constraints on number of outputs p and number of unknown inputs q . However, by making some assumptions on the motion of a camera and the viewed object, the dynamics in Eq. 2-12 can be transformed in the form of Eq. 7-1. In this section, two specific scenarios are discussed.

Example 1: The camera is undergoing arbitrary purely translational motion, i.e., the angular velocities of the camera are zero and the object is moving along a straight line with time-varying unknown velocities. For this case, choices of $\bar{R}(t)$ and $\bar{v}_p(t)$ in Eq. 2-9 become¹ $\bar{R} = I_3$, and $\bar{v}_p(t) = \begin{bmatrix} d_1(t) & 0 & 0 \end{bmatrix}^T$, or $\bar{v}_p(t) = \begin{bmatrix} 0 & d_2(t) & 0 \end{bmatrix}^T$, or $\bar{v}_p(t) = \begin{bmatrix} 0 & 0 & d_3(t) \end{bmatrix}^T$, or $\bar{v}_p(t) = \begin{bmatrix} d_4(t) & d_5(t) & 0 \end{bmatrix}^T$, etc., where $d_i(t) \in \mathbb{R} \forall i = \{1, \dots, 5\}$ is the unknown time-varying object velocity.

¹ w.l.o.g. the camera coordinate frame when the image capture starts can be set as Inertial coordinate frame.

Example 2: A downward looking camera is undergoing arbitrary translational motion along with the angular velocity along the Z-direction (an axis pointing downwards). The object is moving on a ground plane (i.e., X-Y plane) with arbitrary time-varying velocities. In this case, the rotation matrix $\bar{R}(t)$ is given by

$$\bar{R} = \begin{bmatrix} \cos(\theta(t)) & \sin(\theta(t)) & 0 \\ -\sin(\theta(t)) & \cos(\theta(t)) & 0 \\ 0 & 0 & 1 \end{bmatrix} = \begin{bmatrix} \bar{R}_s & 0_{2 \times 1} \\ 0_{1 \times 2} & 1 \end{bmatrix}$$

where $\theta(t) \in [-2\pi, 2\pi)$ is the rotation angle between the current camera coordinate frame and inertial coordinate frame, and $\bar{R}_s(t) \in \mathbb{R}^{2 \times 2}$ represents the upper left 2×2 block of the $\bar{R}(t)$. The object velocity in the inertial frame is represented as $\bar{v}_p(t) = \begin{bmatrix} \bar{d}_1(t) & \bar{d}_2(t) & 0 \end{bmatrix}^T$, where $\bar{d}_1(t), \bar{d}_2(t) \in \mathbb{R}$. The camera angular velocity is such that

$$\bar{R}\bar{v}_p = u \tag{7-13}$$

where $u(t) = \begin{bmatrix} \bar{d}_3(t) & 0 & 0 \end{bmatrix}^T$ or $u(t) = \begin{bmatrix} 0 & \bar{d}_4(t) & 0 \end{bmatrix}^T$, and $\bar{d}_3(t), \bar{d}_4(t) \in \mathbb{R}$ are unknown time-varying quantities. The equality in Eq. 7-13 can be achieved if $\bar{R}_s \begin{bmatrix} \bar{d}_1(t) & \bar{d}_2(t) \end{bmatrix}^T = \bar{u}$, where $\bar{u}(t) = \begin{bmatrix} \bar{d}_5 & 0 \end{bmatrix}^T$ or $\bar{u}(t) = \begin{bmatrix} 0 & \bar{d}_6 \end{bmatrix}^T$, where $\bar{d}_5(t), \bar{d}_6(t) \in \mathbb{R}$. Physically, the condition in Eq. 7-13 represents camera motions such that the heading direction of the camera is parallel or perpendicular to the object's heading direction in the X-Y plane. For example, consider an object undergoing a circular motion in the X-Y plane with unknown time-varying velocities observed by a camera undergoing an arbitrary linear motion in the X-Y-Z plane and circular motion along the downward looking Z-direction.

7.2 Simulation

Consider a moving camera observing an object moving along a straight line. Camera velocities are given by $v_c(t) = \begin{bmatrix} 2 & 1 & 0.5\cos(t/2) \end{bmatrix}^T$ and $\omega(t) = \begin{bmatrix} 0 & 0 & 1 \end{bmatrix}^T$. The object velocity is selected such that $v_p(t) = \begin{bmatrix} 0.5 & 0 & 0 \end{bmatrix}^T$. The camera calibration matrix is

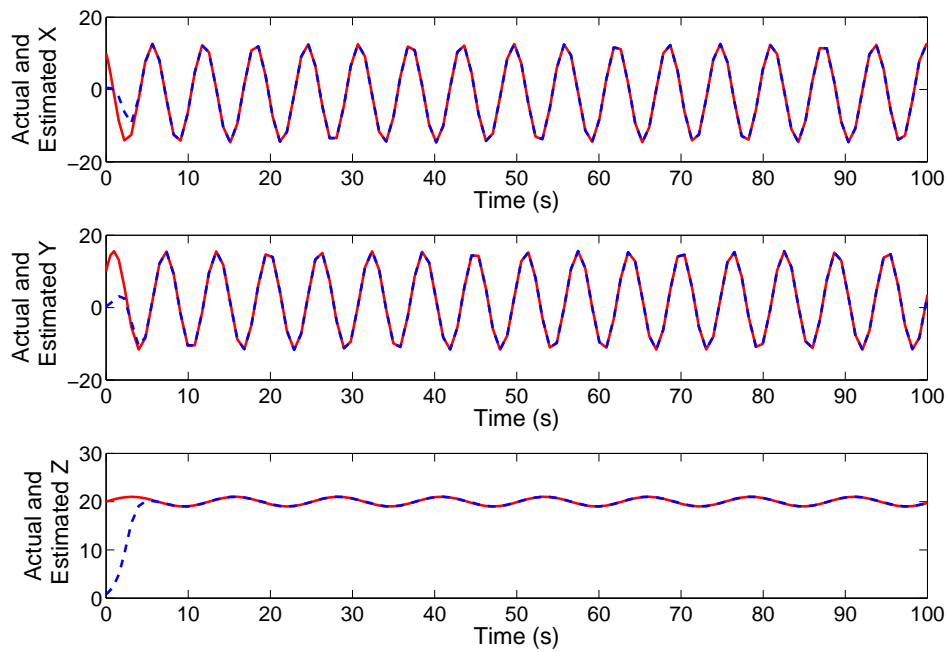


Figure 7-1. Comparison of the actual and estimated X,Y and Z positions of a moving object with respect to a moving camera.

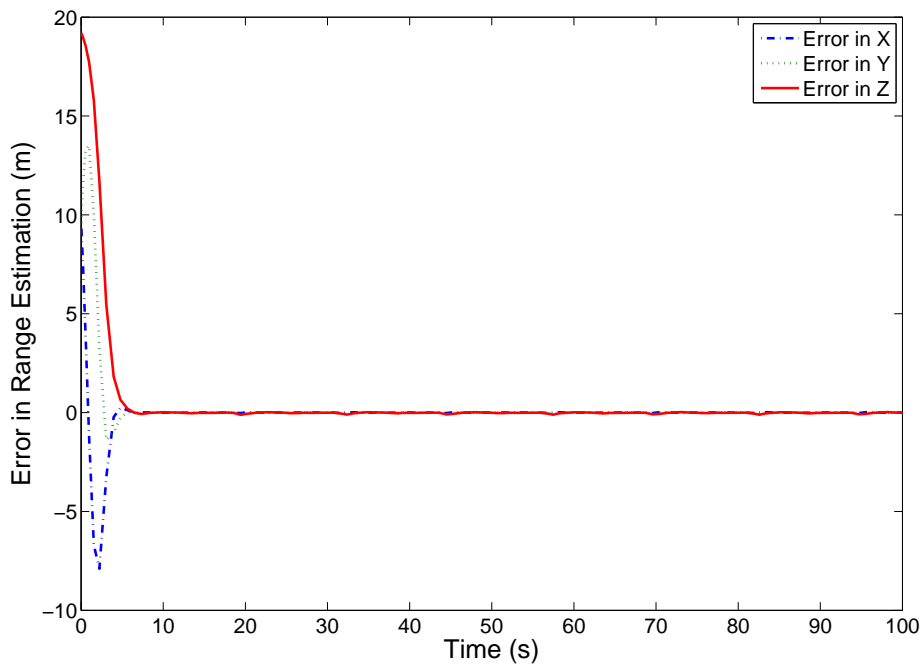


Figure 7-2. Error in the range estimation of the moving object.

given by

$$A_c = \begin{bmatrix} 720 & 0 & 320 \\ 0 & 720 & 240 \\ 0 & 0 & 1 \end{bmatrix}.$$

Matrices A , C and D are

$$A = \begin{bmatrix} 0 & -1 & 2 \\ 1 & 0 & 1 \\ 0 & 0 & 0 \end{bmatrix}, \quad C = \begin{bmatrix} 1 & 0 & 0 \\ 0 & 1 & 0 \end{bmatrix}, \quad D = \begin{bmatrix} 1 \\ 0 \\ 0 \end{bmatrix}.$$

An LMI is formed as shown in Section 6.1.5 of Chapter 6. The matrix Y and the gain matrix K are computed using the LMI feasibility command '*feasp*' in Matlab and are given by

$$K = \begin{bmatrix} 0.8278 & 0 \\ 0 & 0.8278 \\ -1.5374 & 0 \end{bmatrix}, \quad Y = \begin{bmatrix} 0 & 0 \\ 0 & -1 \\ 0 & -1.5374 \end{bmatrix}.$$

Fig. 7-1 shows comparison of the actual and estimated X, Y and Z coordinates of the object in the camera coordinate frame. Fig. 7-2 shows the range estimation error between the moving object and the moving camera.

7.3 Summary

In this chapter, a nonlinear observer is developed to solve the SaMfM problem. The proposed algorithm estimates the structure of a moving object using a moving camera with less restrictive assumptions on the object motion. The object motion is assumed to be along a straight line or in a plane observed by a moving airborne camera. The algorithm improves on our previous work in [119] by relaxing the constant object velocity assumption to arbitrary object motion in a straight line or in a plane. The observer-based approach is causal and does not assume a minimum number of views or feature points. The structure estimation is insensitive to the object motion in the sense that the state estimation is completely decoupled from the object motion which acts as an exogenous

disturbance input under certain conditions on the object motion. Future efforts will focused on designing a reduced-order observer for structure as well as motion estimation.

Chapter 8 CONCLUSION AND FUTURE WORK

8.1 Conclusion

New real-time solutions to a general structure and motion problem in computer vision are presented. As opposed to the traditional batch methods, an observer-based approach is developed. A nonlinear state model is used to derive new reduced-order structure estimation algorithms when the object is stationary and the camera is moving with full or partial camera velocity information. Solutions of the structure estimation of the stationary object have been extended to the moving object moving camera scenario. For the moving object moving camera scenario, the moving object's velocity is considered as an external unknown time-varying disturbance. Two approaches to the observer design in the presence of external unknown disturbance are presented. In the first approach, the disturbance is considered to be a vanishing disturbance. Conditions on the object's motion are developed which satisfies the assumptions required by the observer design. These conditions put certain constraints in the form of differential equations on the moving object's motion and the angular velocity of the camera. For a special case of constant camera angular velocities, an analytical relation between the object's motion and the camera angular velocities is developed where asymptotic estimator convergence can be achieved. In the second approach, a time varying object velocity is considered as an unknown input to the system and an unknown input observer for a general class of nonlinear systems is developed. The UIO approach does not require the external disturbances to be vanishing but requires it to satisfy a minimum phase condition for the transfer function from the disturbance to the output of the system. For the moving camera moving object dynamics the minimum phase condition provides new constraints on the velocity of the moving object and the angular velocity of the camera. These constraints can accommodate a more general moving camera moving object scenario. Results in Chapters 5 and 6 for the moving camera moving object scenario advances the state-of-the-art in terms of amount

of data required and by enabling real-time estimation. The specific contributions of each result are mentioned below.

In Chapter 3, a reduced order nonlinear observer is presented for the structure estimation of points on a stationary object using a moving camera. The observer is globally exponentially stable provided an observability condition is satisfied. The observer is also shown to be exponentially stable under a relaxed observability condition. Hence, the result improves the domain of applicability to a larger set of camera motions than previous algorithms. The observer is shown to be robust against external disturbances. Comparison of the observer performance against two existing observers is presented in theory and in numerical simulations.

Chapter 4 develops a reduced order observer for the estimation of the structure of a stationary target with respect to a moving camera, along with two unknown time-varying linear and angular camera velocities. The observer requires the image coordinates of the feature points on the object, a single linear camera velocity, and the corresponding linear camera acceleration in any one of the three camera coordinate axes. Under a physically motivated PE condition, asymptotic convergence of the observer error is guaranteed. The result advances state of the art SaM algorithms in terms of a fewer number of measurable signals required by the algorithm.

In Chapter 5, a nonlinear observer for moving camera moving object scenario is developed. The object's velocity is considered as an external disturbance. Under a PE condition, Lyapunov analysis is performed to show that the observation error converges to zero. The observer is robust in the sense that the estimation error converges even in the presence of $\mathcal{L}_2[0, \infty)$ time-varying disturbances.

In Chapter 6, an UIO is developed for a general class of nonlinear systems. Necessary and sufficient conditions are developed for the UIO design. The result improves the state of the art UIO algorithms by developing an UIO for a more general class of nonlinear systems. The application of the UIO to the moving camera moving object scenario is

presented in Chapter 7. Conditions on the object motion are developed which satisfies the assumptions of the UIO. The application of the UIO to the moving camera moving object scenario enables solutions to the problems in real-time and significantly advances the state of the art structure and motion algorithms given moving objects in terms of real-time computation, and amount of data required by the estimation algorithm.

8.2 Future Work

The work in this dissertation opens new doors for research in the domain of nonlinear observer design, and structure and motion. In this section, open problems related to the work in this dissertation are discussed. The open problems are segregated into two broad technical disciplines, viz.; Nonlinear Observer and Structure and Motion.

Nonlinear Observer

1. For all the observer designs in this dissertation, the output equation is considered to be continuous. A practically inspired problem in the observer design is: how to design nonlinear observers with the intermittent and/or time-delayed observations. Recently, Kalman filter and extended Kalman filter with intermittent observations have been developed in [120, 121]. The parallels of these results to the general nonlinear observer design should be pursued.
2. In Chapter 5, a very special class of nonlinear systems is considered. One interesting question is can one generalize the output dynamics in Eq. 5-1 to contain nonlinear terms of the unmeasurable state $x(t)$? This extension will increase the application domain of the observer design approach to multiple areas.
3. In Chapter 5, asymptotic error convergence is achieved by assuming that the external disturbance is asymptotically converging to zero. Under suitable conditions, is the asymptotic error convergence achievable with bounded non-vanishing disturbance?
4. In Chapter 5, can the PE assumption be relaxed to show the error convergence? There is related work in [122] which introduced relaxed-PE notion for parameter

identification and adaptive control literature. Similar ideas may be adapted for the observer design to relax the PE assumptions.

5. In Chapter 6, the class of nonlinear systems considered for the UIO has a constant matrix D multiplied by a time-varying disturbance. Designing a UIO for time-varying or state dependent D matrix for the general class of nonlinear systems is an open problem.
6. In Chapter 6, designing necessary and sufficient conditions under which UIO exists for a general class of nonlinear systems is an open problem. Recently, necessary and sufficient conditions are developed for the existence of UIO for state affine systems in [71]. The extension of such results for a more general class of nonlinear systems should be pursued.

Structure and Motion

1. In Chapter 7, the approach for structure and motion estimation of the moving object requires some constraints on the object and camera motions. Existing batch methods solves the problem by putting some geometric constraints on the object trajectory but requires more than two images to perform the estimation. Future efforts should try to incorporate some geometric constraints on the object motion with the state space differential equation model so that a generalized solution to the structure and motion problem can be developed which will potentially relax the existing conditions on the camera and object motion.
2. In this dissertation, the surface of the object is considered as a Lambertian surface, i.e., there is no reflection of the surrounding scene and the feature points on the object can be tracked easily. This observation raises a question: can online solutions be developed for the structure and motion estimation problem when the object's surface is specular, i.e., reflects the surroundings. Recently, in [123, 124] some geometric solutions to the problem are developed. An online solution to this problem does not appear to exist.

Appendix A
PROOF OF POSITIVENESS OF P

Integrating (5-13), the following expression can be obtained

$$P(t) = P(0) - \int_0^t L(\tau) d\tau. \quad (\text{A-1})$$

Using (5-3) and (5-14) the integral of $L(t)$ can be written as

$$\begin{aligned} \int_0^t L(\tau) d\tau &= \int_0^t \dot{e}_1^T(\tau) \chi_1(\tau) d\tau - \rho \int_0^t \dot{e}_1^T(\tau) \operatorname{sgn}(e_1(\tau)) d\tau \\ &\quad + \int_0^t \alpha e_1^T(\tau) (\chi_1(\tau) - \rho \operatorname{sgn}(e_1(\tau))) d\tau. \end{aligned} \quad (\text{A-2})$$

Using integration by parts for the first integral in (A-2) and using the property

$$\int_0^t \dot{e}_1^T(\tau) \operatorname{sgn}(e_1(\tau)) d\tau = \rho \sum_{i=1}^2 |e_{1i}(t)| - \rho \sum_{i=1}^2 |e_{1i}(0)|$$

the integral of $L(t)$ can be expressed as

$$\begin{aligned} \int_0^t L(\tau) d\tau &= e_1^T(t) \chi_1(t) - e_1^T(0) \chi_1(0) - \rho \sum_{i=1}^2 |e_{1i}(t)| + \rho \sum_{i=1}^2 |e_{1i}(0)| \\ &\quad + \alpha \int_0^t e_1^T(\tau) \chi_1(\tau) d\tau - \int_0^t (e_1^T(\tau) \dot{\chi}_1(\tau) + \alpha \rho |e_1(\tau)|) d\tau. \end{aligned} \quad (\text{A-3})$$

Using (A-1) and (A-3), $P(t)$ can be written as

$$\begin{aligned} P(t) &= -e_1^T(t) \chi_1(t) + e_1^T(0) \chi_1(0) + \rho \sum_{i=1}^{n_1} |e_{1i}(t)| - \rho \sum_{i=1}^{n_1} |e_{1i}(0)| \\ &\quad - \alpha \int_0^t e_1^T(\tau) \chi_1(\tau) d\tau + \int_0^t \left(e_1^T(\tau) \dot{\chi}_1(\tau) + \alpha \rho \sum_{i=1}^{n_1} |e_{1i}(\tau)| \right) d\tau \\ &\quad + \rho \sum_{i=1}^{n_1} |e_{1i}(0)| - e_1^T(0) \chi_1(0) \end{aligned}$$

$$\begin{aligned}
P(t) &= -e_1^T(t) \chi_1(t) + \rho \sum_{i=1}^{n_1} |e_{1i}(t)| \\
&\quad - \alpha \int_0^t e_1^T(\tau) \chi_1(\tau) d\tau + \int_0^t (e_1^T(\tau) \dot{\chi}_1(\tau) + \alpha \rho |e_1(\tau)|) d\tau \\
P(t) &\geq \sum_{i=1}^{n_1} |e_{1i}(t)| (\rho_i - |\chi_{1i}(t)|) \\
&\quad + \int_0^t \sum_{i=1}^{n_1} |e_{1i}(\tau)| (\alpha \rho_i - \alpha |\chi_{1i}(\tau)| - |\dot{\chi}_{1i}(\tau)|) d\tau \tag{A-4}
\end{aligned}$$

If ρ is selected according to (5-11), then using (5-9) and (A-4) $P \geq 0$.

Appendix B
OBSERVABILITY CONDITIONS

B.1 Observability Condition in Chapter 4

From Chapter 4, $J(y_1, y_2, b_3) \in \mathbb{R}^{2 \times 3}$ is given by

$$J = \begin{bmatrix} -y_1 b_3 & 1 & 0 \\ -y_2 b_3 & 0 & 1 \end{bmatrix}$$

and

$$J^T J = \begin{bmatrix} (y_1^2 + y_2^2) b_3^2 & -y_1 b_3 & -y_2 b_3 \\ -y_1 b_3 & 1 & 0 \\ -y_2 b_3 & 0 & 1 \end{bmatrix}.$$

Taking the integral of $J^T(y_1, y_2, b_3) J(y_1, y_2, b_3)$ yields

$$\int_t^{t+\delta} J^T J d\tau = \begin{bmatrix} \int_t^{t+\delta} (y_1^2(\tau) + y_2^2(\tau)) b_3^2(\tau) d\tau & \int_t^{t+\delta} -y_1(\tau) b_3(\tau) d\tau & \int_t^{t+\delta} -y_2(\tau) b_3(\tau) d\tau \\ \int_t^{t+\delta} -y_1(\tau) b_3(\tau) d\tau & \delta & 0 \\ \int_t^{t+\delta} -y_2(\tau) b_3(\tau) d\tau & 0 & \delta \end{bmatrix}. \quad (\text{B-1})$$

The conditions for which (B-1) becomes rank 2 are:

1. $b_3(t) = 0 \forall t \in [t, t + \delta]$
2. $y_1(t) = c_1, y_2(t) = c_2$, and $b_3(t) = c_3 \forall t \in [t, t + \delta]$ where $c_i \forall i = \{1, 2, 3\}$ are constants.

The first condition indicates that the camera must be moving in Z-direction during any small duration of time $[t, t + \delta]$. The second condition is satisfied if the image point is not moving for a small duration of time. The image point is constant only if the camera is not moving or if the camera is traveling along the ray projected by the feature point on the camera image.

B.2 Observability Condition in Chapter 5

From Chapter 5,

$$J = \begin{bmatrix} v_{cx} - y_1 v_{cz} & -1 & 0 & y_1 \\ v_{cy} - y_2 v_{cz} & 0 & -1 & y_2 \end{bmatrix}.$$

Let $h_1(t) = v_{cx}(t) - y_1(t)v_{cz}(t)$ and $h_2(t) = v_{cy}(t) - y_2(t)v_{cz}(t)$. The integral of $J^T(v_{cx}, v_{cy}, v_{cz}, y_1, y_2)J(v_{cx}, v_{cy}, v_{cz}, y_1, y_2)$ is given by

$$\int_t^{t+\bar{\varepsilon}} J^T J d\tau = \begin{bmatrix} \int_t^{t+\bar{\varepsilon}} h_1^2(\tau) + h_2^2(\tau) d\tau & \int_t^{t+\bar{\varepsilon}} -h_1(\tau) d\tau \\ \int_t^{t+\bar{\varepsilon}} -h_1(\tau) d\tau & \bar{\varepsilon} \\ \int_t^{t+\bar{\varepsilon}} -h_2(\tau) d\tau & 0 \\ \int_t^{t+\bar{\varepsilon}} y_1(\tau) h_1(\tau) + y_2(\tau) h_2(\tau) d\tau & \int_t^{t+\bar{\varepsilon}} -y_1(\tau) d\tau \\ \int_t^{t+\bar{\varepsilon}} -h_2(\tau) d\tau & \int_t^{t+\bar{\varepsilon}} y_1(\tau) h_1(\tau) + y_2(\tau) h_2(\tau) d\tau \\ 0 & \int_t^{t+\bar{\varepsilon}} -y_1(\tau) d\tau \\ \bar{\varepsilon} & \int_t^{t+\bar{\varepsilon}} -y_2(\tau) d\tau \\ \int_t^{t+\bar{\varepsilon}} -y_2(\tau) d\tau & \int_t^{t+\bar{\varepsilon}} y_1^2(\tau) + y_2^2(\tau) d\tau \end{bmatrix} \quad (\text{B-2})$$

The integral in (B-2) is not full rank if:

1. $y_1(t) = \bar{c}_1$, and $y_2(t) = \bar{c}_2 \forall t \in [t, t + \bar{\varepsilon}]$ where \bar{c}_1, \bar{c}_2 are constants.
2. $h_1(t) = \bar{c}_3$, and $h_2(t) = \bar{c}_4 \forall t \in [t, t + \bar{\varepsilon}]$ where \bar{c}_3, \bar{c}_4 are constants.

Condition 1 can be satisfied only if camera is stationary or if the camera is moving along the projected ray of the feature point on the image plane. For both the cases, $h_1(t) = h_2(t) = 0$, hence, the first condition is a subset of the second condition. The second condition implies the following ratio inequalities,

$$\frac{v_{cx} - \bar{c}_3}{v_{cz}} = \frac{X}{Z}, \text{ and } \frac{v_{cy} - \bar{c}_4}{v_{cz}} = \frac{Y}{Z}. \quad (\text{B-3})$$

The conditions in (B-3) are satisfied if the camera is moving along the ray projected by the feature point on the image plane or if the camera velocities are not persistently changing.

REFERENCES

- [1] F. Morbidi and D. Prattichizzo, “Range estimation from a moving camera: an immersion and invariance approach,” in *Proc. IEEE Int. Conf. Robot. Autom.*, Kobe, Japan, May 2009, pp. 2810–2815.
- [2] A. D. Luca, G. Oriolo, and P. R. Giordano, “Feature depth observation for image-based visual servoing: Theory and experiments,” *Int. J. Robot. Res.*, vol. 27, no. 10, pp. 1093–1116, 2008.
- [3] X. Chen and H. Kano, “State observer for a class of nonlinear systems and its application to machine vision,” *IEEE Trans. Autom. Control*, vol. 49, no. 11, pp. 2085–2091, 2004.
- [4] Y. Ma, S. Soatto, J. Kosecká, and S. Sastry, *An Invitation to 3-D Vision*. Springer, 2004.
- [5] B. Lucas and T. Kanade, “An iterative image registration technique with an application to stereo vision,” in *Int. Joint Conf. Artif. Intell.*, vol. 3. Citeseer, 1981, p. 3.
- [6] H. Bay, T. Tuytelaars, and L. Van Gool, “Surf: Speeded up robust features,” *Lect. Notes Comput. Sci.*, vol. 3951, pp. 404–417, 2006.
- [7] D. G. Lowe, “Distinctive image feature from scale-invariant keypoints,” *Int. J. Comput. Vision*, vol. 60, pp. 91–110, 2004.
- [8] R. Hartley and A. Zisserman, *Multiple View Geometry in Computer Vision*. Cambridge University Press, 2003.
- [9] J. Oliensis, “Exact two-image structure from motion,” *IEEE Trans. Pattern Anal. Mach. Intell.*, vol. 24, no. 12, pp. 1618–2002, 2002.
- [10] —, “A critique of structure-from-motion algorithms,” *Comput. Vis. Image Understand.*, vol. 80, pp. 172–214, 2000.
- [11] P. Sturm and B. Triggs, “A factorization based algorithm for multi-image projective structure and motion,” *Lect. Notes Comput. Sci.*, vol. 1065, pp. 709–720, 1996.
- [12] A. Bartoli and P. Sturm, “Constrained structure and motion from multiple uncalibrated views of a piecewise planar scene,” *Int. J. Comput. Vision*, vol. 52, no. 1, pp. 45–64, 2003.
- [13] —, “Structure-from-motion using lines: Representation, triangulation, and bundle adjustment,” *Comput. Vis. Image Understand.*, vol. 100, no. 3, pp. 416–441, 2005.
- [14] S. Soatto, R. Frezza, and P. Perona, “Motion estimation via dynamic vision,” *IEEE Trans. Autom. Control*, vol. 41, no. 3, pp. 393–413, 1996.

- [15] G. Hu, D. Aiken, S. Gupta, and W. E. Dixon, "Lyapunov-based range identification for paracatadioptric systems," *IEEE Trans. Autom. Control*, vol. 53, no. 7, pp. 1775–1781, Aug. 2008.
- [16] V. Chitrakaran, D. M. Dawson, W. E. Dixon, and J. Chen, "Identification of a moving object's velocity with a fixed camera," *Automatica*, vol. 41, no. 3, pp. 553–562, 2005.
- [17] S. Soatto and P. Perona, "Reducing "structure from motion": A general framework for dynamic vision, part 1: Modeling," *IEEE Trans. Pattern Anal. Mach. Intell.*, vol. 20, no. 9, pp. 933–942, 1998.
- [18] A. Azarbayejani and A. P. Pentland, "Recursive estimation of motion, structure, and focal length," *IEEE Trans. Pattern Anal. Mach. Intell.*, vol. 17, no. 6, pp. 562–575, 1995.
- [19] W. E. Dixon, Y. Fang, D. M. Dawson, and T. J. Flynn, "Range identification for perspective vision systems," *IEEE Trans. Autom. Control*, vol. 48, no. 12, pp. 2232–2238, Dec. 2003.
- [20] G. Quian and R. Chellappa, "Structure from motion using sequential monte carlo methods," *Int. J. Comput. Vision*, vol. 59, pp. 5–31, 2004.
- [21] O. Dahl, F. Nyberg, and A. Heyden, "Nonlinear and adaptive observers for perspective dynamic systems," in *Proc. Am. Control Conf.*, New York City, USA, July 2007, pp. 966–971.
- [22] A. De Luca, G. Oriolo, and P. Giordano, "On-line estimation of feature depth for image-based visual servoing schemes," in *Proc. IEEE Int. Conf. Robot. Autom.*, 2007, pp. 2823–2828.
- [23] M. Jankovic and B. Ghosh, "Visually guided ranging from observations points, lines and curves via an identifier based nonlinear observer," *Syst. Contr. Lett.*, vol. 25, no. 1, pp. 63–73, 1995.
- [24] L. Matthies, T. Kanade, and R. Szeliski, "Kalman filter-based algorithm for estimating depth from image sequence," *Int. J. Comput. Vision*, vol. 3, pp. 209–236, 1989.
- [25] H. Kano, B. K. Ghosh, and H. Kanai, "Single camera based motion and shape estimation using extended Kalman filtering," *Math. Comput. Modell.*, vol. 34, pp. 511–525, 2001.
- [26] A. Chiuso, P. Favaro, H. Jin, and S. Soatto, "Structure from motion causally integrated over time," *IEEE Trans. Pattern Anal. Mach. Intell.*, vol. 24, no. 4, pp. 523–535, 2002.

- [27] D. Karagiannis and A. Astolfi, “A new solution to the problem of range identification in perspective vision systems,” *IEEE Trans. Autom. Control*, vol. 50, no. 12, pp. 2074–2077, 2005.
- [28] L. Ma, C. Cao, N. Hovakimyan, C. Woolsey, and W. E. Dixon, “Fast estimation for range identification in the presence of unknown motion parameters,” *IMA J. Appl. Math.*, vol. 75, no. 2, pp. 165–189, 2010.
- [29] S. Ramalingam, S. Lodha, and P. Sturm, “A generic structure-from-motion framework,” *Comput. Vis. Image. Understand.*, vol. 103, no. 3, pp. 218–228, 2006.
- [30] B. Ghosh and E. Loucks, “A realization theory for perspective systems with applications to parameter estimation problems in machine vision,” *IEEE Trans. Autom. Control*, vol. 41, no. 12, pp. 1706–1722, 1996.
- [31] —, “A perspective theory for motion and shape estimation in machine vision,” *SIAM J. Contr. Optim.*, vol. 33, no. 5, pp. 1530–1559, 1995.
- [32] O. Dahl and A. Heyden, “Dynamic structure from motion based on nonlinear adaptive observers,” in *International Conference on Pattern Recognition*, 2008, pp. 1–4.
- [33] S. Avidan and A. Shashua, “Trajectory triangulation: 3D reconstruction of moving points from a monocular image sequence,” *IEEE Trans. Pattern Anal. Mach. Intell.*, vol. 22, no. 4, pp. 348–357, Apr 2000.
- [34] D. Segal and A. Shashua, “3D reconstruction from tangent-of-sight measurements of a moving object seen from a moving camera,” *Lect. Notes Comput. Sci.*, vol. 1842, pp. 621–631, 2000.
- [35] M. Han and T. Kanade, “Reconstruction of a scene with multiple linearly moving objects,” in *Proc. IEEE Conf. Comput. Vis. Pattern Recognit.*, vol. II, 2000, pp. 542–549.
- [36] P. Sturm, “Structure and motion for dynamic scenes—the case of points moving in planes,” *Lect. Notes Comput. Sci.*, vol. 2351, pp. 867–882, 2002.
- [37] J. Kaminski and M. Teicher, “A general framework for trajectory triangulation,” *J. Math. Imag. Vis.*, vol. 21, no. 1, pp. 27–41, 2004.
- [38] M. Han and T. Kanade, “Reconstruction of a scene with multiple linearly moving objects,” *Int. J. Comput. Vision*, vol. 59, no. 3, pp. 285–300, 2004.
- [39] R. Vidal, Y. Ma, S. Soatto, and S. Sastry, “Two-view multibody structure from motion,” *Int. J. Comput. Vision*, vol. 68, no. 1, pp. 7–25, 2006.
- [40] C. Yuan and G. Medioni, “3D reconstruction of background and objects moving on ground plane viewed from a moving camera,” in *Comput. Vision Pattern Recognit.*, vol. 2, 2006, pp. 2261 – 2268.

- [41] H. Park, T. Shiratori, I. Matthews, and Y. Sheikh, “3D reconstruction of a moving point from a series of 2D projections,” in *Euro. Conf. on Comp. Vision*, vol. 6313, 2010, pp. 158–171.
- [42] A. Aguiar and J. Hespanha, “Robust filtering for deterministic systems with implicit outputs,” *Syst. Contr. Lett.*, vol. 58, no. 4, pp. 263–270, 2009.
- [43] A. Krener and A. Isidori, “Linearization by output injection and nonlinear observers,” *Syst. Contr. Lett.*, vol. 3, no. 1, pp. 47–52, 1983.
- [44] A. Krener and W. Respondek, “Nonlinear observers with linearizable error dynamics,” *SIAM J. Contr. Optim.*, vol. 23, no. 2, pp. 197–216, March 1985.
- [45] N. Kazantzis and C. Kravaris, “Nonlinear observer design using Lyapunov’s auxiliary theorem,” *Syst. Contr. Lett.*, vol. 35, no. 5, pp. 241–247, 1998.
- [46] A. Krener and M. Xiao, “Nonlinear observer design in Siegel domain,” *SIAM J. Contr. Optim.*, vol. 41, no. 3, pp. 932–953, 2002.
- [47] V. Andrieu and L. Praly, “On the existence of a Kazantzis-Kravaris/Luenberger observer,” *SIAM J. Contr. Optim.*, vol. 45, no. 2, pp. 432–456, 2006.
- [48] J. P. Gauthier, H. Hammouri, and S. Othman, “A simple observer for nonlinear systems applications to bioreactors,” *IEEE Trans. Autom. Control*, vol. 37, no. 6, pp. 875–880, 1992.
- [49] J. P. Gauthier and I. A. K. Kupka, “Observability and observers for nonlinear systems,” *SIAM J. Contr. Optim.*, vol. 32, no. 4, pp. 975–994, 1994.
- [50] A. Atassi and H. Khalil, “A separation principle for the stabilization of a class of nonlinear systems,” *IEEE Trans. Autom. Control*, vol. 44, no. 9, pp. 1672–1687, 1999.
- [51] F. Thau, “Observing the state of non-linear dynamic systems,” *Int. J. Control*, vol. 17, no. 3, pp. 471–479, 1973.
- [52] R. Rajamani, “Observers for Lipschitz nonlinear systems,” *IEEE Trans. Autom. Control*, vol. 43, no. 3, pp. 397–401, Mar. 1998.
- [53] A. Pertew, A. Marquez, and Q. Zhao, “ H_∞ observer design for Lipschitz nonlinear systems,” *IEEE Trans. on Autom. Control*, vol. 51, no. 7, pp. 1211–1216, 2006.
- [54] M. Chen and C. Chen, “Robust nonlinear observer for Lipschitz nonlinear systems subject to disturbances,” *IEEE Trans. Autom. Control*, vol. 52, no. 12, pp. 2365–2369, 2007.
- [55] J. C. Doyle and G. Stein, “Robustness with observers,” *IEEE Trans. Autom. Contr.*, vol. 24, no. 4, pp. 607–611, 1979.

- [56] A. Morgan and K. Narendra, "On the stability of nonautonomous differential equations $\dot{x} = [A + B(t)]x$ with skew symmetric matrix $B(t)$," *SIAM J. Contr. Optim.*, vol. 15, pp. 163–176, 1977.
- [57] D. Karagiannis, D. Carnevale, and A. Astolfi, "Invariant manifold based reduced order observer design for nonlinear systems," *IEEE Trans. on Autom. Control*, vol. 53, no. 11, pp. 2602–2614, 2008.
- [58] G. Basile and G. Marro, "On the observability of linear, time-invariant systems with unknown inputs," *J. Optimiz. Theory App.*, vol. 3, pp. 410–415, 1969.
- [59] S. Bhattacharyya, "Observer design for linear systems with unknown inputs," *IEEE Trans. Autom. Control*, vol. 23, no. 3, pp. 483–484, Jun. 1978.
- [60] P. Kudva, N. Viswanadham, and A. Ramakrishna, "Observers for linear systems with unmeasurable disturbances," *IEEE Trans. on Autom. Control*, vol. 25, pp. 113–115, 1980.
- [61] N. Kobayashi and T. Nakamizo, "An observer design for linear systems with unknown inputs," *Int. J. Control*, vol. 35, pp. 605–619, 1982.
- [62] F. Fairman, S. Mahil, and L. Luk, "Disturbance decoupled observer design via singular value decomposition," *IEEE Trans. on Autom. Control*, vol. 29, pp. 84–86, 1984.
- [63] Y. Guan and M. Saif, "A novel approach to the design of unknown input observers," *IEEE Trans. Autom. Control*, vol. 36, no. 5, pp. 632–635, May 1991.
- [64] M. Hou and P. Muller, "Design of observers for linear systems with unknown inputs," *IEEE Trans. Autom. Control*, vol. 37, no. 6, pp. 871–875, Jun. 1992.
- [65] F. Yang and R. Wilde, "Design of observers for linear systems with unknown inputs," *IEEE Trans. on Autom. Control*, vol. 37, pp. 871–875, 1992.
- [66] M. Darouach, M. Zasadzinski, and S. Xu, "Full-order observers for linear systems with unknown inputs," *IEEE Trans. Autom. Control*, vol. 39, no. 3, pp. 606–609, Mar. 1994.
- [67] C.-C. Tsui, "A new design approach to unknown input observers," *IEEE Trans. Autom. Control*, vol. 41, no. 3, pp. 464–468, Mar. 1996.
- [68] T. Floquet and J. Barbot, "A sliding mode approach of unknown input observers for linear systems," in *IEEE Conf. Decision and Control*, vol. 2, 2004, pp. 1724–1729.
- [69] J. Moreno, "Unknown input observers for SISO nonlinear systems," in *IEEE Conf. Decision and Control*, vol. 1, 2000, pp. 790–801.

- [70] A. Pertew, H. Marquez, and Q. Zhao, "Design of unknown input observers for Lipschitz nonlinear systems," in *Proc. of American Control Conf.*, 2005, pp. 4198–4203.
- [71] H. Hammouri and Z. Tmar, "Unknown input observer for state affine systems: A necessary and sufficient condition," *Automatica*, vol. 46, pp. 271–278, 2010.
- [72] M. Hautus, "Strong detectability and observers," *Lin. Algebra. Appl.*, vol. 50, pp. 353–368, 1983.
- [73] T. Floquet, J. Barbot, W. Perruquetti, and M. Djemai, "On the robust fault detection via sliding mode perturbation observer," *Int. J. Control*, vol. 77, pp. 622–629, 2004.
- [74] F. Bejarano, L. Fridman, and A. Poznyak, "Exact state estimation for linear systems with unknown inputs based on hierarchical super-twisting algorithm," *Int. J. Robust Nonlinear Contr.*, vol. 17, pp. 1734–1753, 2007.
- [75] K. Kalsi, J. Lian, S. Hui, and S. Zak, "Sliding-mode observers for systems with unknown inputs: a high-gain approach," *Automatica*, vol. 46, no. 2, pp. 347–353, 2010.
- [76] D. Koenig and S. Mammar, "Design of a class of reduced order unknown inputs nonlinear observer for fault diagnosis," in *Proc. of American Control Conf.*, vol. 3, 2001, pp. 2143–2147.
- [77] W. Chen and M. Saif, "Fault detection and isolation based on novel unknown input observer design," in *Proc. of American Control Conf.*, 2006.
- [78] ———, "Unknown input observer design for a class of nonlinear systems: an LMI approach," in *Proc. of American Control Conf.*, 2006.
- [79] F. Liu, M. Farza, and M. M'Saad, "Unknown input observers design for a class of nonlinear systems - application to biochemical process," in *IFAC Symp. Robust Control Design*, 2006.
- [80] L. Fridman, Y. Shtessel, C. Edwards, and G. Yan, X, "Higher-order sliding-mode observer for state estimation and input reconstruction in nonlinear systems," *Int. J. Robust Nonlinear Contr.*, vol. 18, pp. 399–412, 2007.
- [81] J. A. Moreno and D. Dochain, "Global observability and detectability analysis of uncertain reaction systems and observer design," *Int. J. Control*, vol. 81, pp. 1062–1070, 2008.
- [82] R. J. Patton and J. Chen, "Optimal selection of unknown input distribution matrix in the design of robust observers for fault diagnosis." *Automatica*, vol. 29, pp. 837–841, 1993.

- [83] C. De Persis and A. Isidori, "A geometric approach to nonlinear fault detection and isolation," *IEEE Trans. on Autom. Control*, vol. 46, pp. 853–865, 2001.
- [84] H. Hammouri, P. Kabore, and M. Kinnaert, "Geometric approach to fault detection and isolation for bilinear systems." *IEEE Trans. on Autom. Control*, vol. 46, no. 9, pp. 1451–1455, 2001.
- [85] H. Hammouri, M. Kinnaert, and E. H. El Yaagoubi, "Observer based approach to fault detection and isolation for nonlinear systems." *IEEE Trans. on Autom. Control*, vol. 44, pp. 1879–1884, 1999.
- [86] B. Xian, D. M. Dawson, M. S. de Queiroz, and J. Chen, "A continuous asymptotic tracking control strategy for uncertain nonlinear systems," *IEEE Trans. Autom. Control*, vol. 49, pp. 1206–1211, 2004.
- [87] P. M. Patre, W. MacKunis, K. Kaiser, and W. E. Dixon, "Asymptotic tracking for uncertain dynamic systems via a multilayer neural network feedforward and RISE feedback control structure," *IEEE Trans. Autom. Control*, vol. 53, no. 9, pp. 2180–2185, 2008.
- [88] A. Behal, W. E. Dixon, B. Xian, and D. M. Dawson, *Lyapunov-Based Control of Robotic Systems*. CRC Press, 2009.
- [89] O. Faugeras, *Three-Dimensional computer vision*. Cambridge, Massachusetts: The MIT Press, 2001.
- [90] Z. Zhang and A. Hanson, "3D reconstruction based on homography mapping," in *Proc. ARPA Image Underst. Workshop*, Palm Springs CA, 1996.
- [91] S. Hutchinson, G. Hager, and P. Corke, "A tutorial on visual servo control," *IEEE Trans. Robot. Autom.*, vol. 12, no. 5, pp. 651–670, Oct. 1996.
- [92] H. Khalil, "Adaptive output feedback control of nonlinear systems represented by input-output models," *IEEE Trans. Autom. Control*, vol. 41, no. 2, p. 177, 1996.
- [93] X. Chen and H. Kano, "A new state observer for perspective systems," *IEEE Trans. Autom. Control*, vol. 47, no. 4, pp. 658–663, 2002.
- [94] C. Chicone, *Ordinary Differential Equations with Applications*, 2nd ed. Springer, 2006.
- [95] S. Sastry and M. Bodson, *Adaptive Control: Stability, Convergence, and Robustness*. Upper Saddle River, NJ: Prentice-Hall, 1989.
- [96] H. K. Khalil, *Nonlinear Systems*, 3rd ed. Prentice Hall, 2002.
- [97] N. Stefanovic, M. Ding, and L. Pavel, "An application of L2 nonlinear control and gain scheduling to erbium doped fiber amplifiers," *Control Eng. Pract.*, vol. 15, pp. 1107–1117, 2007.

- [98] R. Kelly, V. Santibanez, and A. Loria, *Control of Robot Manipulators in Joint Space*. Springer, 2005.
- [99] F. Nagata, K. Kuribayashi, K. Kiguchi, and K. Watanabe, “Simulation of fine gain tuning using genetic algorithms for model-based robotic servo controllers,” in *Proc. Int. Sym. Comput. Intell. Robot. Autom.*, 20-23 June 2007, pp. 196–201.
- [100] T. Fujinaka, Y. Kishida, M. Yoshioka, and S. Omatu, “Stabilization of double inverted pendulum with self-tuning neuro-PID,” in *Proc. IEEE-INNS-ENNS Int. Joint Conf. Neural Netw.*, vol. 4, 24–27 July 2000, pp. 345–348.
- [101] N. J. Killingsworth and M. Krstic, “PID tuning using extremum seeking: online, model-free performance optimization,” *IEEE Contr. Syst. Mag.*, vol. 26, no. 1, pp. 70–79, 2006.
- [102] K. Åström, T. Hägglund, C. Hang, and W. Ho, “Automatic tuning and adaptation for PID controllers—a survey,” *Control Eng. Pract.*, vol. 1, no. 4, pp. 669–714, 1993.
- [103] Z. Zhang, “A flexible new technique for camera calibration,” *IEEE Trans. Pattern Anal. Mach. Intell.*, vol. 22, no. 11, pp. 1330–1334, 2000.
- [104] W. Rudin, *Principles of Mathematical Analysis*. McGraw-Hill, 1976.
- [105] F. M. Callier and C. A. Desoer, *Multivariable Feedback Systems*. Springer-Verlag, 1982.
- [106] A. Krener, *The convergence of the minimum energy estimator*, ser. Lect. Notes in Contr. and Inform. Sci. Springer-Verlag, 2003.
- [107] R. Marino, G. Santosuosso, and P. Tomei, “Robust adaptive observer for nonlinear systems with bounded disturbances,” *IEEE Trans. Autom. Contr.*, vol. 46, no. 6, p. 967972, 2001.
- [108] A. Filippov, “Differential equations with discontinuous right-hand side,” *Am. Math. Soc. Transl.*, vol. 42 no. 2, pp. 199–231, 1964.
- [109] G. V. Smirnov, *Introduction to the theory of differential inclusions*. American Mathematical Society, 2002.
- [110] B. Paden and S. Sastry, “A calculus for computing Filippov’s differential inclusion with application to the variable structure control of robot manipulators,” *IEEE Trans. Circuits Syst.*, vol. 34 no. 1, pp. 73–82, 1987.
- [111] F. H. Clarke, *Optimization and nonsmooth analysis*. SIAM, 1990.
- [112] D. Shevitz and B. Paden, “Lyapunov stability theory of nonsmooth systems,” *IEEE Trans. Autom. Control*, vol. 39 no. 9, pp. 1910–1914, 1994.
- [113] H. K. Khalil, *Nonlinear Systems*, 2nd ed. Prentice Hall, 1996.

- [114] K. Narendra and A. Annaswamy, *Stable adaptive systems*. Prentice-Hall, Inc., 1989.
- [115] E. Yaz and A. Azemi, “Observer design for discrete and continuous nonlinear stochastic systems,” *Int. J. Syst. Sci.*, vol. 24, no. 12, pp. 2289–2302, 1993.
- [116] L. Xie and P. P. Khargonekar, “Lyapunov-based adaptive state estimation for a class of nonlinear stochastic systems,” in *Proc. of American Controls Conf.*, Baltimore, MD, 2010, pp. 6071–6076.
- [117] D. Bernstein, *Matrix Mathematics*. Princeton Univ Pr, 2005.
- [118] P. Gahinet, A. Nemirovskii, A. Laub, and M. Chilali, “The LMI control toolbox,” in *IEEE Conf. Decision and Control*, vol. 3, 1994, pp. 2038–2041.
- [119] A. P. Dani, Z. Kan, N. Fischer, and W. E. Dixon, “Structure and motion estimation of a moving object using a moving camera,” in *Proc. Am. Control Conf.*, Baltimore, MD, 2010.
- [120] B. Sinopoli, L. Schenato, M. Franceschetti, K. Poolla, M. Jordan, and S. Sastry, “Kalman filtering with intermittent observations,” *IEEE Trans. Autom. Contr.*, vol. 49, no. 9, pp. 1453–1464, 2004.
- [121] S. Kluge, K. Reif, and M. Brokate, “Stochastic stability of the extended Kalman filter with intermittent observations,” *IEEE Trans. Autom. Contr.*, vol. 55, no. 2, pp. 514–518, 2010.
- [122] E. Panteley, A. Loria, and A. Teel, “Relaxed persistency of excitation for uniform asymptotic stability,” *IEEE Trans. Autom. Contr.*, vol. 46, no. 12, pp. 1874–1886, 2001.
- [123] S. Roth and M. Black, “Specular flow and the recovery of surface structure,” in *Computer Vision and Pattern Recognition*, 2006.
- [124] Y. Adato, Y. Vasilyev, T. Zickler, and O. Ben-Shahar, “Shape from specular flow,” *IEEE Pattern Recognit. and Machine Intell.*, vol. 32, no. 11, pp. 2054–2070, 2010.

BIOGRAPHICAL SKETCH

Ashwin Dani was born in Nagpur, India. He received his Bachelor of Engineering degree in mechanical engineering from College of Engineering Pune (COEP), India. After his graduation in 2005, he was hired by International Business Machines (IBM) as a graduate engineer from 2005 to 2006. He then joined the Nonlinear Controls and Robotics (NCR) research group to pursue his doctoral research, under the advisement of Warren E. Dixon. He has worked as an intern at Mitsubishi Electric Research Labs, Cambridge MA, during January of 2009 to May 2009 and May 2010 to August 2010 on observer design for distributed parameter systems. He received his Ph.D. from the University of Florida in the Summer of 2011. From August 2011 onward he will be a post-doctoral fellow with the University of Illinois at Urbana-Champaign.